

# Synthetic Hectorite in Solvent Mixtures and resulting Nanocomposites

Dissertation

zur Erlangung des akademischen Grades einer  
Doktorin der Naturwissenschaften (Dr. rer. nat.)  
an der Fakultät für Biologie, Chemie und Geowissenschaften  
der Universität Bayreuth

vorgelegt von

**Lina Mayr**  
geboren in Bamberg

Bayreuth, 2020



Die vorliegende Arbeit wurde in der Zeit von November 2016 bis Oktober 2020 in Bayreuth am Lehrstuhl für Anorganische Chemie I unter Betreuung von Herrn Prof. Dr. Josef Breu angefertigt.

Vollständiger Abdruck der von der Fakultät für Biologie, Chemie und Geowissenschaften der Universität Bayreuth genehmigten Dissertation zur Erlangung des akademischen Grades einer Doktorin der Naturwissenschaften (Dr. rer. nat.).

Dissertation eingereicht am: 28.10.2020

Zulassung durch die Promotionskommission: 04.11.2020

Wissenschaftliches Kolloquium: 31.03.2021

Amtierender Dekan: Prof. Dr. Matthias Breuning

Prüfungsausschuss:

Prof. Dr. Josef Breu (Gutachter)

Prof. Dr. Seema Agarwal (Gutachterin)

Prof. Dr. Markus Retsch (Vorsitz)

Prof. Dr. Birgit Weber



Meiner lieben Familie

What we know is a drop.  
What we don't know is an ocean.

*Isaac Newton*



---

## Table of Contents

List of Abbreviations .....	III
1 Summary .....	1
2 Zusammenfassung.....	3
3 Introduction.....	7
3.1 Hectorite .....	8
3.1.1 Structural properties .....	8
3.1.2 Swelling in water .....	9
3.1.3 Swelling in organic solvents .....	11
3.2 Polymer clay nanocomposites .....	13
3.2.1 Preparation of polymer clay nanocomposites .....	13
3.2.2 Properties and application of polymer clay nanocomposites.....	14
3.2.3 Polymer nanocomposite foams .....	18
3.3 Pickering emulsions .....	22
3.3.1 General aspects of Pickering emulsions .....	22
3.3.2 Clay Pickering emulsions .....	24
3.3.3 Encapsulation in Pickering emulsions .....	26
3.4 Scope of the thesis.....	27
4 Synopsis .....	29
4.1 Swelling of sodium hectorite in ternary solvent mixtures.....	30
4.2 Polymer clay nanocomposite foams made via high internal phase emulsions .....	32
4.3 Sustained release of fragrances from clay Pickering emulsions .....	34
5 Literature.....	37
6 Results.....	47
6.1 Osmotic swelling of sodium hectorite in ternary solvent mixtures: nematic liquid crystals in hydrophobic media .....	47
6.2 Structural and mechanical impact of synthetic clay in composite foams made via high internal phase emulsions .....	61

---

6.3	Encapsulation of fragrance in aqueous emulsions by delaminated synthetic hectorite	79
7	List of Publications	91
8	Acknowledgement	93
9	Erklärung des Verfassers	95

---

## List of Abbreviations

Not included in this list: Units and chemical formulas

$\alpha$	aspect ratio (diameter/height)
$\gamma_{OP}$	interfacial tension between oil and particle
$\gamma_{OW}$	interfacial tension between oil and water
$\gamma_{WP}$	interfacial tension between water and particle
$\Delta\varepsilon$	change in strain
$\Delta\sigma$	change in stress
$\Delta G$	energy difference
$\theta$	contact angle
$\mu$	geometrical factor (4/9)
$\rho$	foam density
$\rho_{rel}$	relative foam density
$\rho_s$	density of the solid bulk polymer
$\sigma_{YS}$	yield stress
$\phi$	volume fraction
$A$	surface area
$A_{OP}$	interface area between oil and particle
$A_{OW}$	interface area between oil and water
$A_{WP}$	interface area between water and particle
CTAB	cetyltrimethylammonium bromide
$d$	layer distance / separation
$D$	diffusivity
DMSO	dimethyl sulfoxide
$E$	Young's modulus
$E_c$	Young's modulus of the composite
$E_f$	Young's modulus of the filler
$E_m$	Young's modulus of the matrix
$E_s$	Young's modulus of the solid bulk polymer
eq.	equation
Hec	hectorite
HecPEHMA	hectorite modified with ammonium terminated poly (2-ethylhexyl methacrylate)
HIPE	high internal phase emulsion

---

mol.-%	molar percentage
NaHec	sodium fluorohectorite
NMR	nuclear magnetic resonance spectroscopy
O-MMT	commercial organophilized montmorillonite
OS	octahedral sheet
$P$	permeability
$P_0$	permeability of the matrix
$P_c$	permeability of the composite
$P_{rel}$	relative permeability
PEHMA	poly(2-ethyl hexyl methacrylate)
PEI	poly(ethylene imine)
PMMA	poly(methyl methacrylate)
$pfu$	per formula unit
PVP	polyvinylpyrrolidone
$R$	radius
r.h.	relative humidity
$S$	solubility
SAXS	small angle X-ray scattering
SEM	scanning electron microscopy
$t$	layer thickness
TS	tetrahedral sheet
UV	ultra violet
vol.-%	volume percentage
WL	water layer
wt.-%	weight percentage

# 1 Summary

In this thesis, hectorite, a layered silicate, was investigated in different solvent mixtures and was, then, used for the preparation of nanocomposites with different application possibilities. Osmotic swelling of hectorite in water offers an easy way to gain single 1 nm thick layers with a huge aspect ratio. For many applications like gas barrier, composites with such layers are desired. As many polymers are insoluble in water, organic solvents or solvent mixtures that enable osmotic swelling are needed. In the first part of this thesis, the swelling of sodium hectorite (NaHec) in different ternary mixtures consisting of methanol, acetonitrile, ethylene glycol, glycerol carbonate or water was investigated. It was found that in ternary mixtures, less water was necessary to trigger osmotic swelling than in corresponding binary mixtures. In this way, the water content could be reduced to 10 vol.-% using a mixture of methanol (70 vol.-%), water and acetonitrile (20 vol.-%). In a system with glycerol carbonate, a solvent that can also be polymerized, and methanol, only negligible amounts of water were necessary for osmotic swelling. Thus, hydrophilic NaHec could be osmotically swollen almost without water which extends its application possibilities. Furthermore, it was found that in binary mixtures of water with one organic solvent, the dipole moment of the latter determines the swelling behavior. The smaller the dipole moment, the more water was necessary to allow for osmotic swelling. However, for ternary systems, this simple correlation does not exist. A quantitative study of the osmotic swelling of NaHec in a ternary solvent mixture revealed a similar behavior like the osmotic swelling in water. The layer separation increased with increasing amount of solvent indicating complete osmotic swelling.

Whereas completely miscible solvents were used for the swelling studies, the other two parts of this thesis are dealing with emulsions of immiscible solvents.

In the second part, high internal phase emulsions (HIPEs) in which the external phase consisted of polymerizable molecules were used as templates for polymer foam composites. Hectorite was modified with a custom-made organo-cation (HecPEHMA) to disperse it in the external phase of a HIPE. Upon polymerization of this phase, open-cell composite foams with relative densities of 4–7 % could be synthesized. The mechanics of the foams were studied by compression tests depending on the filler content and the relative density of the foams. With only 2 % HecPEHMA, the Young's modulus could be increased up to a factor of four. To investigate the mechanism of the strengthening, HecPEHMA was also incorporated in bulk polymer plates and their tensile properties were tested. However, the filler led to a weakening of the polymer concluding that the strengthening of the foams was not due to a reinforcement

of the material. Instead, the foam mechanics were determined by the foam morphology. The foams with 2 % HecPEHMA had larger cells, thicker struts and a more consistent structure. Most probably, HecPEHMA acted as a Pickering emulsifier stabilizing the emulsion in addition to the molecular surfactant. This then led to an improved foam structure which simultaneously improved the mechanics. Contrary, a commercial organophilized montmorillonite (O-MMT) filler could not enhance the foam mechanics, most likely as its surface modification could not provide a Pickering effect.

In the third part, hectorite was used to encapsulate a fragrance mixture in aqueous emulsions. In many applications, not a single fragrance is used but a mixture of different volatile substances. These fragrances usually differ in their vapor pressures and therefore, the composition of the mixture changes upon evaporation. Thus, unselective barriers are needed to maintain the original scent impression. As nanocomposite films with hectorite provide excellent gas barriers, it seems promising to use hectorite for barrier capsules as well. However, pristine hectorite is too hydrophilic to stabilize emulsion droplets. Therefore, hectorite was *in-situ* modified with polycationic poly(ethylene imine) (PEI) during the emulsification. The evaporation of a model fragrance mixture (eucalyptol, limonene,  $\alpha$ -pinene and ethyl-2-methylbutyrate) from such emulsions was investigated. By applying hectorite layers at the water-oil-interface, the release could be significantly retarded in comparison with an emulsion that was solely stabilized with PEI. The release rates were no longer determined by their vapor pressures. All fragrances are hydrophobic but differ in their water solubility. As the capsule wall which consisted of hectorite and PEI was most probably swollen with water, the relative solubility of the fragrances in the capsule wall might be similar to the water solubility. Fragrances which have a higher water solubility diffuse faster through the capsule wall and were thus, released faster. By comparing emulsions made with different ratios between PEI and hectorite, it could be shown that the release was further retarded by lowering the amount of PEI. This is due to an increased tortuosity in the capsule wall. An additional chemical cross-linking of PEI could further improve the retardation of the fragrances.

This work is a cumulative thesis. A detailed description of the results can be found in the attached publications.

## 2 Zusammenfassung

In dieser Arbeit wurde Hectorit, ein Schichtsilikat, in verschiedenen Lösemittelgemischen untersucht und dann für die Herstellung von Nanokompositen mit unterschiedlichen Anwendungsmöglichkeiten verwendet.

Die osmotische Quellung von Hectorit in Wasser bietet eine einfache Möglichkeit, einzelne, 1 nm dicke Schichten mit einem sehr großen Aspektverhältnis herzustellen. Für viele Anwendungen wie beispielsweise als Gasbarriere, sind Komposite mit solchen Schichten wünschenswert. Da viele Polymere nicht wasserlöslich sind, werden organische Lösemittel oder Lösemittelmischungen, die eine osmotische Quellung erlauben, benötigt. Im ersten Teil dieser Arbeit wurde das Quellungsverhalten von Natriumhectorit (NaHec) in verschiedenen ternären Lösemittelmischungen, bestehend aus Methanol, Acetonitril, Ethylenglykol, Glycerincarboxat oder Wasser, untersucht. Es wurde festgestellt, dass in ternären Gemischen weniger Wasser notwendig war, um eine osmotische Quellung einzuleiten als in entsprechenden binären Mischungen. So konnte der Wassergehalt auf 10 vol.-% reduziert werden indem ein Gemisch aus Methanol (70 vol.-%), Wasser und Acetonitril (20 vol.-%) verwendet wurde. In einem System mit Glycerincarboxat, einem Lösemittel, das gleichzeitig polymerisiert werden kann, und Methanol waren nur vernachlässigbar kleine Mengen Wasser für eine osmotische Quellung notwendig. Hydrophiler NaHec konnte also nahezu ohne Wasser osmotisch gequollen werden, was seine Anwendungsmöglichkeiten erweitert. Weiterhin wurde festgestellt, dass das Quellungsverhalten in binären Mischungen (Wasser und ein organisches Lösemittel) vom Dipolmoment des organischen Lösemittels bestimmt wird. Je kleiner das Dipolmoment ist, desto mehr Wasser ist notwendig, um eine osmotische Quellung zu realisieren. Diese einfache Korrelation ist allerdings nicht auf ternäre Mischungen übertragbar. Eine quantitative Untersuchung der osmotischen Quellung von NaHec in einem ternären Gemisch ergab ein ähnliches Verhalten wie bei der osmotischen Quellung in Wasser. Der Schichtabstand nahm mit zunehmender Lösungsmittelmenge zu, was eine vollständige osmotische Quellung anzeigt.

Während für die Quellungsstudien komplett mischbare Lösemittel verwendet wurden, befassen sich die beiden anderen Teile dieser Arbeit mit Emulsionen von nicht mischbaren Lösemitteln. Im zweiten Teil wurden Emulsionen mit einem großen Anteil an interner Phase (*high internal phase emulsion*, HIPE), bei denen die externe Phase polymerisiert werden konnte, als Template für Polymerschäume verwendet. Hectorit wurde mit einem maßgeschneiderten Organokation modifiziert (HecPEHMA), um ihn in der externen Phase einer HIPE zu dispergieren. Durch die

Polymerisation dieser Phase konnten offenzellige Schäume mit relativen Dichten von 4 – 7 % hergestellt werden. Die mechanischen Eigenschaften dieser Schäume wurden in Abhängigkeit von Dichte und Füllstoffgehalt mittels Druckversuchen untersucht. Mit nur 2 % HecPEHMA konnte der Young'sche Modul im Vergleich zu einem Schaum ohne Füllstoff um bis zu einem Faktor von vier gesteigert werden. Um den Mechanismus der Verstärkung zu untersuchen, wurde HecPEHMA auch in Polymerplatten eingebracht und deren Zugeigenschaften getestet. Allerdings bewirkte der Füllstoff eine Schwächung des Polymers, was zu der Schlussfolgerung führte, dass die Steigerung des Young'schen Moduls der Schäume nicht von einer Verstärkung des Materials kommt. Stattdessen wurden die mechanischen Eigenschaften von der Schaummorphologie bestimmt. Die Schäume mit 2 % HecPEHMA hatten größere Zellen, dickere Stege und eine konsistentere Struktur. Höchstwahrscheinlich fungierte HecPEHMA als Pickering-Emulgator, der in Kombination mit den molekularen Tensiden die Emulsion stabilisierte. Dies führte zu einer verbesserten Schaummorphologie, was wiederum die mechanischen Eigenschaften verbesserte. Im Gegensatz dazu konnte ein kommerzieller organophiler Montmorillonit (O-MMT) als Füllstoff die Schaummechanik nicht verbessern, da seine Oberflächenmodifikation vermutlich keinen Pickering-Effekt erzielen konnte.

Im dritten Teil dieser Arbeit wurde Hectorit dazu verwendet, Duftstoffe in wässrigen Emulsionen einzukapseln. In vielen Anwendungen werden keine einzelnen Duftstoffe eingesetzt, sondern eine Mischung aus verschiedenen flüchtigen Substanzen. Diese Duftstoffe unterscheiden sich üblicherweise durch ihre Dampfdrücke und daher ändert sich beim Verdunsten die Zusammensetzung der Mischung. Somit werden nicht-selektive Barrieren benötigt, um den ursprünglichen Geruchseindruck zu erhalten. Da Nanokomposit-Filme mit Hectorit exzellente Barrieren darstellen, scheint es vielversprechend, Hectorit auch für Barriere kapseln zu verwenden. Allerdings ist reiner Hectorit zu hydrophil, um Emulsionen zu stabilisieren. Daher wurde der Hectorit *in-situ*, also während der Emulgierung, mit dem Polykation Polyethylenimin (PEI) modifiziert. Das Verdunsten einer beispielhaften Duftstoffmischung (Eucalyptol, Limonen,  $\alpha$ -Pinen und Ethyl-2-methylbutyrat) aus solchen Emulsionen wurde untersucht. Durch den Einsatz von Hectoritplättchen an der Öl-Wasser-Grenzfläche konnte die Freisetzung im Vergleich zu einer Emulsion, die nur von PEI stabilisiert wurde, signifikant verlangsamt werden. Dabei wurde die Freisetzungsrates nicht länger durch die Dampfdrücke bestimmt. Alle Duftstoffe sind hydrophob, unterscheiden sich aber durch ihre Wasserlöslichkeit. Da die Kapselwand aus Hectorit und PEI besteht und damit höchstwahrscheinlich mit Wasser gequollen ist, könnte die relative Löslichkeit der Duftstoffe

in der Kapselwand ähnlich zu der in Wasser sein. Duftstoffe, die eine höhere Wasserlöslichkeit besitzen, diffundierten schneller durch die Kapselwand und wurden demzufolge schneller freigesetzt. Ein Vergleich von Kapseln, die mit unterschiedlichen Verhältnissen zwischen Hectorit und PEI hergestellt wurden, zeigte, dass die Freisetzung weiter verzögert werden konnte indem die Menge an PEI reduziert wurde. Dies ist auf eine Verlängerung der mittleren Wegstrecke (erhöhte Tortuosität) in der Kapselwand zurückzuführen. Ein zusätzliches chemisches Quervernetzen von PEI konnte die Freisetzung der Duftstoffe weiter verzögern.

Diese Arbeit ist eine kumulative Dissertation. Eine detaillierte Beschreibung der Ergebnisse befindet sich in den angehängten Publikationen.



### 3 Introduction

The first handed down description of a polymer is the recipe of a resin made of casein in 1530.<sup>[1]</sup> Already in this description, the various application possibilities, for example as tabletop or cups, were mentioned. However, polymers, or more commonly plastics, had their great breakthrough in the 20<sup>th</sup> century. Since then, polymers can be found nearly everywhere in daily life. Due to their light weight, easy processability and various utilization possibilities, polymers are often the material of choice.<sup>[2]</sup> Application areas are for example packaging, insulation, technical devices like computers or mobile phones and medical technology.<sup>[1-2]</sup>

However, for some applications, neat polymers do not fulfill the required specifications like mechanical properties, flame retardancy or resistance against heat, oxidation or UV irradiation.<sup>[1]</sup> One way to improve polymer properties is the use of additives. Molecular additives can be used to improve the resistance against UV radiation, to change the crystallinity or for plasticizing effects.<sup>[1]</sup> However, some of them are repeatedly criticized due to their toxicity.<sup>[3-4]</sup> Other important additives are solid fillers which are used to produce composites. In general, composites are solids consisting of two or more components where at least one component is dispersed in another.<sup>[2]</sup> Two of the most common fillers are carbon and glass fibers.<sup>[5]</sup> Such polymer composites are used in aircrafts or sport equipment for instance. While preserving the light weight of the polymer, fiber reinforced composites exhibit enhanced mechanical strength.

If the dispersed phase in composites has at least one dimension in the nanometer-scale, a nanocomposite is obtained.<sup>[6]</sup> Spherical nanoparticles have all three dimensions in this scale. Various metal and metal oxide nanoparticles can be used to improve electrical, optical and mechanical properties.<sup>[7]</sup> Fibers or tubes have two dimensions in the nanometer-scale. For example, carbon nanotube composites can be used as cathodes.<sup>[8]</sup> If only one dimension is in the nanometer-scale, platelets are obtained (also referred to as two-dimensional particles). One representative of this material class are clays. They have been used for a long time in several applications. Already in Mayan paintings, clay mixed with dye molecules was found to yield a color which is resistant against acids and biocorrosion.<sup>[9]</sup> Furthermore, clay is used in many ceramics like porcelain, in papers and in cosmetics.<sup>[10]</sup> In polymers, clay is used as filler to improve gas barrier,<sup>[11-12]</sup> flame retardancy<sup>[13-14]</sup> and mechanical strength.<sup>[15-16]</sup> Prominent examples of clays are montmorillonite, kaolinite and hectorite.<sup>[10]</sup>

### 3.1 Hectorite

#### 3.1.1 Structural properties

Hectorite belongs to the class of layered silicates (phyllosilicates). In general, layered silicates are composed of tetrahedral and octahedral sheets. Tetrahedral sheets (TS) are built from  $\text{SiO}_4$  tetrahedra which are connected via three basal oxygen atoms (Figure 1). In this way, an infinite hexagonal sheet is formed. This sheet is condensed with an octahedral sheet (OS) via its apical oxygen atoms. Depending on the kind of phyllosilicate, the corners of the octahedra are occupied by oxygen, hydroxide or fluoride. Various cations like  $\text{Mg}^{2+}$ ,  $\text{Li}^+$ ,  $\text{Al}^{3+}$ ,  $\text{Fe}^{2+}$  or  $\text{Fe}^{3+}$  can be allocated in the centers of the octahedra.<sup>[10]</sup> There are several properties that are used to classify layered silicates. One way is the classification by the connection of tetrahedral and octahedral sheets to form clay layers. In a 1:1 layered silicate, one tetrahedral sheet is condensed with one octahedral sheet, whereas in a 2:1 layered silicate, one octahedral sheet is sandwiched between two tetrahedral sheets (Figure 1).<sup>[10, 17]</sup>

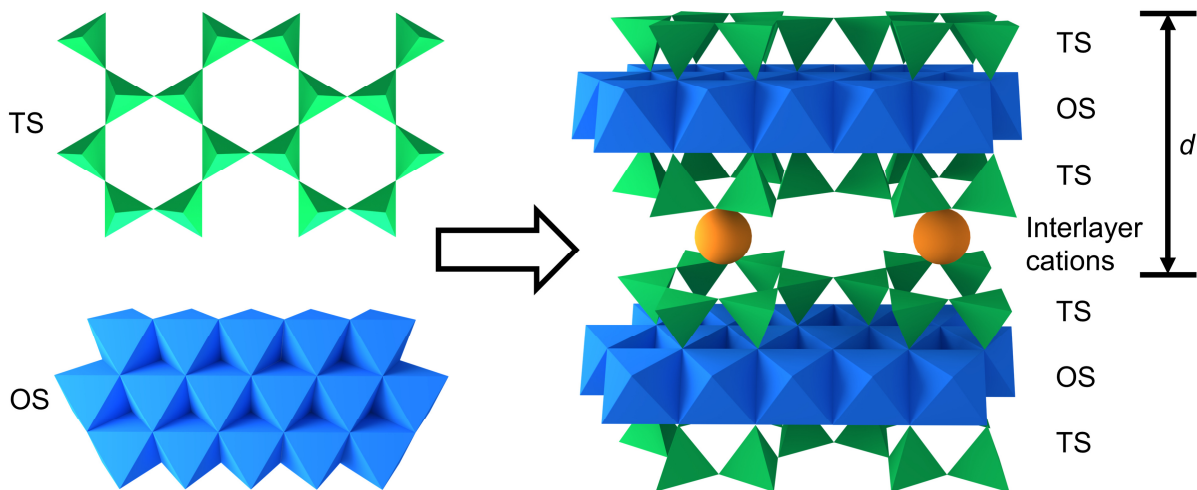


Figure 1: Structure of individual tetrahedral (green) and octahedral (blue) sheets and their combination to 2:1 layered silicates.

Furthermore, layered silicates can be divided into dioctahedral and trioctahedral depending on the occupation of the cations in the octahedral sheet.<sup>[18]</sup> In trioctahedral layered silicates, all octahedral sites are occupied whereas in dioctahedral layered silicates only 2/3 are occupied. One example of a trioctahedral 2:1 layered silicate is talc with the chemical formula  $\text{Mg}_3\text{Si}_4\text{O}_{10}(\text{OH})_2$ .<sup>[19]</sup> Talc is a non-charged layered silicate. From this structure, charged layered silicates can be derived. By partial isomorphic substitution of divalent  $\text{Mg}^{2+}$  by monovalent  $\text{Li}^+$  in the octahedral sheet, a negative charge is generated within the layer. This negative charge is compensated by hydrated or non-hydrated cations between the layers. These interlayer cations can easily be exchanged against other inorganic or organic cations which offers tunable

properties of the clay material (see chapter 3.2.1).<sup>[20-21]</sup> Depending on the type and hydration of the interlayer cation, layered silicates exhibit certain layer separations  $d$  (Figure 1).

Further classification of layered silicates is done by their layer charge. A net layer charge per formula unit (*pfu*) of 0.2 – 0.6 refers to the class of smectites, which includes hectorite and montmorillonite.<sup>[18]</sup> The latter is a natural clay with a dioctahedral character and one of the most used clays in industrial applications.<sup>[10, 22]</sup>

In this work, a synthetic sodium fluorohectorite (NaHec,  $[\text{Na}_{0.5}][\text{Mg}_{2.5}\text{Li}_{0.5}][\text{Si}_4]\text{O}_{10}\text{F}_2$ ) was used.<sup>[23-24]</sup> It belongs to the trioctahedral 2:1 layered silicates and has a layer charge of 0.5 *pfu*. It is synthesized in a closed molybdenum crucible at 1750 °C followed by tempering for six weeks at 1045 °C.<sup>[24]</sup> Whereas natural layered silicates suffer from inhomogeneous charge distributions, this synthesis ensures a statistical distribution of the cations in the octahedral sheet resulting in a phase pure material with homogenous charge distribution. This causes a homogenous intracrystalline reactivity and concomitantly a homogenous swelling behavior.<sup>[24]</sup>

### 3.1.2 Swelling in water

As mentioned before, sodium cations in the interlayer space can be hydrated, which is also known as crystalline swelling.<sup>[25]</sup> Depending on the relative humidity (r.h.), discrete hydration steps occur.<sup>[26]</sup> Starting with a fully dried NaHec and increasing the relative humidity above 22 %, a transition to the 1 water layer (WL) hydrate takes place. A 2 WL hydrate is obtained when exceeding 64 % r.h. These hydration steps correspond to a  $d$ -spacing of 0.96 nm (0 WL), 1.24 nm (1 WL) and 1.55 nm (2 WL), respectively. For the 1 WL hydrate of a sodium hectorite with a layer charge of 0.7 *pfu*, it was shown, that sodium cations are located close to one tetrahedral sheet and are coordinated by three basal oxygen atoms. On the opposite side, sodium cations are coordinated by three water molecules. In the 2 WL hydrate, sodium cations are coordinated by six water molecules and are located in the middle of the interlayer space.<sup>[27]</sup>

Whereas crystalline swelling occurs at different values of relative humidity, osmotic swelling sets in, when NaHec is dispersed in liquid water. Due to repulsive forces between negatively charged layers, they are pushed apart from each other. This results in delaminated 1 nm thick layers while preserving the original width.<sup>[24]</sup> Due to their huge aspect ratio  $\alpha$  ( $\text{diameter/height} \approx 20000$ ), the individual nanoplatelets cannot freely rotate even in dilute suspensions.<sup>[26]</sup> Thus, they align – depending on the volume fraction – more or less parallel to each other to form nematic phases.<sup>[28]</sup> These nematic phases can easily be visualized between two crossed polarizers (Figure 2A). Furthermore, they can be evidenced by small angle X-ray scattering (SAXS) and thereof, the average distance between the platelets can be determined.<sup>[26]</sup>

Osmotic swelling of NaHec in water exhibits two regimes depending on its volume fraction  $\phi$  (Figure 2B). At high volume fractions of NaHec ( $\phi > 0.025$ ), the distance between adjacent layers  $d$  is determined by eq. (1), with the layer thickness  $t = 0.96$  nm.

$$d = t \cdot \phi^{-1} \quad (1)$$

At a volume fraction of  $\phi = 0.025$ , a kink is observed. Below this value, the distance between the layers scales with eq. (2).<sup>[26]</sup>

$$d \sim \phi^{-0.66} \quad (2)$$

This kind of crossover was also observed for other clay materials like nontronites and montmorillonites but its reason is not clear.<sup>[28]</sup>

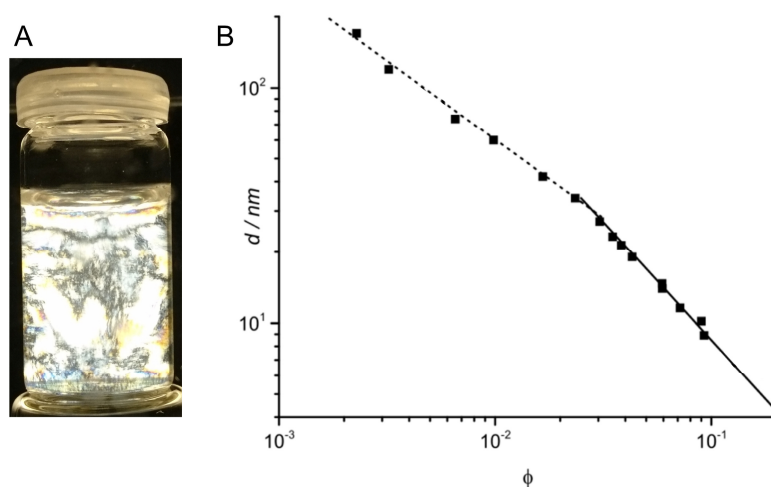


Figure 2: A: Aqueous suspension of 0.1 vol-% NaHec between two crossed polarizers showing birefringence because of the formation of a nematic phase. B: Osmotic swelling of NaHec exhibiting two regimes depending on the volume fraction (Reprinted with permission from reference<sup>[26]</sup>. Copyright (2016) American Chemical Society.).

Whether osmotic swelling sets in or not strongly depends on the charge density of the layered silicate and the interlayer cation.<sup>[29]</sup> Osmotic swelling requires interlayer cations with a certain steric demand and upon hydration a critical  $d$ -spacing has to be surpassed.<sup>[30]</sup> Whereas sodium smectites delaminate in water up to a layer charge of 0.55 *pfu*, higher charged layered silicates need larger interlayer cations like *N*-methyl-D-glucamine to fulfill these criteria.<sup>[31]</sup> Furthermore, osmotic swelling can be suppressed by an increasing ionic background or by adding organic solvents.<sup>[32]</sup>

### 3.1.3 Swelling in organic solvents

Even though osmotic swelling of clay minerals in organic solvents is hampered, crystalline swelling of different clay materials in organic solvents or solvent mixtures could be observed.<sup>[33-35]</sup> Intercalation of neutral solvents in layered silicates is influenced by interactions between solvent molecules and interlayer cations. Possible interactions include hydrogen bonds, ion-dipole interactions, coordination bonds and van-der-Waals interactions.<sup>[21]</sup> Intercalation complexes of sodium or calcium can be formed with a large variety of solvents like alcohols,<sup>[33-34]</sup> acetone,<sup>[33]</sup> dimethyl sulfoxide (DMSO),<sup>[35]</sup> aromatic heterocycles,<sup>[36]</sup> different formamides<sup>[35]</sup> and different acetamides.<sup>[35]</sup> The stability of interlayer complexes is strongly dependent on the polarizing power of the interlayer cation. For acrylonitrile montmorillonite complexes, Yamanaka et al. found that the stronger the polarizing power is, the stronger the attraction between the cation and acrylonitrile is.<sup>[37]</sup>

The most prominent examples of interlayer complexes are made with ethylene glycol and glycerol. These complexing agents are used for identification and quantification of different clay minerals. Ethylene glycol can be intercalated as mono- or bilayer resulting in a specific *d*-spacing depending on charge density and interlayer cation.<sup>[21, 38]</sup>

Exchanging the inorganic interlayer cations against organo-cations like quaternary alkylammonium compounds renders the clay surface hydrophobic.<sup>[39]</sup> Such clay materials can intercalate neutral organic molecules like alcohols or hydrocarbons.<sup>[40-41]</sup> However, complete delamination is hard to achieve as there are strong van-der-Waals interactions between the alkylammonium chains.<sup>[21]</sup>

Different attempts regarding different decisive parameters were made to explain the swelling behavior of clays with organic solvents. If the interlayer cation and the solvent molecule exhibit strong interactions, a complete solvation occurs pushing the cation to the center of the interlayer space. If the interaction is less, solvation is incomplete and the cation is still coordinated by basal oxygen atoms.<sup>[42]</sup> One parameter that describes the strength of a Lewis base is the Gutmann donor number.<sup>[43]</sup> Thus, it describes the ability of a solvent to coordinate to a cation. For the swelling of sodium montmorillonite with a variety of organic solvents, a Gutmann donor number of at least 14 was found to be necessary to remove sodium cations from the hexagonal cavities to allow a complete solvation.<sup>[44]</sup> A correlation between the degree of swelling and the donor number of the solvent was also found for formamide-montmorillonite complexes.<sup>[45]</sup> A different approach was done by Graber and Mingelgrin. They applied regular solution theory, which is normally used for polymer solutions, to explain swelling maxima of different clays with a variety of solvents.<sup>[46]</sup>

In solvent mixtures, different regimes of swelling can be observed. For example, Brindley studied the swelling of different montmorillonites in binary mixtures of DMSO and water.<sup>[47]</sup> Depending on the interlayer cation ( $\text{Li}^+$ ,  $\text{Na}^+$  and  $\text{K}^+$ ), osmotic swelling was observed up to a DMSO content of 45, 30 and 10 mol.-%, respectively. Beyond that, only crystalline swelling was obtained. More recently, the swelling of NaHec in mixtures of acetonitrile and water was studied.<sup>[48]</sup> Here, osmotic swelling occurred up to 65 vol.-% acetonitrile. When more acetonitrile was added, crystalline swelling with a step-like decrease in  $d$ -spacing was observed.

## 3.2 Polymer clay nanocomposites

### 3.2.1 Preparation of polymer clay nanocomposites

Since the first experiments of Toyota, clay-polymer nanocomposites are of large interest in research and industry. In this pioneering work, a mixture of  $\epsilon$ -caprolactam and montmorillonite, which was organophilized by the intercalation of a  $\omega$ -amino acid, was polymerized *in-situ* resulting in exfoliated clay layers within Nylon 6.<sup>[49]</sup> Contrary, melt compounding of Nylon 6 with montmorillonite resulted in clay aggregates.<sup>[50]</sup> This work shows the importance of the preparation method of nanocomposites and of the organophilization of clay.

The most important preparation methods for polymer clay nanocomposites are the following three: the already mentioned *in-situ* polymerization, melt compounding and solution blending.<sup>[51]</sup> For *in-situ* polymerization, clay is dispersed in a monomer which swells the interlayer (usually in the crystalline swelling regime). Then, polymerization is initiated and takes place inside and outside the clay layers. During polymerization, individual clay layers are pushed apart resulting in larger layer separations up to single clay layers.<sup>[52]</sup> Depending on the monomer, this method can be done with or without organic modification of the clay.<sup>[52]</sup> Mixing clay with liquid pre-polymers which are cross-linked afterwards is in close relation to this method.<sup>[53-54]</sup>

Melt compounding involves dispersion of clay in a polymer melt. This is only possible for polymers that have a melt or glass temperature below the decomposition temperature. Furthermore, if the clay was modified previously, this organic modifier has to be stable at high temperatures. The polymer melt can be extruded in several forms (e.g. by injection molding) enabling various applications which makes this method interesting for industry.<sup>[52, 55]</sup> However, one disadvantage of this method is that clay is applied in a dry state and thus, remains in band-like aggregates which cannot be disaggregated by shear forces during melt compounding.<sup>[56]</sup>

This problem is overcome in solution blending. Here, a clay dispersion is mixed with a polymer solution in the same solvent.<sup>[57]</sup> Afterwards, the solvent is removed resulting in a nanocomposite. In this method, clay is introduced in dispersion which reduces the amount of band-like aggregates and thus, gives a better dispersion in the polymer matrix later.<sup>[56]</sup>

In general, the interfacial tension between filler and matrix has to be similar to get a good dispersion. If a polymer is water soluble, pristine hydrophilic clay can be used. For example, hectorite polyvinylpyrrolidone (PVP) nanocomposites could be produced by spray coating of a suspension of delaminated NaHec and PVP in water.<sup>[58]</sup> The resulting films consisted of highly ordered Bragg stacks made from the two alternating components. Other examples of

nanocomposites with hydrophilic pristine clays were made with poly (vinyl alcohol),<sup>[59]</sup> glycol chitosan,<sup>[11]</sup> or poly (ethylene glycol).<sup>[60]</sup>

However, a lot of polymers are not water soluble and therefore, clays need to be organophilized to render the surface hydrophobic and to ensure a good compatibility with the matrix. Therefore, inorganic interlayer cations are exchanged against organic cations.<sup>[61]</sup> In commercial organophilic clays, this is often done by quaternary alkyl ammonium compounds containing (hydrogenated) tallow groups.<sup>[62-63]</sup> Furthermore, custom-made modifiers are used in research to improve the compatibility between filler and matrix.<sup>[64]</sup> Modifiers that are chemically similar to the matrix can provide an excellent dispersion of the filler in the matrix resulting in almost no clay stacks.<sup>[65]</sup> If nanocomposites are prepared by *in-situ* polymerization, a strong interaction between clay and polymer can be achieved if clay is modified with an organo-cation which can be polymerized. For example, ammonium compounds with acrylate groups were used for modification.<sup>[66-68]</sup> Moreover, *in-situ* polymerization can be initiated from the clay surface. Therefore, azo-compounds<sup>[69-70]</sup> or peroxides<sup>[71-72]</sup> with one or two cationic ammonium groups were used as modifier. With this method, even controlled polymerizations like atom transfer radical polymerization<sup>[15, 73]</sup> or reversible addition-fragmentation chain transfer polymerization<sup>[74]</sup> are possible.

### 3.2.2 Properties and application of polymer clay nanocomposites

#### *Mechanical reinforcement*

For the reinforcement of polymers by the incorporation of fillers, the mechanics of the filler is of crucial importance. Due to the anisotropic shape of the clay layers, the mechanical properties are anisotropic as well. The in-plane modulus of single NaHec layers was determined by a wrinkling method.<sup>[75]</sup> Therefore, single clay layers were deposited on a stretched substrate. Upon relaxation of the substrate, NaHec formed wrinkles which allowed for the calculation of the in-plane modulus (142 GPa). If NaHec is not present as a single layer but as double layer, the in-plane modulus is increased to 171 GPa.<sup>[76]</sup> Similar values were reported for the in-plane moduli of micas (2:1 layered silicates with non-hydrated cations).<sup>[77-78]</sup> The cross-plane modulus of NaHec is significantly smaller as determined by Brillouin light spectroscopy (25 GPa).<sup>[58]</sup>

Polymers generally exhibit several important mechanical parameters including Young's modulus, tensile strength, elongation at break and toughness. Often, mechanical parameters are determined by a tensile test where a test specimen is stretched applying a constant strain rate.

The Young's modulus  $E$  is then determined by the quotient of the change in tensile stress  $\Delta\sigma$  and the change in strain  $\Delta\varepsilon$  in the linear regime at the beginning of the test:<sup>[79]</sup>

$$E = \frac{\Delta\sigma}{\Delta\varepsilon} \quad (3)$$

Especially the Young's modulus can be improved if clay is used as filler. In polymer clay nanocomposites, the applied stress can be transferred to the filler which has a higher modulus than the matrix. One model to predict the increase in modulus is the Halpin-Tsai-theory (eq. (4)).<sup>[80-81]</sup> Thereby, the modulus of the composite  $E_c$  is dependent on the moduli of filler  $E_f$  and matrix  $E_m$ , the volume fraction of the filler  $\phi$ , its aspect ratio  $\alpha$  and a factor  $\eta$  which is defined in eq. (5).

$$\frac{E_c}{E_m} = \frac{1 + 2 \cdot 0.66 \cdot \alpha \cdot \eta \cdot \phi}{1 - \eta \cdot \phi} \quad (4)$$

$$\eta = \frac{\frac{E_f}{E_m} - 1}{\frac{E_f}{E_m} + 2 \cdot 0.66 \cdot \alpha} \quad (5)$$

From eq. (4), it is clear that the aspect ratio is a crucial factor determining the reinforcement of nanocomposites (Figure 3A). For example, at a filler content of 0.05, increasing the aspect ratio from 100 to 20000 increases the modulus of about 20%. Thus, maximizing the aspect ratio by delaminating clay into single layers by repulsive osmotic swelling can achieve the best reinforcement. Furthermore, the relative reinforcement that is possible at a given volume fraction and aspect ratio strongly depends on the modulus of the matrix (Figure 3B). Softer polymers like polyethylene (0.1 – 0.7 GPa<sup>[82]</sup>) can be greater reinforced than stiffer polymers like poly(methyl methacrylate) (PMMA, 2.5 – 3.3 GPa<sup>[82]</sup>).

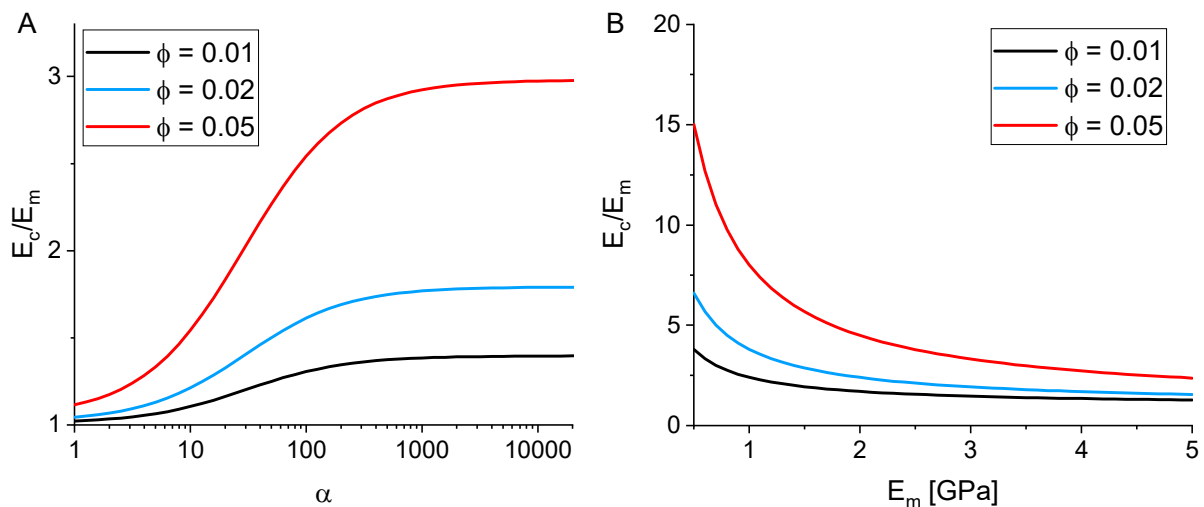


Figure 3: Reinforcement effect of clay in nanocomposites depending on the aspect ratio (A) and the matrix modulus (B) according to Halpin-Tsai ( $E_f = 142$  GPa; A:  $E_m = 3.5$  GPa; B:  $\alpha = 20000$ ).

In the early works of Toyota, tensile strength and modulus of Nylon 6 could be significantly enhanced with only 5 wt.-% montmorillonite.<sup>[50]</sup> However, these composites suffered from reduced elongation at break. For brittle polymer matrices like PMMA, the incorporation of nanofillers usually results in an increased modulus, but in decreased values for strength, strain and toughness.<sup>[83-84]</sup> However, the incorporation of a synthetic mica-like clay with a tailored surface modification led to PMMA nanocomposites with increased modulus and toughness while preserving the tensile strength which was not possible with a commercial organoclay.<sup>[85]</sup> Thus, it is obvious that the surface modification and consequently the dispersion quality is crucial for successfully improving the mechanical properties of polymer clay nanocomposites.

#### *Barrier properties*

Another important benefit of polymer clay nanocomposites is an improved gas barrier. The key parameter that describes the barrier properties of a material is the permeability  $P$ . In general, the permeability can be expressed by the product of diffusivity  $D$  and solubility  $S$ :<sup>[86]</sup>

$$P = D \cdot S \quad (6)$$

Thus, the higher the solubility of the permeate in the matrix is, the worse the barrier is. The diffusivity can be reduced by the incorporation of clay. Inorganic clay platelets are assumed to be impermeable.<sup>[87]</sup> Nielsen described that the diffusion path for permeate molecules is significantly prolonged by increasing tortuosity (Figure 4A and B).<sup>[88]</sup> One modification of his approach which provides realistic values was made by Cussler (eq. (7)).<sup>[87, 89]</sup>

$$P_{rel} = \frac{P_c}{P_0} = \left( 1 + \mu \frac{\alpha^2 \phi^2}{1 - \phi} \right)^{-1} \quad (7)$$

Here,  $P_{rel}$  is the relative permeability,  $P_c$  and  $P_0$  are the permeability of the composite and the neat matrix polymer, respectively,  $\mu$  is a geometrical factor (4/9 for hexagonal platelets),  $\alpha$  is the aspect ratio and  $\phi$  the volume fraction of the filler. The permeability is mainly dependent on the aspect ratio of the clay platelets and the filler content. Increasing the aspect ratio improves the barrier properties significantly (Figure 4C). Thus, a good dispersion in ideally, single clay sheets in the polymer matrix is crucial.

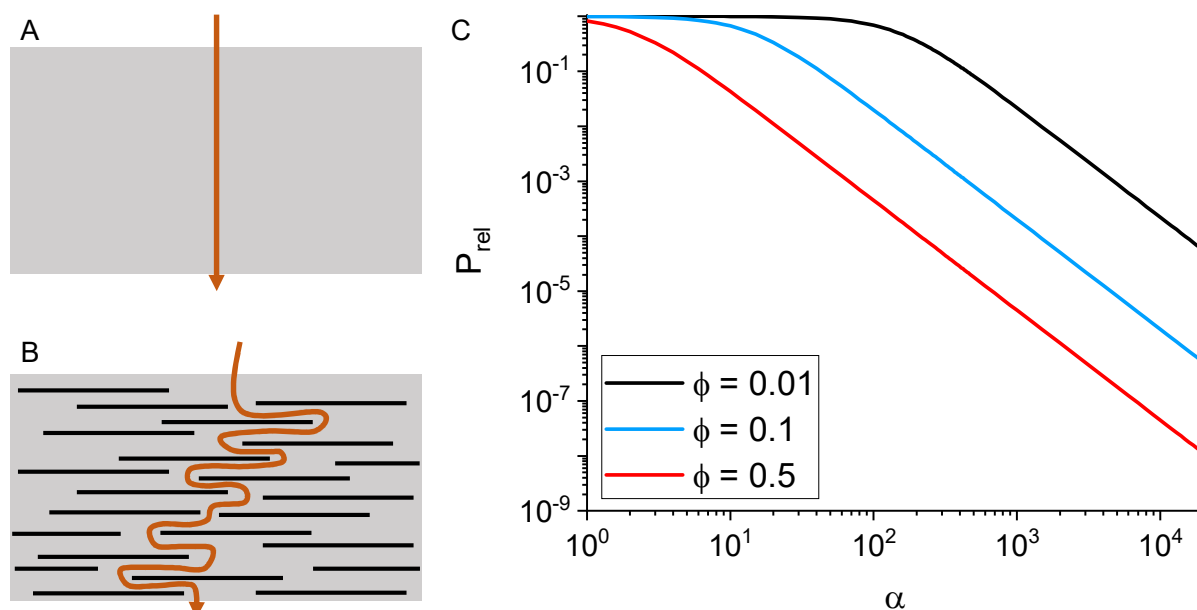


Figure 4: A, B: Diffusion pathways of a permeate through a polymer and a polymer clay nanocomposite, respectively. C: Relative permeability according to Cussler's model in dependency on the aspect ratio and the volume fraction of the platy filler.

Various examples of polymer clay nanocomposite films with superior barrier against water vapor,<sup>[90-91]</sup> oxygen<sup>[12, 92]</sup> or helium<sup>[93-94]</sup> were reported. One important application for barrier films is food packaging.<sup>[62]</sup> A nanocomposite coating of glycol chitosan and NaHec on polylactic acid provided excellent barrier against oxygen and is at the same time biodegradable.<sup>[11]</sup> Another important application is the protection of (opto)electronic devices with films that show high barrier properties against water vapor and oxygen.<sup>[53]</sup>

Not only barrier properties of flat films are important but also of microcapsules. Usually, microcapsules are used to encapsulate active materials like drugs, fragrances, flavors or reactive substances.<sup>[95-96]</sup> This is often done with the purpose of protecting the active material from chemical reactions or to control their release. Similar to flat films, the barrier properties of microcapsules can be enhanced by the incorporation of clay.<sup>[97-99]</sup> For example, poly(urea formaldehyde) microcapsules showed sustained release of dimethyl phthalate with montmorillonite as filler.<sup>[98]</sup> This observation is attributed to the fact that clay can block pores in the capsule wall but also to the increased tortuosity.

### 3.2.3 Polymer nanocomposite foams

In general, foams are materials in which a gas is dispersed in a solid or liquid matrix.<sup>[100]</sup> This chapter focuses on solid polymer foams which means that the gas is dispersed in a polymer matrix. Polymer foams find applications in many areas like lightweight constructions, insulation or cushioning.<sup>[1]</sup> However, they often suffer from bad flame retardancy or bad mechanical properties. Solid foams are generally divided into two groups: closed-cell foams and open-cell foams (sometimes also called sponges or porous solids).<sup>[101]</sup> In closed-cell polymer foams, the cells are separated from each other by polymer walls. This makes these foams useful for thermal insulation.<sup>[1]</sup> In contrast to that, cells in open-cell foams are interconnected with each other. Therefore, these foams find applications in sound insulation. Furthermore, they can absorb liquids as their pores are accessible.<sup>[102]</sup>

For many applications, for instance cushioning, the compression properties of foams are decisive. These are often measured by compressing a test specimen by a constant strain rate. Analogous to the Young's (tensile) modulus, the compression modulus is determined by the quotient of the change in compression stress  $\Delta\sigma$  and the change in strain  $\Delta\varepsilon$  in the linear regime at the beginning of the test (eq. (3), Figure 5). Another key parameter is the yield stress or elastic collapse  $\sigma_{YS}$  where the struts begin to buckle which results in a plateau of the stress-strain curve (Figure 5). The curve rises again when the foam is densified.<sup>[101]</sup>

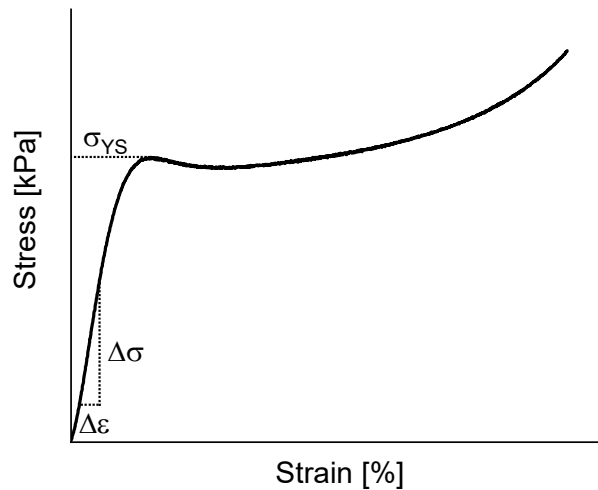


Figure 5: Exemplary stress strain curve of an elastomeric foam upon compression.

One of the most important parameters determining the foam mechanics is the relative density  $\rho_{rel}$  which can be calculated by dividing the apparent foam density  $\rho$  by the density of the corresponding solid bulk polymer  $\rho_s$ :<sup>[101]</sup>

$$\rho_{rel} = \frac{\rho}{\rho_s} \quad (8)$$

Several attempts have been made to find a relationship between the relative density and the foam mechanics. One of the simplest models to calculate the compression modulus and the elastic collapse of elastomeric foams (eq. (9) and (10)) was made by Gibson and Ashby.<sup>[101]</sup> Here,  $E$  and  $E_s$  are the moduli of the foam and the solid bulk polymer, respectively.

$$\frac{E}{E_s} = \rho_{rel}^2 \quad (9)$$

$$\frac{\sigma_{YS}}{E_s} = 0.05 \cdot \rho_{rel}^2 \quad (10)$$

In these equations, it is assumed that the foam mechanics are solely determined by the foam density and the polymer material. Concomitantly, the foam morphology is uniform and has no influence on the mechanics. However, simulations showed that a foam is weaker if irregularities are observed.<sup>[103-104]</sup>

Polymer foams can be made in several ways. One of the most important class of polymer foams are polyurethanes. They are made by polyaddition of diisocyanates and diols. If water is added, it reacts with isocyanates producing carbon dioxide which foams the polymer.<sup>[102]</sup> Incorporation of clay in such foams has two opposing effects. On the one hand, clay acts as nucleation agent which promotes smaller cells and on the other hand, adsorbed water acts as (additional) blowing agent which leads to larger cells.<sup>[105]</sup> While for small clay amounts the nucleation effect prevails, the effect of adsorbed water dominates for larger amounts.<sup>[106]</sup> Moreover, clay could improve the compressive properties of the foams.<sup>[105-107]</sup>

Furthermore, polymer foams can be made by addition of a blowing agent like pentane or carbon dioxide to a polymer melt.<sup>[102]</sup> In this way, a large variety of polymers can be foamed. Again, clay in such foams can reduce the cell size.<sup>[108-109]</sup> Furthermore, the mechanical properties and flame retardancy could be improved.<sup>[110]</sup>

Another attractive way to produce polymer foams is the use of high internal phase emulsions (HIPE) as templates.<sup>[111]</sup> In general, emulsions consist of immiscible liquids (usually water and oil) and (at least) one liquid is dispersed as droplets in a second continuous liquid (for stabilization of emulsions see chapter 3.3.1). By definition, in a HIPE, the internal phase exceeds 74 vol.-%. This is the volume fraction of close packing spheres. Thus, in a HIPE, the internal phase is present as polydisperse or polyhedral droplets.<sup>[112]</sup> To use HIPEs as templates for foams, the external phase needs to be polymerizable. For the foam preparation, firstly, the internal phase is added to the stirred external phase. To ensure emulsification, the external phase usually contains surfactants. Then, the external phase is polymerized resulting in a wet foam which then, can be washed and dried (Figure 6).<sup>[112]</sup> Polymerization can be initiated from the

internal or the external phase and this is often done by a thermal radical initiator. During polymerization, volume shrinkage of the external phase occurs. This shrinkage is not macroscopic, but internal which leads to ruptures of the thin monomer films between droplets.<sup>[113]</sup> Thus, most foams made via HIPEs are open-cell foams. However, to achieve this, two parameters are important: volume fraction of the internal phase and surfactant concentration, whereas the latter is more significant.<sup>[114]</sup> High surfactant concentrations are necessary to get open-cell foams which is related to thinner monomer films between the droplets.<sup>[112]</sup> Another important factor determining the morphology is the salt concentration in the internal aqueous phase. Higher salt concentrations produce smaller cells.<sup>[115]</sup> Moreover, higher stirring speeds also reduce the cell size.<sup>[116-117]</sup> Foams based on HIPEs can be made from oil-in-water or water-in-oil emulsions. For water-in-oil emulsions, the oil phase often consists of styrene as monomer and divinylbenzene as cross-linker.<sup>[112]</sup> However, (meth)acrylates and other monomers can also be used.<sup>[118-120]</sup>

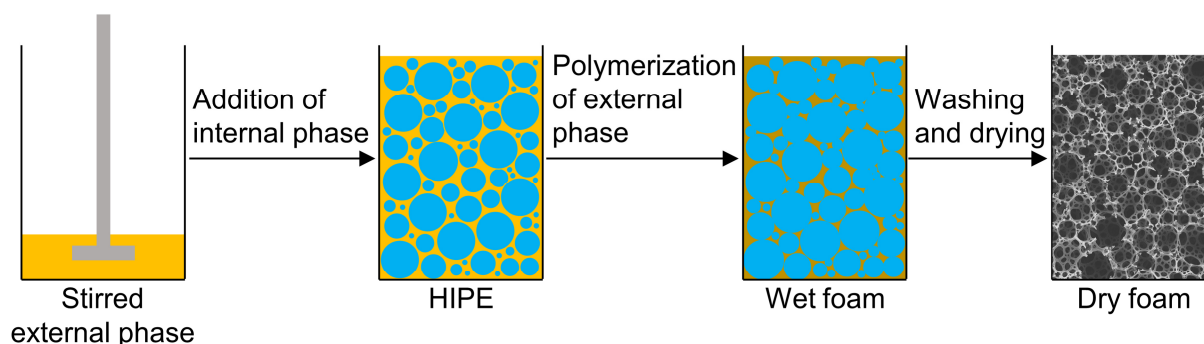


Figure 6: Scheme of the preparation of foams based on HIPEs: To the stirred oil phase, the aqueous phase is added resulting in a HIPE, then the oil phase is polymerized and the resulting foam is washed and dried.

The properties of foams based on HIPEs can be adjusted in several ways which makes them useful for many applications like filtration media, catalyst supports or absorbent materials.<sup>[121-124]</sup> One way is the application of monomers with functional groups followed by post-modification of the foam. For instance, monomers with amino groups can be used to graft poly peptides to the foam. These foams have a pH-sensitive hydrophilicity and can be used for bioconjugations.<sup>[125]</sup> Another way to adjust foam properties is the incorporation of fillers. Silica nanoparticles can significantly enhance the compression modulus and the crush strength of foams.<sup>[126]</sup>

Nanoparticles cannot only be used for reinforcement but also as Pickering emulsifiers (chapter 3.3.1) for the HIPE.<sup>[123, 127]</sup> However, open-cell foams are difficult to realize when nanoparticles are the only emulsifier.<sup>[128]</sup> Nanoparticles at the water-oil-interface act like a barrier preventing the thin monomer films to rupture. This can be avoided by using an additional molecular surfactant.<sup>[129]</sup>

As clay is able to reinforce bulk polymers, it is also applied in foams based on HIPEs to improve the mechanical properties. Therefore, clay can be dispersed in the internal or in the external (monomer) phase. For the latter case, the polymerization of the HIPE can be considered as *in-situ* polymerization (chapter 3.2.1).

Applying a commercial organophilized montmorillonite in foams made from styrene, divinylbenzene and acrylonitrile resulted in smaller cell sizes indicating that clay can act as co-surfactant.<sup>[130]</sup> However, for most composite foams, the Young's modulus was decreased compared to the unfilled foam. A decreasing cell size was not only found for organophilized montmorillonite, but also for sodium montmorillonite added in the aqueous phase of water-in-oil HIPEs.<sup>[120, 131]</sup>

As mentioned in chapter 3.2.1, a stronger binding between clay and matrix can be achieved by modifying the clay surface with a reactive compound. These clay materials are able to improve foam mechanics and can lead to smaller cell sizes.<sup>[132-133]</sup> Lépine et al. modified montmorillonite with an ammonium compound bearing a vinylbenzyl group.<sup>[134]</sup> This clay material was able to significantly increase the Young's modulus of polystyrene foams. In contrast, sodium montmorillonite applied through the aqueous phase had no impact on the foam properties.

In summary, applying clay in nanocomposite foams based on HIPEs to improve its mechanics has some crucial factors. To ensure a good dispersion of clay in the monomer and later in the polymer matrix, appropriate modification is of great importance. Furthermore, there are two ways in which clay can affect the foam mechanics. On the one hand, clay can reinforce the polymer similar to a Halpin-Tsai mechanism. On the other hand, a co-surfactant effect of clay cannot be ruled out. This can change the foam morphology which itself has a large impact on the mechanical properties.<sup>[103, 135]</sup>

### 3.3 Pickering emulsions

#### 3.3.1 General aspects of Pickering emulsions

Emulsions are dispersions of at least two immiscible liquids (usually water and oil) and find many applications in daily life as detergents, cosmetics or in the textile industry.<sup>[136]</sup> In an emulsion, the internal phase is dispersed as droplets in the external continuous phase. To stabilize these droplets, often molecular surfactants are used. Such molecules exhibit a hydrophilic and a hydrophobic part which allows them to mediate between water and oil phase. However, the surfactants are not fixed at the water-oil-interface but they are moving between different droplets.<sup>[100]</sup>

For more than 100 years, it is known, that not only molecular surfactants are able to adsorb at a water-oil-interface, but also solid particles.<sup>[137]</sup> Particle stabilized emulsions are named after Spencer U. Pickering who published the first paper on this topic.<sup>[138]</sup> To obtain stable Pickering emulsions, parameters like the size and shape of the particles and their wettability are important. The latter can be expressed by the contact angle  $\theta$ . (Figure 7A).<sup>[100]</sup>

Driving force for particles to adsorb at an interface is the reduction of interfacial tension. Concomitantly, moving a particle with radius  $R$  from the interface (Figure 7A) completely into one phase (e.g. water, Figure 7B) costs energy. This process generates new interfaces between water and particle ( $A_{WP}$ ) and between oil and water ( $A_{OW}$ ). Simultaneously, the interface between oil and particle ( $A_{OP}$ ) is displaced (Figure 7A).

$$A_{WP} = 2\pi R^2 (1 - \cos\theta) \quad (11)$$

$$A_{OW} = \pi R^2 (1 - \cos^2\theta) \quad (12)$$

$$A_{OP} = 2\pi R^2 (1 - \cos\theta) \quad (13)$$

Neglecting gravitational forces, the energy difference can be calculated as follows.<sup>[100]</sup>

$$\begin{aligned} \Delta G &= A_{OW}\gamma_{OW} + A_{WP}\gamma_{WP} - A_{OP}\gamma_{OP} \\ &= R^2\pi\gamma_{OW} (1 - \cos\theta)^2 \end{aligned} \quad (14)$$

Here,  $\gamma$  is the interfacial tension between two phases (oil, water or particle). Analogous, the energy that is necessary to detach a particle from the interface into the oil phase is determined by eq. (15).

$$\Delta G = R^2\pi\gamma_{OW} (1 + \cos\theta)^2 \quad (15)$$

From eq. (14) and (15) it is clear, that the wettability of the particles is essential for stabilizing an interface. If the particles are very hydrophilic ( $\theta \ll 90^\circ$ ) or very hydrophobic ( $\theta \gg 90^\circ$ ), they can easily be removed from the interface and will be immersed in the water or in the oil phase, respectively (Figure 7C). Thus, an intermediate wettability with a contact angle around  $90^\circ$  is

desired for stabilizing Pickering emulsions. Then, the energy that is required to remove particles from the interface is usually orders of magnitude larger than the thermal energy.<sup>[139]</sup> Consequently, particles located at a water-oil-interface can be assumed to be irreversibly trapped and coalescence is prevented much better than in emulsions stabilized by molecular surfactants.<sup>[140]</sup>

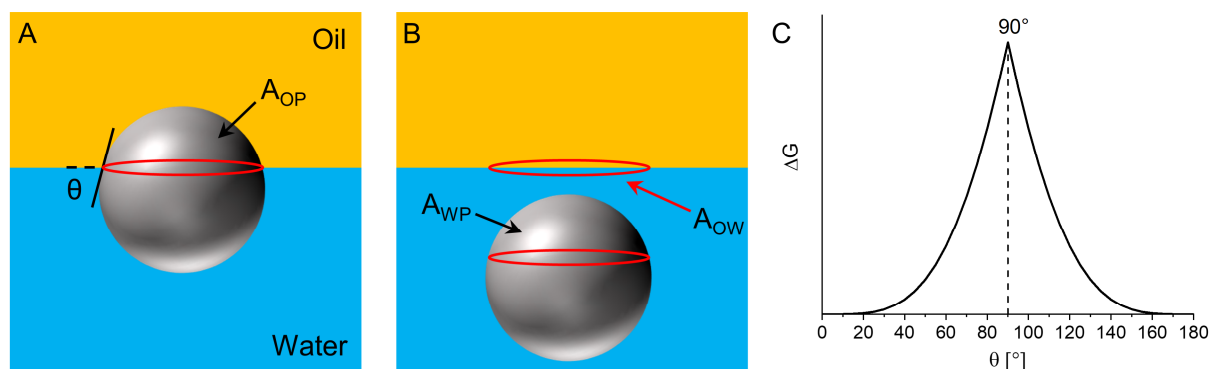


Figure 7: A: Particle at the water-oil-interface. B: Particle completely immersed in the water phase. C: Energy which is necessary to remove a particle from the interface in dependency on the contact angle  $\theta$ .

The wettability of the particles not only determines their stability at the interface but also which kind of emulsion is formed.<sup>[139]</sup> If particles are slightly hydrophilic ( $\theta < 90^\circ$ ), water is the continuous phase (Figure 8A). Contrary, if particles are better wetted by the oil phase ( $\theta > 90^\circ$ ), a water-in-oil emulsion is formed (Figure 8B).

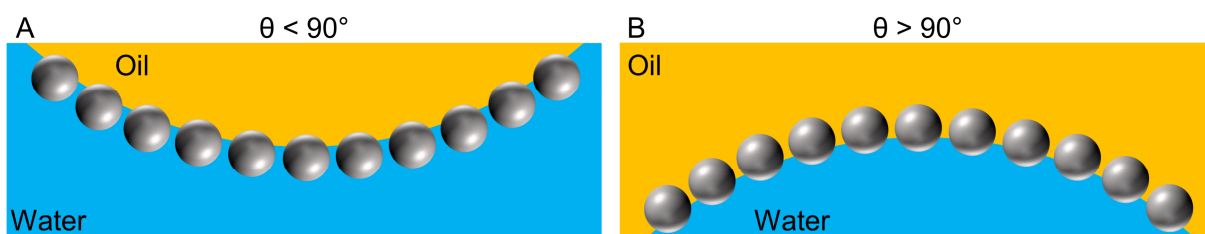


Figure 8: Slightly hydrophilic particles stabilizing an oil-in-water emulsion (A) and slightly hydrophobic particles stabilizing a water-in-oil emulsion (B).

### 3.3.2 Clay Pickering emulsions

Besides spherical particles, two-dimensional particles can also be used to stabilize Pickering emulsions. The most prominent examples for such particles are layered silicates and graphene oxides.<sup>[141]</sup> Contrary to isotropic, spherical particles (Figure 9A), two-dimensional, anisotropic particles can theoretically have different orientations at the interface. However, due to their large aspect ratio, the energetically favored orientation is parallel to the interface (Figure 9B).<sup>[142]</sup> Neglecting the edges, the energy required to detach a platelet (with the surface area  $A$ ) from the interface is given by eq. (16).<sup>[143]</sup>

$$\Delta G = A\gamma_{OW} (1 \pm \cos\theta) \quad (16)$$

Analogous to spherical particles, the stability of platelets at an interface is strongly dependent on the wettability. Again, a contact angle close to  $90^\circ$  is desired. Due to their parallel alignment to the interface, platelets (or discs like in Figure 9B) desorb less likely from the interface than spheres with the same diameter (Figure 9C).<sup>[141, 144]</sup>

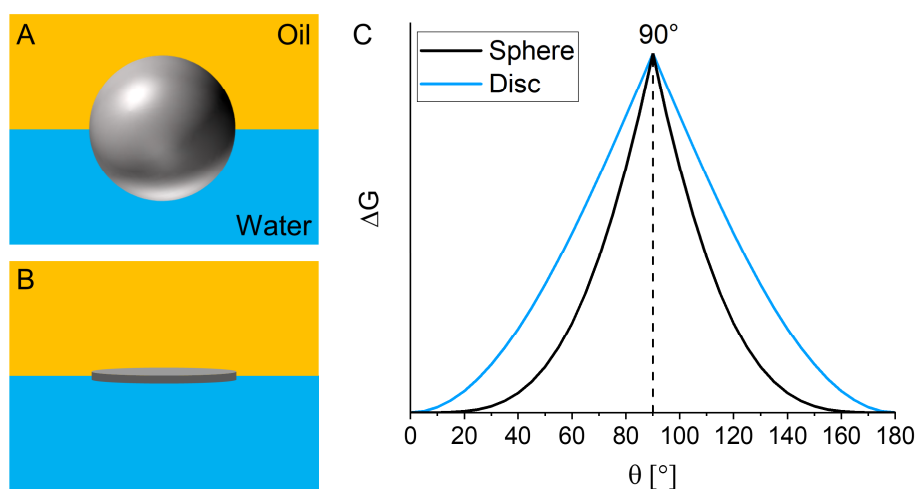


Figure 9: Sphere (A) and disc (B) with the same diameter located at the interface and the corresponding energy (C) that is necessary to detach them from the surface.

Pure layered silicates are very hydrophilic and are not able to stabilize emulsions. However, if high salt concentrations are added, the repulsive forces between the layers are screened, the zeta potential is lowered and the clay layers aggregate. Ashby and Binks found that concentrations of 0.1 M NaCl and 1.5 – 3.5 wt.-% Laponite (a synthetic smectite with a diameter of about 30 nm) were necessary to produce stable toluene-in-water emulsions.<sup>[145]</sup> At these concentrations, Laponite effectively covered the interface and prevents coalescence. However, a further increase of the NaCl concentration (0.5 M) resulted in larger clay aggregates which were less efficient in adsorbing at the interface and the emulsions underwent coalescence.<sup>[146]</sup> The oil droplet size was independent of the clay concentration but highly dependent on the oil volume fraction.<sup>[145]</sup> Whereas these emulsions were made with aggregated clay, stable

emulsions could also be produced from clay in a gel-like state. In this state, clay particles form interconnected networks in water. Then, the oil droplets are not only stabilized by clay at the interface but also by the incorporation in the network.<sup>[147]</sup>

Accumulation of clay at a water-oil-interface cannot only be achieved by increasing salt concentration but also by adding nonionic co-surfactants like glycerol monostearate or deca (ethylene glycol) hexadecyl ether.<sup>[148]</sup> Another option to produce clay Pickering emulsions involves modified clay platelets. The wettability of the anionic clay surface can be adjusted by an organic cation. The choice and the amount of modifier plays a significant role on the type of emulsion. This can be seen particularly when modifying montmorillonite with cetyltrimethylammonium bromide (CTAB).<sup>[149]</sup> Adsorption of small amounts of CTAB renders the montmorillonite surface slightly hydrophobic which allows the stabilization of oil-in-water emulsions. Increasing the amount of CTAB increases the surface hydrophobicity which results in a phase inversion to water-in-oil emulsions. When so much CTAB is added that it forms bilayers on the clay surface, the particles become hydrophilic and the emulsion is again oil-in-water type.

Compared with CTAB, more stable oil-in-water emulsions could be made with a more hydrophilic quaternary ammonium compound.<sup>[150]</sup> However, a salt concentration of at least 0.01 M NaCl was necessary to avoid phase separation. Similar to the Laponite stabilized emulsions, salt is necessary to screen repulsive forces and triggers clay aggregation at the interface. Furthermore, in these emulsions it was shown that clay stacks of four layers lie parallel to the interface whereas a significant amount of clay is still dispersed in the continuous water phase. That the dispersion of modified clay and its network formation in the continuous phase can have a benefit on the emulsion stability was also shown when montmorillonite was modified with short chain amines.<sup>[151]</sup>

#### 3.3.3 Encapsulation in Pickering emulsions

One possible application of Pickering emulsions is encapsulation. For instance, encapsulation of volatile substances requires sustained release. It was shown that volatile oils (present as droplet phase) evaporated slower from Pickering emulsions than from conventional emulsions.<sup>[152]</sup> The particles at the interface created a barrier for the oil. This barrier could be further improved if the particles at the interface were compressed to a dense film.

Furthermore, two-dimensional graphene oxide as Pickering emulsifier showed better barrier properties compared to spherical particles.<sup>[144]</sup> Multiple layers of graphene oxide generate tortuosity comparable to nanocomposite films (chapter 3.2.2).

Moreover, Pickering emulsions can be used to prepare colloidosomes by connecting the particles at the interface resulting in a capsule.<sup>[153]</sup> This can be done for example by chemical cross-linking, thermal annealing or physical complexation.<sup>[153-154]</sup> Colloidosomes can be used to encapsulate for instance dyes, drugs or enzymes.<sup>[155-157]</sup> Montmorillonite and Laponite are both able to stabilize oil-in-water emulsions when they were modified with poly(ethylene imine) (PEI). Subsequent crosslinking of PEI with a diglycidyl ether provided the formation of colloidosomes.<sup>[158-159]</sup> However, dye release studies showed that the resulting shell was disordered and thus, highly permeable.<sup>[159]</sup>

### 3.4 Scope of the thesis

Applying two-dimensional fillers in polymers offers beneficial properties like improvement in barrier or mechanics. Synthetic NaHec possesses superior charge homogeneity which allows for osmotic swelling in water resulting in single 1 nm thick layers. Thus, it has a high aspect ratio which makes NaHec an ideal filler in composites for various applications. Osmotic swelling of NaHec is only known in water or aqueous solutions of organic solvents with high water content (> 35 vol.-%). However, many polymers are not soluble in such mixtures. To enable the fabrication of polymer clay nanocomposites without modifying the clay surface, polymer and clay need to be dispersed in the same solvent system. Consequently, there is a demand for solvent systems that contain as less water as possible but still offer osmotic swelling. Such systems were investigated in chapter 6.1. Here, three solvents which are completely miscible were combined.

Moreover, the combination of immiscible solvents also provides interesting applications. For example, HIPEs with a polymerizable continuous phase can be used as templates for polymer foams. The mechanical properties of polymer foams with a certain density mainly depend on two aspects: the mechanics of the foam material and the foam morphology. Thus, the dispersion of clay in the continuous phase of a HIPE can in principle have different impacts on the resulting foam. On the one hand, clay can enhance the mechanical properties of the strut material. On the other hand, clay is a surface active material and can influence the emulsion stability which in turn can affect the foam morphology. In chapter 6.2, the influence of two clay fillers on the mechanics and the morphology of foams was investigated. Therefore, a synthetic hectorite which was modified with a custom-made organo-cation was compared with a commercial organophilized montmorillonite.

Another important application of emulsions are fragrance-in-water emulsions. Thereby, unselective release of different fragrances is desirable to maintain the fragrance composition. Since clays are surface active materials, they can be used to stabilize emulsions by a Pickering effect. Furthermore, clay significantly improves the barrier properties of polymer films which makes them suitable candidates for encapsulation of volatile substances. Thus, clay was fixed with polycationic PEI at the interface to produce hybrid capsules. The release of a fragrance mixture thereof was explored in chapter 6.3.



## 4 Synopsis

This thesis contains three publications dealing with hectorite in different liquid mixtures which can be used for the fabrication of nanocomposites (Figure 10).

For many applications, delaminated layers with a maximized aspect ratio are important. For an easy fabrication of nanocomposites, delamination of NaHec in a solvent that also dissolves the desired (hydrophobic) polymer is preferable. One step in this direction is described in chapter 6.1. Here, the swelling of NaHec in different ternary mixtures was investigated looking for compositions with a low water content that allow for osmotic swelling.

In the other two publications, emulsions are used to fabricate nanocomposites. In chapter 6.2, a high internal water-in-oil emulsion was used as template to synthesize polymer foams. Modified hectorite was applied as filler to enhance the mechanical properties. Furthermore, its influence on the foam morphology was investigated.

In chapter 6.3, the Pickering effect of hectorite layers was used to stabilize fragrance-in-water emulsions. NaHec and PEI were combined at the interface to form hybrid capsules. The release of volatile substances from these capsules was investigated.

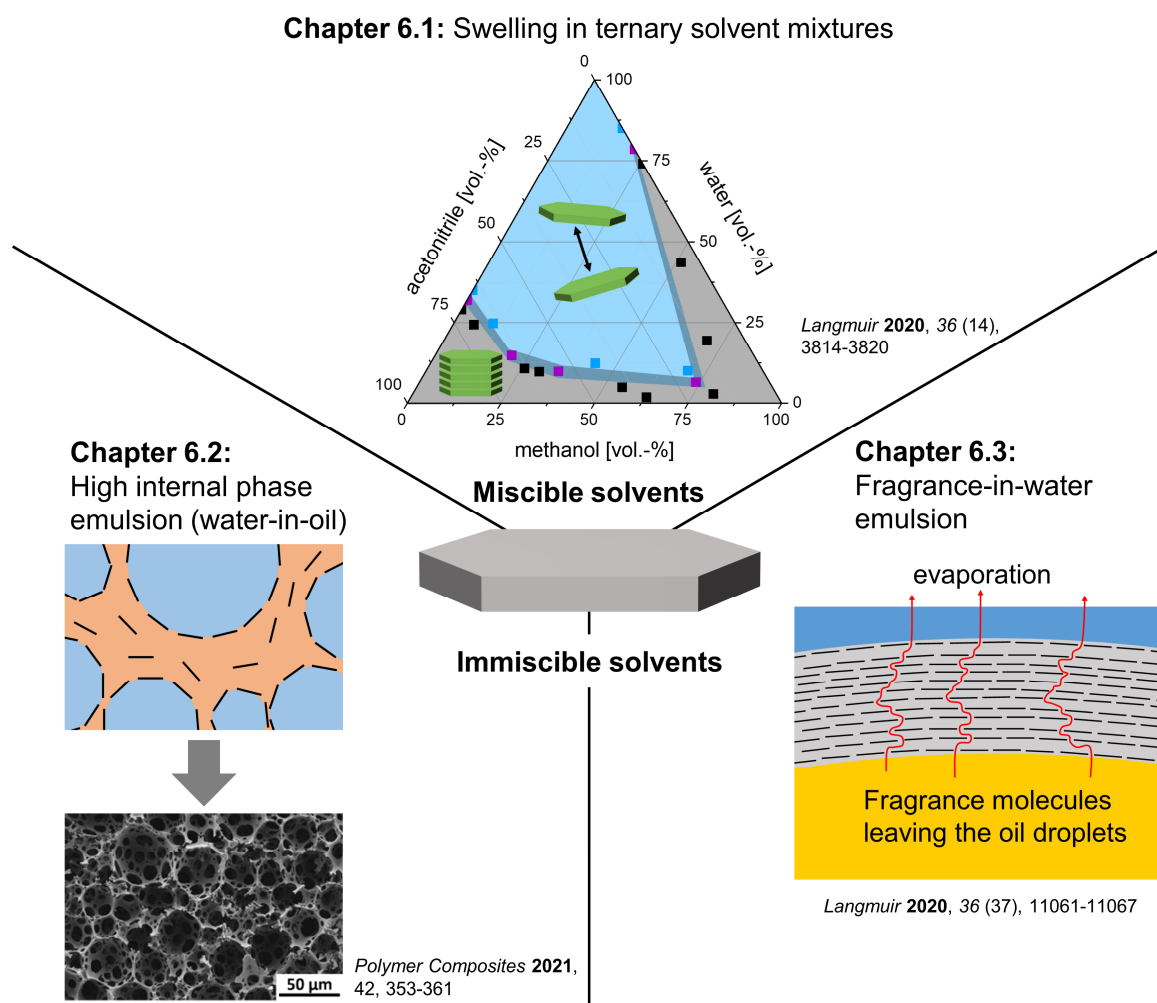


Figure 10: Schematic representation of the three topics of this thesis.

#### 4.1 Swelling of sodium hectorite in ternary solvent mixtures

For many applications of polymer clay nanocomposites, clay with a high aspect ratio is of great importance. NaHec spontaneously delaminates in water by osmotic swelling resulting in nanoplatelets with an aspect ratio of about 20000. This allows for an easy synthesis of nanocomposites consisting of water soluble polymers with perfectly delaminated hectorite platelets. However, many polymers are not water soluble which demands for delamination by osmotic swelling in organic media or their aqueous mixtures.

Swelling of NaHec in three different ternary mixtures was investigated. Therefore, NaHec was swollen in defined mixtures of three solvents for five days to reach equilibrium. Gel-like samples were further analyzed by SAXS to prove delamination. Samples with sediments were analyzed by X-ray diffraction to prove for crystalline swelling.

The first ternary mixture consisted of methanol, water and acetonitrile. In previous studies, it was shown that NaHec swells osmotically in aqueous acetonitrile up to 65 vol.-% acetonitrile (chapter 3.1.3). For higher acetonitrile contents, only crystalline swelling could be observed. In aqueous methanol, only 15 vol.-% methanol was allowed to achieve osmotic swelling. In ternary mixtures, less water was necessary for osmotic swelling of NaHec (Figure 11A). The lowest water content of 10 vol.-% was found at 70 vol.-% methanol and 20 vol.-% acetonitrile. Unexpectedly, this composition contains more methanol than acetonitrile although methanol needs more water in binary aqueous mixtures than acetonitrile to set in osmotic swelling.

In the next mixture, ethylene glycol was used instead of methanol as it is well-known for its intercalation in smectites (chapter 3.1.3). In aqueous ethylene glycol less water was necessary for osmotic swelling compared with aqueous methanol. Again, in a ternary mixture with acetonitrile, less water was necessary for osmotic swelling compared to the corresponding binary aqueous mixtures (Figure 11B). However, applying ethylene glycol-water-acetonitrile, the lowest water content was higher (17 vol.-%) than in the mixture of methanol-water-acetonitrile.

In a third mixture, glycerol carbonate was used in combination with water and methanol. Glycerol carbonate is not only a solvent but also a potential monomer which can be polymerized. This ternary mixture exhibited the largest area of osmotic swelling in the phase diagram (Figure 11C). Two mixtures were found that allowed for osmotic swelling without any water added. Only the interlayer water applied through the 1 WL hydrate was present.

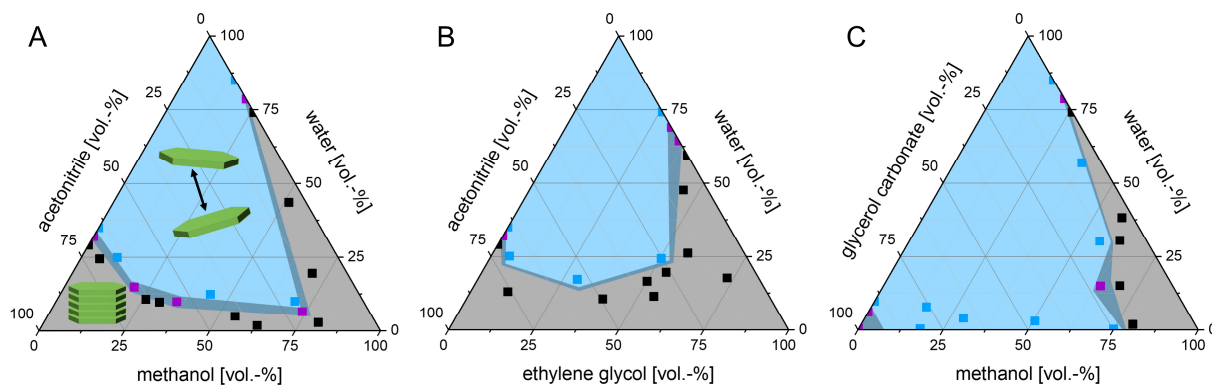


Figure 11: Phase diagrams of NaHec swollen in different ternary solvent mixtures (A: methanol-water-acetonitrile, B: ethylene glycol-water-acetonitrile, C: methanol-water-glycerol carbonate). Black: crystalline swollen, purple: crystalline and osmotically swollen NaHec coexist, blue: osmotically swollen. (Reprinted with permission from reference<sup>[160]</sup>. Copyright (2020) American Chemical Society.)

In literature, several attempts were made to explain swelling of clays with organic molecules (chapter 3.1.3). However, parameters like Hildebrand solubility parameter, relative permittivity, or Gutmann donor number showed no correlation with the minimum water content that was necessary for osmotic swelling in binary mixtures of water with acetonitrile, methanol, ethylene glycol or glycerol carbonate. Indeed, a correlation with the dipole moment was found: less water was necessary if the dipole moment of the organic solvent was larger. However, this correlation could not be transferred to ternary systems.

Furthermore, a quantitative study of the swelling in one exemplary solvent mixture (44 vol.-% methanol, 12 vol.-% water, 44 vol.-% acetonitrile) was done. NaHec was osmotically swollen in this mixture at different volume ratios. The swelling behavior in this mixture was similar to the swelling in pure water (chapter 3.1.2) showing two regimes. At high NaHec contents ( $\phi > 0.05$ ), the distance between adjacent platelets scaled with  $\phi^{-1}$  indicating quantitative osmotic swelling. For  $\phi < 0.05$ , the distance scaled with  $\phi^{-0.5}$ .

The results showed that osmotic swelling of NaHec is possible with only small water contents applying ternary solvent mixtures. Although the swelling behavior in ternary mixtures could not be explained, the reduction of water amount that is necessary for osmotic swelling may ease the synthesis of nanocomposites with polymers that are not soluble in water.

## 4.2 Polymer clay nanocomposite foams made via high internal phase emulsions

Layered silicates are often used as fillers in polymer clay nanocomposites to enhance the mechanical properties. One interesting material class are polymer foams made from high internal phase emulsions (HIPE). Therefore, the continuous phase of the emulsion consists of polymerizable molecules and accounts for less than 26 vol.-%. In this work, water-in-oil emulsions were made where the oil phase contained 2-ethylhexyl acrylate and ethylene glycol dimethacrylate. Polymerization of the emulsion yielded open-cell foams with relative densities between 4 and 7 %. Compression tests showed that the moduli of these foams strongly depended on the foam density ( $E \sim \rho_{rel}^{3.2}$ ). For the preparation of nanocomposites, hectorite platelets with a diameter of 0.2  $\mu\text{m}$  were modified with a custom-made oligomeric organocation (poly (2-ethyl hexyl methacrylate), PEHMA) which was similar to one of the monomers. The modified hectorite (HecPEHMA) was transferred from tetrahydrofuran to the oil phase without drying to avoid aggregation of the platelets. HecPEHMA was applied at 0.5 – 2 wt.-% and in all cases, open-cell foams could be achieved. With 0.5 % HecPEHMA, foam mechanics did not change compared to the unfilled foams. However, with only 1 and 2 % HecPEHMA, the compression moduli could be significantly enhanced (Figure 12). Like in the unfilled foams, the mechanics of these foams strongly depended on their relative densities. However, the dependency changed to  $E \sim \rho_{rel}^{1.4-1.6}$ . This resulted in a more pronounced strengthening at lower relative densities. The compression moduli of foams with a relative density of about 4 % could be doubled with only 1 % HecPEHMA and increased up to four times with 2 % HecPEHMA. This increase is significantly larger than what would be expected applying Halpin-Tsai theory which indicates that it is not or not only due to a reinforcement of the struts.

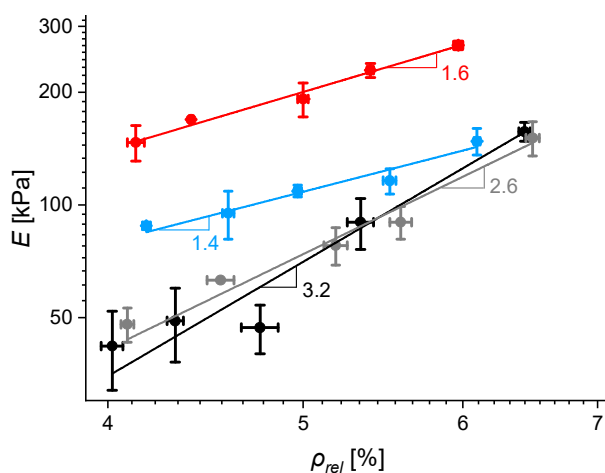


Figure 12: Compression moduli depending on the relative density (black: no filler; grey: 0.5 % HecPEHMA, blue: 1 % HecPEHMA, red: 2 % HecPEHMA; numbers next to the triangles represent slopes in double-log plot). (Reprinted with permission from reference<sup>[161]</sup>. Copyright (2020) John Wiley and Sons.)

In addition to HecPEHMA, a commercial organophilized montmorillonite (O-MMT) with a similar size was used as filler for comparison. However, applying 1 % O-MMT did not change the mechanics and 2 % O-MMT led to a significant weakening of the foams. The difference between the two fillers may be due to their different surface modification (custom-made oligomeric organo-cation *vs.* alkyl ammonium).

To investigate the strengthening mechanism of HecPEHMA in the foams, the influence of HecPEHMA on bulk polymer plates of the same composition was investigated. Furthermore, a detailed analysis of the foam structures was made.

The mechanics of polymer plates without filler and with 2 % HecPEHMA were compared. In tensile tests, the nanocomposite showed lower values of tensile strength, strain at break and Young's modulus compared to the unfilled polymer. This indicates that HecPEHMA is not able to reinforce the polymer struts in the foams and foam strengthening has to have another reason. In general, the foam structure can crucially influence the mechanics. Therefore, scanning electron microscopy (SEM) images of an unfilled foam and a foam with 2 % HecPEHMA were compared. It was shown that the composite foam had larger cells, larger windows (between the cells) and thicker struts. Furthermore, the unfilled foam had a more inconsistent structure. This means that there were different regions with locally different densities (Figure 13A). In contrast to that, the foam with 2 % HecPEHMA had a more consistent structure (Figure 13B).

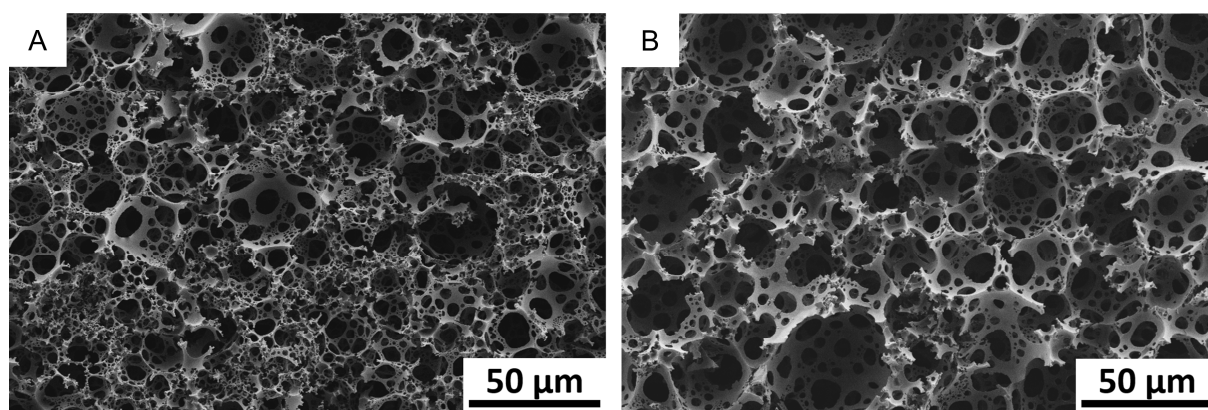


Figure 13: SEM images of an unfilled foam (A) and a foam with 2 % HecPEHMA (B). (Reprinted with permission from reference<sup>[161]</sup>. Copyright (2020) John Wiley and Sons.)

From these results, it was concluded that the increase in foam mechanics was due to an improvement in foam structure. This is most likely caused by a Pickering effect of HecPEHMA. Clay platelets can lie at the oil-water-interface enhancing the emulsion stability. The custom-made modifier is chemically similar to the monomers and thus may provide better Pickering efficiency than O-MMT.

### 4.3 Sustained release of fragrances from clay Pickering emulsions

Emulsions of volatile fragrances are important for applications like cosmetics or detergents. For this, the emulsions should encapsulate the fragrances and provide sustained release. As polymer clay nanocomposite films offer excellent barriers against gas molecules (chapter 3.2.2), it looks encouraging to use clay for the encapsulation of fragrances. Pure hectorite (Hec) is too hydrophilic to stabilize emulsions. Therefore, it was modified with poly(ethylene imine) (PEI). As the polycationic PEI would instantly lead to uncontrolled flocculation of Hec, the modification was done quasi *in-situ*. Therefore, Hec was dispersed in water and mixed with the oil phase. During mixing, a PEI solution was added to fix Hec as multilayer stacks at the interface. Whereas the ratio between Hec and oil phase was constant, the mass ratio between PEI and Hec was varied between 0.5 and 1.25. For comparison, an emulsion only with PEI was made. All Hec/PEI Pickering emulsions showed good stability as no creaming or phase separation was observed. Furthermore, the droplet size did not change within two weeks. The emulsions with PEI:Hec = 0.75 – 1.25 all had similar droplet diameters of 18 – 23  $\mu\text{m}$  whereas PEI:Hec = 0.5 resulted in larger droplets with a mean diameter of 58  $\mu\text{m}$ . Contrary to the Pickering emulsions, the emulsion stabilized only with PEI creamed and a significant amount of larger droplets was observed after two weeks.

To investigate the barrier properties of the Hec/PEI hybrid capsules, a mixture of five fragrances was applied as oil phase. Citronellol has a relatively low vapor pressure and its amount is therefore assumed to be constant. It is used as a reference for the other fragrances (eucalyptol, limonene,  $\alpha$ -pinene and ethyl-2-methylbutyrate). While shaking in an open vial, the composition of the emulsions was determined by  $^1\text{H}$  nuclear magnetic resonance spectroscopy every two days. The fragrances differ in their vapor pressures and in their water solubility. In the emulsion solely stabilized by PEI, all volatile fragrances were released after ten days. Thereby, the release order was determined by the vapor pressure of the individual fragrances. Ethyl-2-methylbutyrate which has the highest vapor pressure was released fastest whereas eucalyptol which has the lowest vapor pressure was released slowest.

In the Pickering emulsions, the vapor pressure was no longer rate determining. Here, the rate determining step was the diffusion of the fragrances through the capsule wall. Hec will provide tortuosity which unselectively retards fragrance diffusion. Thus, the release rate was determined by the solubility of the fragrances in the capsule wall. While PEI rendered the Hec surface slightly more hydrophobic, it was still hydrophilic and could swell with water. Limonene and  $\alpha$ -pinene, which were released slowest from Pickering emulsions, are the least water soluble

fragrances suggesting that they are also the least soluble in the capsule wall. Contrary, the fragrance with the highest water solubility, ethyl-2-methylbutyrate, was released fastest.

The capsule wall consisted of Hec layers with PEI in between. Thus, the lower the amount of PEI, the smaller would be the distance between two adjacent Hec layers. This increased the tortuosity and consequently enhanced the barrier properties. Indeed, the emulsion with the lowest PEI:Hec ratio (0.50) showed the best barrier for all fragrances (Figure 14).

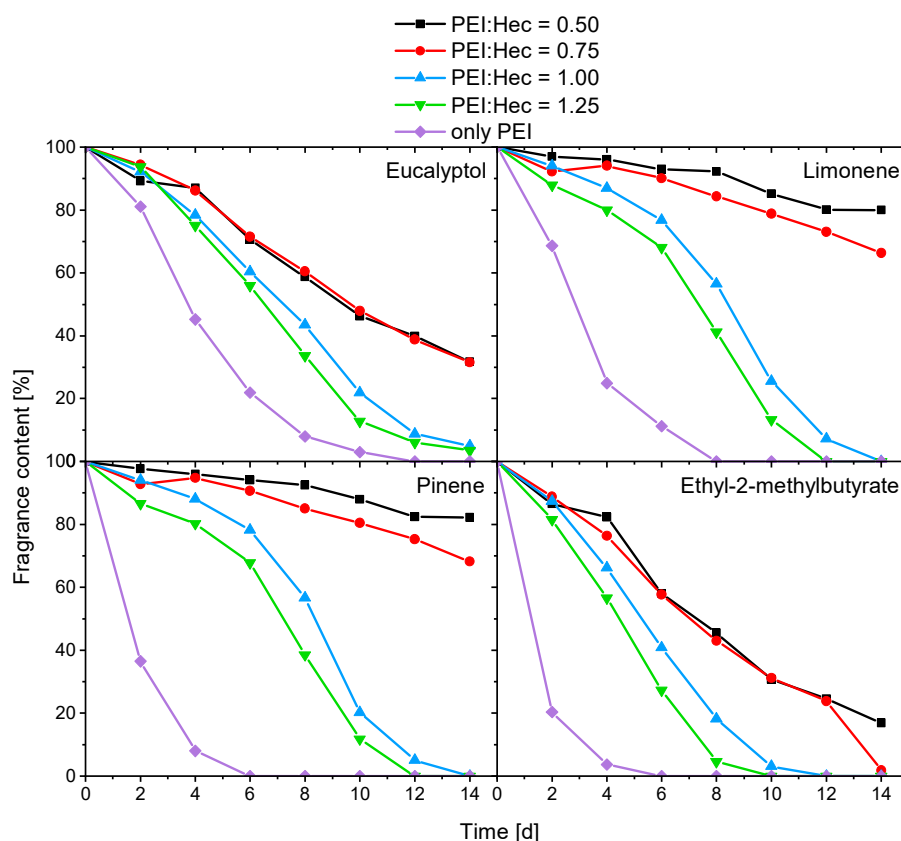


Figure 14: Fragrance release from emulsions with varying ratio of PEI:Hec. (Reprinted with permission from reference<sup>[162]</sup>. Copyright (2020) American Chemical Society.)

In a subsequent step, PEI was cross-linked by polypropylene diglycidyl ether dissolved in the oil phase. The cross-linked emulsion showed good stability and similar droplet sizes as the corresponding non-cross-linked emulsion. Again, the release rates of the fragrances were determined by their solubility in the capsule wall. Furthermore, cross-linking could make an additional contribution to the barrier.

It was shown that the quasi *in-situ* fixing of Hec with PEI at the water-oil-interface resulted in stable fragrance-in-water emulsions. Moreover, the hybrid capsules provided good barrier properties by tortuosity in the wall.



## 5 Literature

- [1] Kaiser, W. *Kunststoffchemie für Ingenieure*. 3 ed.; Carl Hanser Verlag: München, 2011
- [2] Michler, G. H.; Baltá-Calleja, F. J. *Nano- and Micromechanics of Polymers*. Carl Hanser Verlag: München, 2012
- [3] Bundesinstitut für Risikobewertung: DPHP in Spielzeug nachgewiesen: BfR bewertet Risiko des Weichmachers. <https://www.bfr.bund.de/cm/343/dphp-in-spielzeug-nachgewiesen-bfr-bewertet-risiko-des-weichmachers.pdf> (accessed 06.08.2020).
- [4] Verordnung (EU) 2017/227 der Kommission. <https://eur-lex.europa.eu/legal-content/DE/TXT/PDF/?uri=CELEX:32017R0227&from=DE> (accessed 06.08.2020).
- [5] Altin Karataş, M.; Gökkaya, H. A review on machinability of carbon fiber reinforced polymer (CFRP) and glass fiber reinforced polymer (GFRP) composite materials. *Defence Technology* **2018**, *14* (4), 318-326.
- [6] Schadler, L. S. Polymer-based and Polymer-filled Nanocomposites. In *Nanocomposite Science and Technology*, Ajayan, P. M.; Schadler, L. S.; Braun, P. V., Eds. Wiley-VCH Verlag GmbH & Co. KGaA: Weinheim, 2003; pp 77-154.
- [7] Balazs, A. C.; Emrick, T.; Russell, T. P. Nanoparticle polymer composites: where two small worlds meet. *Science* **2006**, *314* (5802), 1107-1110.
- [8] Yu, Z.; Niu, X.; Liu, Z.; Pei, Q. Intrinsically stretchable polymer light-emitting devices using carbon nanotube-polymer composite electrodes. *Adv. Mater.* **2011**, *23* (34), 3989-3994.
- [9] José-Yacamán, M.; Rendón, L.; Arenas, J.; Serra Puche, M. C. Maya Blue Paint: An Ancient Nanostructured Material. *Science* **1996**, *273* (5272), 223-225.
- [10] Bergaya, F.; Lagaly, G. General Introduction: Clays, Clay Minerals, and Clay Science. In *Handbook of Clay Science*, Bergaya, F.; Theng, B. K. G.; Lagaly, G., Eds. Elsevier: Amsterdam, 2006; pp 1-18.
- [11] Habel, C.; Schöttle, M.; Daab, M.; Eichstaedt, N. J.; Wagner, D.; Bakhshi, H.; Agarwal, S.; Horn, M. A.; Breu, J. High-Barrier, Biodegradable Food Packaging. *Macromol. Mater. Eng.* **2018**, *303* (10), 1800333.
- [12] Grunlan, J. C.; Grigorian, A.; Hamilton, C. B.; Mehrabi, A. R. Effect of clay concentration on the oxygen permeability and optical properties of a modified poly(vinyl alcohol). *J. Appl. Polym. Sci.* **2004**, *93* (3), 1102-1109.
- [13] Morgan, A. B.; Wilkie, C. A. *Flame retardant polymer nanocomposites*. John Wiley Sons, Inc.: Hoboken, New Jersey, 2007
- [14] Schütz, M. R.; Kalo, H.; Lunkenbein, T.; Breu, J.; Wilkie, C. A. Intumescent-like behavior of polystyrene synthetic clay nanocomposites. *Polymer* **2011**, *52* (15), 3288-3294.
- [15] Ziadeh, M.; Weiss, S.; Fischer, B.; Förster, S.; Altstädt, V.; Müller, A. H. E.; Breu, J. Towards completely miscible PMMA nanocomposites reinforced by shear-stiff, nano-mica. *J. Colloid Interface Sci.* **2014**, *425*, 143-151.
- [16] Morits, M.; Verho, T.; Sorvari, J.; Liljeström, V.; Kostianen, M. A.; Gröschel, A. H.; Ikkala, O. Toughness and Fracture Properties in Nacre-Mimetic Clay/Polymer Nanocomposites. *Adv. Funct. Mater.* **2017**, *27* (10), 1605378.

- [17] Brigatti, M. F.; Galan, E.; Theng, B. K. G. Structures and Mineralogy of Clay Minerals. In *Handbook of Clay Science*, Bergaya, F.; Theng, B. K. G.; Lagaly, G., Eds. Elsevier: Amsterdam, 2006; pp 19-86.
- [18] Martin, R. T.; Bailey, S. W.; Eberl, D. D.; Fanning, D. S.; Guggenheim, S.; Kodama, H.; Pevear, D. R.; Srodon, J.; Wicks, F. J. Report of the Clay Minerals Society Nomenclature Committee: Revised Classification of Clay Materials. *Clays Clay Miner.* **1991**, *39* (3), 333-335.
- [19] Holleman, A. F.; Wiberg, N.; Wiberg, E. *Lehrbuch der Anorganischen Chemie*. 102 ed.; Walter de Gruyter & Co.: Berlin, 2007
- [20] Stöter, M.; Rosenfeldt, S.; Breu, J. Tunable Exfoliation of Synthetic Clays. *Annu. Rev. Mater. Res.* **2015**, *45*, 129-151.
- [21] Lagaly, G.; Ogawa, M.; Dékány, I. Clay Mineral Organic Interactions. In *Handbook of Clay Science*, Bergaya, F.; Theng, B. K. G.; Lagaly, G., Eds. Elsevier: Amsterdam, 2006; pp 309-377.
- [22] Harvey, C. C.; Lagaly, G. Conventional Applications. In *Handbook of Clay Science*, Bergaya, F.; Theng, B. K. G.; Lagaly, G., Eds. Elsevier: Amsterdam, 2006; pp 501-540.
- [23] Breu, J.; Seidl, W.; Stoll, A. J.; Lange, K. G.; Probst, T. U. Charge Homogeneity in Synthetic Fluorohectorite. *Chem. Mater.* **2001**, *13* (11), 4213-4220.
- [24] Stöter, M.; Kunz, D. A.; Schmidt, M.; Hirsemann, D.; Kalo, H.; Putz, B.; Senker, J.; Breu, J. Nanoplatelets of sodium hectorite showing aspect ratios of approximately 20000 and superior purity. *Langmuir* **2013**, *29* (4), 1280-1285.
- [25] Madsen, F. T.; Müller-Vonmoos, M. The swelling behaviour of clays. *Appl. Clay Sci.* **1989**, *4* (2), 143-156.
- [26] Rosenfeldt, S.; Stöter, M.; Schlenk, M.; Martin, T.; Albuquerque, R. Q.; Förster, S.; Breu, J. In-Depth Insights into the Key Steps of Delamination of Charged 2D Nanomaterials. *Langmuir* **2016**, *32* (41), 10582-10588.
- [27] Kalo, H.; Milius, W.; Breu, J. Single crystal structure refinement of one- and two-layer hydrates of sodium fluorohectorite. *RSC Adv.* **2012**, *2* (22), 8452-8459.
- [28] Michot, L. J.; Bihannic, I.; Maddi, S.; Funari, S. S.; Baravian, C.; Levitz, P.; Davidson, P. Liquid-crystalline aqueous clay suspensions. *Proc. Natl. Acad. Sci. USA* **2006**, *103* (44), 16101-16104.
- [29] Kalo, H.; Möller, M. W.; Kunz, D. A.; Breu, J. How to maximize the aspect ratio of clay nanoplatelets. *Nanoscale* **2012**, *4* (18), 5633-5639.
- [30] Daab, M.; Eichstaedt, N. J.; Habel, C.; Rosenfeldt, S.; Kalo, H.; Schießling, H.; Förster, S.; Breu, J. Onset of Osmotic Swelling in Highly Charged Clay Minerals. *Langmuir* **2018**, *34* (28), 8215-8222.
- [31] Daab, M.; Eichstaedt, N. J.; Edenharter, A.; Rosenfeldt, S.; Breu, J. Layer charge robust delamination of organo-clays. *RSC Adv.* **2018**, *8* (50), 28797-28803.
- [32] Lagaly, G.; Ziesmer, S. Colloid chemistry of clay minerals: the coagulation of montmorillonite dispersions. *Adv. Colloid Interface Sci.* **2003**, *100-102*, 105-128.
- [33] Bissada, K. K.; Johns, W. D.; Cheng, F. S. Cation-dipole interactions in clay organic complexes. *Clay Miner.* **1967**, *7* (2), 155-166.

- [34] Dowdy, R. H.; Mortland, M. M. Alcohol-Water Interactions on Montmorillonite Surfaces. I. Ethanol. *Clays Clay Miner.* **1967**, *15* (1), 259-271.
- [35] Olejnik, S.; Posner, A. M.; Quirk, J. P. Swelling of Montmorillonite in Polar Organic Liquids. *Clays Clay Miner.* **1974**, *22* (4), 361-365.
- [36] Greene-Kelly, R. Sorption of aromatic organic compounds by montmorillonite. Part 1.- Orientation studies. *Trans. Faraday Soc.* **1955**, *51*, 412-424.
- [37] Yamanaka, S.; Kanamaru, F.; Koizumi, M. Role of interlayer cations in the formation of acrylonitrile-montmorillonite complexes. *J. Phys. Chem.* **1974**, *78* (1), 42-44.
- [38] MacEwan, D. M. C. The identification and estimation of the montmorillonite group of minerals, with special reference to soil clays. *J. Soc. Chem. Ind.* **1946**, *65* (10), 298-304.
- [39] Jordan, J. W. Organophilic Bentonites. I. Swelling in Organic Liquids. *J. Phys. Colloid Chem.* **1949**, *53* (2), 294-306.
- [40] Slabaugh, W. H.; Hiltner, P. A. Swelling of alkylammonium montmorillonites. *J. Phys. Chem.* **1968**, *72* (12), 4295-4298.
- [41] Moraru, V. N. Structure formation of alkylammonium montmorillonites in organic media. *Appl. Clay Sci.* **2001**, *19* (1-6), 11-26.
- [42] Lagaly, G. Clay-organic interactions. *Phil. Trans. R. Soc. Lond. A* **1997**, *311* (1517), 315-332.
- [43] Gutmann, V. Solvent effects on the reactivities of organometallic compounds. *Coord. Chem. Rev.* **1976**, *18* (2), 225-255.
- [44] Berkheiser, V.; Mortland, M. M. Variability in Exchange Ion Position in Smectite: Dependence on Interlayer Solvent. *Clays Clay Miner.* **1975**, *23* (5), 404-410.
- [45] Onikata, M.; Kondo, M.; Yamanaka, S. Swelling of Formamide-Montmorillonite Complexes in Polar Liquids. *Clays Clay Miner.* **1999**, *47* (5), 678-681.
- [46] Graber, E. R.; Mingelgrin, U. Clay swelling and regular solution theory. *Environ. Sci. Technol.* **1994**, *28* (13), 2360-2365.
- [47] Brindley, G. W. Intracrystalline Swelling of Montmorillonites in Water-Dimethylsulfoxide Systems. *Clays Clay Miner.* **1980**, *28* (5), 369-372.
- [48] Kunz, R.; Amschler, S.; Edenharter, A.; Mayr, L.; Herlitz, S.; Rosenfeldt, S.; Breu, J. Giant Multistep Crystalline vs. Osmotic Swelling of Synthetic Hectorite in Aqueous Acetonitrile. *Clays Clay Miner.* **2019**, *67* (6), 481-487.
- [49] Usuki, A.; Kojima, Y.; Kawasumi, M.; Okada, A.; Fukushima, Y.; Kurauchi, T.; Kamigaito, O. Synthesis of nylon 6-clay hybrid. *J. Mater. Res.* **1993**, *8* (5), 1179-1184.
- [50] Okada, A.; Usuki, A. Twenty Years of Polymer-Clay Nanocomposites. *Macromol. Mater. Eng.* **2006**, *291* (12), 1449-1476.
- [51] Albdiry, M. T.; Yousif, B. F.; Ku, H.; Lau, K. T. A critical review on the manufacturing processes in relation to the properties of nanoclay/polymer composites. *J. Compos. Mater.* **2012**, *47* (9), 1093-1115.
- [52] Alexandre, M.; Dubois, P. Polymer-layered silicate nanocomposites: Preparation, properties and uses of a new class of materials. *Mater. Sci. Eng., R* **2000**, *28* (1-2), 1-63.

- [53] Kunz, D. A.; Schmid, J.; Feicht, P.; Erath, J.; Fery, A.; Breu, J. Clay-based nanocomposite coating for flexible optoelectronics applying commercial polymers. *ACS Nano* **2013**, *7* (5), 4275-4280.
- [54] Triantafyllidis, K. S.; Xidas, P. I.; Pinnavaia, T. J. Alternative Synthetic Routes to Epoxy Polymer - Clay Nanocomposites using Organic or Mixed-Ion Clays Modified by Protonated Di/Triamines (Jeffamines). *Macromol. Symp.* **2008**, *267* (1), 41-46.
- [55] Müller, K.; Bugnicourt, E.; Latorre, M.; Jorda, M.; Echegoyen Sanz, Y.; Lagaron, J. M.; Miesbauer, O.; Bianchin, A.; Hankin, S.; Böhlz, U.; Perez, G.; Jesdinszki, M.; Lindner, M.; Scheuerer, Z.; Castelló, S.; Schmid, M. Review on the Processing and Properties of Polymer Nanocomposites and Nanocoatings and Their Applications in the Packaging, Automotive and Solar Energy Fields. *Nanomaterials* **2017**, *7* (4), 74.
- [56] Ziadeh, M.; Fischer, B.; Schmid, J.; Altstädt, V.; Breu, J. On the importance of specific interface area in clay nanocomposites of PMMA filled with synthetic nano-mica. *Polymer* **2014**, *55* (16), 3770-3781.
- [57] Sinha Ray, S.; Okamoto, M. Polymer/layered silicate nanocomposites: A review from preparation to processing. *Prog. Polym. Sci.* **2003**, *28* (11), 1539-1641.
- [58] Wang, Z.; Rolle, K.; Schilling, T.; Hummel, P.; Philipp, A.; Kopera, B. A. F.; Lechner, A. M.; Retsch, M.; Breu, J.; Fytas, G. Tunable Thermoelastic Anisotropy in Hybrid Bragg Stacks with Extreme Polymer Confinement. *Angew. Chem., Int. Ed.* **2020**, *59* (3), 1286-1294.
- [59] Ogata, N.; Kawakage, S.; Ogihara, T. Poly(vinyl alcohol)-clay and poly(ethylene oxide)-clay blends prepared using water as solvent. *J. Appl. Polym. Sci.* **1997**, *66* (3), 573-581.
- [60] Habel, C.; Maiz, J.; Olmedo-Martínez, J. L.; López, J. V.; Breu, J.; Müller, A. J. Competition between nucleation and confinement in the crystallization of poly(ethylene glycol)/ large aspect ratio hectorite nanocomposites. *Polymer* **2020**, *202*, 122734.
- [61] Alateyah, A. I.; Dhakal, H. N.; Zhang, Z. Y. Processing, Properties, and Applications of Polymer Nanocomposites Based on Layer Silicates: A Review. *Adv. Polym. Technol.* **2013**, *32* (4), 21368.
- [62] Bumbudsanpharoke, N.; Ko, S. Nanoclays in Food and Beverage Packaging. *J. Nanomater.* **2019**, *2019*, 1-13.
- [63] Kotal, M.; Bhowmick, A. K. Polymer nanocomposites from modified clays: Recent advances and challenges. *Prog. Polym. Sci.* **2015**, *51*, 127-187.
- [64] Schütz, M. R.; Kalo, H.; Lunkenbein, T.; Gröschel, A. H.; Müller, A. H. E.; Wilkie, C. A.; Breu, J. Shear stiff, surface modified, mica-like nanoplatelets: A novel filler for polymer nanocomposites. *J. Mater. Chem.* **2011**, *21* (32), 12110-12116.
- [65] Kunz, R.; Martin, T.; Callsen, C.; Hutschreuther, J.; Altstädt, V.; Breu, J. Thermal expansion of clay polymer nanocomposites as a function of aspect ratio and filler content. *Polymer* **2019**, *169*, 74-79.
- [66] Samakande, A.; Hartmann, P. C.; Cloete, V.; Sanderson, R. D. Use of acrylic based surfmers for the preparation of exfoliated polystyrene-clay nanocomposites. *Polymer* **2007**, *48* (6), 1490-1499.
- [67] Zeng, C.; Lee, L. J. Poly(methyl methacrylate) and Polystyrene/Clay Nanocomposites Prepared by in-Situ Polymerization. *Macromolecules* **2001**, *34* (12), 4098-4103.

- [68] Su, S.; Wilkie, C. A. Exfoliated poly(methyl methacrylate) and polystyrene nanocomposites occur when the clay cation contains a vinyl monomer. *J. Polym. Sci., Part A: Polym. Chem.* **2003**, *41* (8), 1124-1135.
- [69] Fan, X.; Xia, C.; Advincula, R. C. Grafting of Polymers from Clay Nanoparticles via In Situ Free Radical Surface-Initiated Polymerization: Monocationic versus Bicationic Initiators. *Langmuir* **2003**, *19* (10), 4381-4389.
- [70] Uthirakumar, P.; Nahm, K. S.; Hahn, Y. B.; Lee, Y.-S. Preparation of polystyrene/montmorillonite nanocomposites using a new radical initiator-montmorillonite hybrid via in situ intercalative polymerization. *Eur. Polym. J.* **2004**, *40* (11), 2437-2444.
- [71] Albrecht, M.; Ehrler, S.; Mühlebach, A. Nanocomposites from Layered Silicates: Graft Polymerization with Intercalated Ammonium Peroxides. *Macromol. Rapid Commun.* **2003**, *24* (5/6), 382-387.
- [72] Velten, U.; Shelden, R. A.; Caseri, W. R.; Suter, U. W.; Li, Y. Polymerization of Styrene with Peroxide Initiator Ionically Bound to High Surface Area Mica. *Macromolecules* **1999**, *32* (11), 3590-3597.
- [73] Böttcher, H.; Hallensleben, M. L.; Nuß, S.; Wurm, H.; Bauer, J.; Behrens, P. Organic/inorganic hybrids by 'living'/controlled ATRP grafting from layered silicates. *J. Mater. Chem.* **2002**, *12* (5), 1351-1354.
- [74] Samakande, A.; Sanderson, R. D.; Hartmann, P. C. RAFT-mediated polystyrene-clay nanocomposites prepared by making use of initiator-bound MMT clay. *Eur. Polym. J.* **2009**, *45* (3), 649-657.
- [75] Kunz, D. A.; Erath, J.; Kluge, D.; Thurn, H.; Putz, B.; Fery, A.; Breu, J. In-plane modulus of singular 2:1 clay lamellae applying a simple wrinkling technique. *ACS Appl. Mater. Interfaces* **2013**, *5* (12), 5851-5855.
- [76] Stöter, M.; Gödrich, S.; Feicht, P.; Rosenfeldt, S.; Thurn, H.; Neubauer, J. W.; Seuss, M.; Lindner, P.; Kalo, H.; Möller, M.; Fery, A.; Förster, S.; Papastavrou, G.; Breu, J. Controlled Exfoliation of Layered Silicate Heterostructures into Bilayers and Their Conversion into Giant Janus Platelets. *Angew. Chem., Int. Ed.* **2016**, *55* (26), 7398-7402.
- [77] Vaughan, M. T.; Guggenheim, S. Elasticity of muscovite and its relationship to crystal structure. *J. Geophys. Res. Solid Earth* **1986**, *91* (B5), 4657-4664.
- [78] McNeil, L. E.; Grimsditch, M. Elastic moduli of muscovite mica. *J. Phys.: Condens. Matter* **1993**, *5* (11), 1681-1690.
- [79] Elias, H.-G. *Makromoleküle - Band 4: Anwendungen von Polymeren*. 6 ed.; Wiley VCH Verlag GmbH & Co. KGaA: Weinheim, 2003
- [80] Halpin, J. C.; Kardos, J. L. The Halpin-Tsai equations: A review. *Polym. Eng. Sci.* **1976**, *16* (5), 344-352.
- [81] Wu, Y.-P.; Jia, Q.-X.; Yu, D.-S.; Zhang, L.-Q. Modeling Young's modulus of rubber-clay nanocomposites using composite theories. *Polym. Test.* **2004**, *23* (8), 903-909.
- [82] Brostow, W. Mechanical Properties. In *Physical Properties of Polymers Handbook*, 2 ed.; Mark, J. E., Ed. Springer Science+Business Media, LLC: New York, 2007; pp 423-445.
- [83] Liaw, J. H.; Hsueh, T. Y.; Tan, T.-S.; Wang, Y.; Chiao, S.-M. Twin-screw compounding of poly(methyl methacrylate)/clay nanocomposites: effects of compounding temperature and matrix molecular weight. *Polym. Int.* **2007**, *56* (8), 1045-1052.

- [84] Tiwari, R. R.; Natarajan, U. Thermal and mechanical properties of melt processed intercalated poly(methyl methacrylate)-organoclay nanocomposites over a wide range of filler loading. *Polym. Int.* **2008**, *57* (5), 738-743.
- [85] Fischer, B.; Ziadeh, M.; Pfaff, A.; Breu, J.; Altstädt, V. Impact of large aspect ratio, shear-stiff, mica-like clay on mechanical behaviour of PMMA/clay nanocomposites. *Polymer* **2012**, *53* (15), 3230-3237.
- [86] Saritha, A.; Kuruvilla, J. Barrier Properties of Nanocomposites. In *Polymer Composites - Volume 2*, Thomas, S.; Joseph, K.; Malhotra, S. K.; Goda, K.; Sreekala, M. S., Eds. Wiley-VCH Verlag GmbH & Co. KGaA: Weinheim, 2013; pp 185-200.
- [87] DeRocher, J. P.; Gettelfinger, B. T.; Wang, J.; Nuxoll, E. E.; Cussler, E. L. Barrier membranes with different sizes of aligned flakes. *J. Membr. Sci.* **2005**, *254* (1-2), 21-30.
- [88] Nielsen, L. E. Models for the Permeability of Filled Polymer Systems. *J. Macromol. Sci. (Chem.)*, **A** **1967**, *1* (5), 929-942.
- [89] Cussler, E. L.; Hughes, S. E.; Ward, W. J.; Aris, R. Barrier membranes. *J. Membr. Sci.* **1988**, *38* (2), 161-174.
- [90] Tsurko, E. S.; Feicht, P.; Habel, C.; Schilling, T.; Daab, M.; Rosenfeldt, S.; Breu, J. Can high oxygen and water vapor barrier nanocomposite coatings be obtained with a waterborne formulation? *J. Membr. Sci.* **2017**, *540*, 212-218.
- [91] Kalendova, A.; Merinska, D.; Gerard, J. F.; Slouf, M. Polymer/clay nanocomposites and their gas barrier properties. *Polym. Compos.* **2013**, *34* (9), 1418-1424.
- [92] Schilling, T.; Habel, C.; Rosenfeldt, S.; Röhr, M.; Breu, J. Impact of Ultraconfinement on Composite Barriers. *ACS Appl. Polym. Mater.* **2020**, *2* (7), 3010-3015.
- [93] Habel, C.; Tsurko, E. S.; Timmins, R. L.; Hutschreuther, J.; Kunz, R.; Schuchardt, D. D.; Rosenfeldt, S.; Altstädt, V.; Breu, J. Lightweight Ultra-High-Barrier Liners for Helium and Hydrogen. *ACS Nano* **2020**, *14* (6), 7018-7024.
- [94] Tzeng, P.; Lugo, E. L.; Mai, G. D.; Wilhite, B. A.; Grunlan, J. C. Super hydrogen and helium barrier with polyelectrolyte nanobrick wall thin film. *Macromol. Rapid Commun.* **2015**, *36* (1), 96-101.
- [95] Latnikova, A.; Jobmann, M. Towards Microcapsules with Improved Barrier Properties. *Top. Curr. Chem.* **2017**, *375* (3), 64.
- [96] He, L.; Hu, J.; Deng, W. Preparation and application of flavor and fragrance capsules. *Polym. Chem.* **2018**, *9* (40), 4926-4946.
- [97] Chuanjie, F.; Xiaodong, Z. Preparation and barrier properties of the microcapsules added nanoclays in the wall. *Polym. Adv. Technol.* **2009**, *20* (12), 934-939.
- [98] Jagtap, S. B.; Mohan, M. S.; Shukla, P. G. Improved performance of microcapsules with polymer nanocomposite wall: Preparation and characterization. *Polymer* **2016**, *83*, 27-33.
- [99] Mozaffari, S. M.; Beheshty, M. H. Nanoclay-modified microcapsules as a latent curing agent in epoxy. *Polym. Bull.* **2020**
- [100] Butt, H.-J.; Graf, K.; Kappl, M. *Physics and Chemistry of Interfaces*. Wiley-VCH Verlag GmbH & Co. KGaA: Weinheim, 2003

- [101] Gibson, L. J.; Ashby, M. F. *Cellular solids*. 2 ed.; Cambridge University Press: Cambridge, 1997
- [102] Koltzenburg, S.; Maskos, M.; Nuyken, O. *Polymere: Synthese, Eigenschaften und Anwendungen*. Springer Spektrum: Berlin, Heidelberg, 2014
- [103] Sotomayor, O. E.; Tippur, H. V. Role of cell regularity and relative density on elastoplastic compression response of 3-D open-cell foam core sandwich structure generated using Voronoi diagrams. *Acta Mater.* **2014**, *78*, 301-313.
- [104] Zhu, H. X.; Hobdell, J. R.; Windle, A. H. Effects of cell irregularity on the elastic properties of open-cell foams. *Acta Mater.* **2000**, *48* (20), 4893-4900.
- [105] Xu, Z.; Tang, X.; Gu, A.; Fang, Z. Novel preparation and mechanical properties of rigid polyurethane foam/organoclay nanocomposites. *J. Appl. Polym. Sci.* **2007**, *106* (1), 439-447.
- [106] Istrate, O. M.; Chen, B. Relative modulus–relative density relationships in low density polymer–clay nanocomposite foams. *Soft Matter* **2011**, *7* (5), 1840-1848.
- [107] Cao, X.; Lee, L. J.; Widya, T.; Macosko, C. Polyurethane/clay nanocomposites foams: processing, structure and properties. *Polymer* **2005**, *46* (3), 775-783.
- [108] Lee, Y. H.; Wang, K. H.; Park, C. B.; Sain, M. Effects of clay dispersion on the foam morphology of LDPE/clay nanocomposites. *J. Appl. Polym. Sci.* **2007**, *103* (4), 2129-2134.
- [109] Zeng, C.; Han, X.; Lee, L. J.; Koelling, K. W.; Tomasko, D. L. Polymer–Clay Nanocomposite Foams Prepared Using Carbon Dioxide. *Adv. Mater.* **2003**, *15* (20), 1743-1747.
- [110] Han, X.; Zeng, C.; Lee, L. J.; Koelling, K. W.; Tomasko, D. L. Extrusion of polystyrene nanocomposite foams with supercritical CO<sub>2</sub>. *Polym. Eng. Sci.* **2003**, *43* (6), 1261-1275.
- [111] Silverstein, M. S. PolyHIPEs: Recent advances in emulsion-templated porous polymers. *Prog. Polym. Sci.* **2014**, *39* (1), 199-234.
- [112] Cameron, N. R. High internal phase emulsion templating as a route to well-defined porous polymers. *Polymer* **2005**, *46* (5), 1439-1449.
- [113] Cameron, N. R.; Sherrington, D. C.; Albiston, L.; Gregory, D. P. Study of the formation of the open-cellular morphology of poly(styrene/divinylbenzene) polyHIPE materials by cryo-SEM. *Colloid Polym. Sci.* **1996**, *274* (6), 592-595.
- [114] Williams, J. M.; Wroblewski, D. A. Spatial distribution of the phases in water-in-oil emulsions. Open and closed microcellular foams from cross-linked polystyrene. *Langmuir* **1988**, *4* (3), 656-662.
- [115] Williams, J. M.; Gray, A. J.; Wilkerson, M. H. Emulsion stability and rigid foams from styrene or divinylbenzene water-in-oil emulsions. *Langmuir* **1990**, *6* (2), 437-444.
- [116] Abbasian, Z.; Moghbeli, M. R. Open porous emulsion-templated monoliths: Effect of the emulsion preparation conditions on the foam microstructure and properties. *J. Appl. Polym. Sci.* **2009**, *116* (2), 986-994.
- [117] Choi, J. S.; Chun, B. C.; Lee, S. J. Effect of rubber on microcellular structures from high internal phase emulsion polymerization. *Macromol. Res.* **2003**, *11* (2), 104-109.
- [118] Gurevitch, I.; Silverstein, M. S. Nanoparticle-based and organic-phase-based AGET ATRP polyHIPE synthesis within pickering HIPEs and surfactant-stabilized HIPEs. *Macromolecules* **2011**, *44*, 3398-3409.

- [119] Çıra, F.; Mert, E. H. PolyHIPE/pullulan composites derived from glycidyl methacrylate and 1,3-butanediol dimethacrylate-based high internal phase emulsions. *Polymer Engineering & Science* **2015**, *55* (11), 2636-2642.
- [120] Berber, E.; Çıra, F.; Mert, E. H. Preparation of porous polyester composites via emulsion templating: Investigation of the morphological, mechanical, and thermal properties. *Polym. Compos.* **2016**, *37* (5), 1531-1538.
- [121] Zhang, H.; Cooper, A. I. Synthesis and applications of emulsion-templated porous materials. *Soft Matter* **2005**, *1* (2), 107-113.
- [122] Pulko, I.; Krajnc, P. High internal phase emulsion templating - a path to hierarchically porous functional polymers. *Macromol. Rapid Commun.* **2012**, *33* (20), 1731-1746.
- [123] Qu, Q.; Pan, J.; Yin, Y.; Wu, R.; Shi, W.; Yan, Y.; Dai, X. Synthesis of macroporous polymer foams via pickering high internal phase emulsions for highly efficient 2,4,5-trichlorophenol removal. *J. Appl. Polym. Sci.* **2015**, *132* (6), 41430.
- [124] Gao, H.; Peng, Y.; Pan, J.; Zeng, J.; Song, C.; Zhang, Y.; Yan, Y.; Shi, W. Synthesis and evaluation of macroporous polymerized solid acid derived from Pickering HIPEs for catalyzing cellulose into 5-hydroxymethylfurfural in an ionic liquid. *RSC Adv.* **2014**, *4* (81), 43029-43038.
- [125] Audouin, F.; Fox, M.; Larragy, R.; Clarke, P.; Huang, J.; O'Connor, B.; Heise, A. Polypeptide-Grafted Macroporous PolyHIPE by Surface-Initiated *N*-Carboxyanhydride (NCA) Polymerization as a Platform for Bioconjugation. *Macromolecules* **2012**, *45* (15), 6127-6135.
- [126] Haibach, K.; Menner, A.; Powell, R.; Bismarck, A. Tailoring mechanical properties of highly porous polymer foams: Silica particle reinforced polymer foams via emulsion templating. *Polymer* **2006**, *47* (13), 4513-4519.
- [127] Shin, H.; Kim, S.; Han, Y.; Kim, K.; Choi, S. Q. Preparation of a monolithic and macroporous superabsorbent polymer via a high internal phase Pickering emulsion template. *J. Appl. Polym. Sci.* **2019**, *136* (42), 48133.
- [128] Ikem, V. O.; Menner, A.; Bismarck, A. High internal phase emulsions stabilized solely by functionalized silica particles. *Angew. Chem., Int. Ed.* **2008**, *47* (43), 8277-8279.
- [129] Zou, S.; Yang, Y.; Liu, H.; Wang, C. Synergistic stabilization and tunable structures of Pickering high internal phase emulsions by nanoparticles and surfactants. *Colloids Surf., A* **2013**, *436*, 1-9.
- [130] Abbasian, Z.; Moghbeli, M. R. Preparation of highly open porous styrene/acrylonitrile and styrene/acrylonitrile/organoclay polymerized high internal phase emulsion (PolyHIPE) foams via emulsion templating. *J. Appl. Polym. Sci.* **2011**, *119* (6), 3728-3738.
- [131] Ahmed, M. S.; Lee, Y. H.; Park, C. B.; Atalla, N. Effect of nanoclay on the microcellular structure and morphology of high internal phase emulsion (HIPE) foams. *Asia-Pac. J. Chem. Eng.* **2009**, *4* (2), 120-124.
- [132] Çıra, F.; Berber, E.; Şen, S.; Mert, E. H. Preparation of polyHIPE/clay composites by using a reactive intercalant. *J. Appl. Polym. Sci.* **2015**, *132* (4), 41333.
- [133] Yüce, E.; Mert, E. H.; Şen, S.; Saygı, S.; San, N. Properties and applications of nanoclay reinforced open-porous polymer composites. *J. Appl. Polym. Sci.* **2017**, *134* (46), 45522.
- [134] Lépine, O.; Birot, M.; Deleuze, H. Elaboration of open-cell microcellular nanocomposites. *J. Polym. Sci., Part A: Polym. Chem.* **2007**, *45* (18), 4193-4203.

- [135] Luxner, M. H.; Stampfl, J.; Pettermann, H. E. Numerical simulations of 3D open cell structures – influence of structural irregularities on elasto-plasticity and deformation localization. *Int. J. Solids Struct.* **2007**, *44* (9), 2990-3003.
- [136] Förster, T.; von Rybinski, W. Applications of Emulsions. In *Modern Aspects of Emulsion Science*, Binks, B. P., Ed. Royal Society of Chemistry: Cambridge, 1998; pp 395-426.
- [137] Ramsden, W. Separation of solids in the surface-layers of solutions and suspensions. *Proc. R. Soc. Lond.* **1904**, *72* (477-486), 156-164.
- [138] Pickering, S. U. Emulsions. *J. Chem. Soc., Trans.* **1907**, *91*, 2001-2021.
- [139] Binks, B. P. Particles as surfactants - similarities and differences. *Curr. Opin. Colloid Interface Sci.* **2002**, *7* (1-2), 21-41.
- [140] Tadros, T. F. *Emulsions*. Walter de Gruyter GmbH: Berlin/Boston, 2016
- [141] Wei, P.; Luo, Q.; Edgehouse, K. J.; Hemmingsen, C. M.; Rodier, B. J.; Pentzer, E. B. 2D Particles at Fluid-Fluid Interfaces: Assembly and Templating of Hybrid Structures for Advanced Applications. *ACS Appl. Mater. Interfaces* **2018**, *10* (26), 21765-21781.
- [142] Tiwari, R. R.; Paul, D. R. Effect of organoclay on the morphology, phase stability and mechanical properties of polypropylene/polystyrene blends. *Polymer* **2011**, *52* (4), 1141-1154.
- [143] Texter, J. Graphene oxide and graphene flakes as stabilizers and dispersing aids. *Curr. Opin. Colloid Interface Sci.* **2015**, *20* (5-6), 454-464.
- [144] Creighton, M. A.; Ohata, Y.; Miyawaki, J.; Bose, A.; Hurt, R. H. Two-dimensional materials as emulsion stabilizers: interfacial thermodynamics and molecular barrier properties. *Langmuir* **2014**, *30* (13), 3687-3696.
- [145] Ashby, N. P.; Binks, B. P. Pickering emulsions stabilised by Laponite clay particles. *Phys. Chem. Chem. Phys.* **2000**, *2* (24), 5640-5646.
- [146] Gholamipour-Shirazi, A.; Carvalho, M. S.; Fossum, J. O. Controlled microfluidic emulsification of oil in a clay nanofluid: Role of salt for Pickering stabilization. *Eur. Phys. J. Special Topics* **2016**, *225* (4), 757-765.
- [147] Garcia, P. C.; Whitby, C. P. Laponite-stabilised oil-in-water emulsions: viscoelasticity and thixotropy. *Soft Matter* **2012**, *8* (5), 1609-1615.
- [148] Lagaly, G.; Reese, M.; Abend, S. Smectites as colloidal stabilizers of emulsions. *Appl. Clay Sci.* **1999**, *14* (1-3), 83-103.
- [149] Zhang, J.; Li, L.; Xu, J.; Sun, D. Effect of cetyltrimethylammonium bromide addition on the emulsions stabilized by montmorillonite. *Colloid Polym. Sci.* **2013**, *292* (2), 441-447.
- [150] Cui, Y.; Threlfall, M.; van Duijneveldt, J. S. Optimizing organoclay stabilized Pickering emulsions. *J. Colloid Interface Sci.* **2011**, *356* (2), 665-671.
- [151] Li, W.; Yu, L.; Liu, G.; Tan, J.; Liu, S.; Sun, D. Oil-in-water emulsions stabilized by Laponite particles modified with short-chain aliphatic amines. *Colloids Surf., A* **2012**, *400*, 44-51.
- [152] Binks, B. P.; Fletcher, P. D. I.; Holt, B. L.; Beaussoubre, P.; Wong, K. Selective retardation of perfume oil evaporation from oil-in-water emulsions stabilized by either surfactant or nanoparticles. *Langmuir* **2010**, *26* (23), 18024-18030.

- [153] Thompson, K. L.; Williams, M.; Armes, S. P. Colloidosomes: synthesis, properties and applications. *J. Colloid Interface Sci.* **2015**, *447*, 217-228.
- [154] Yow, H. N.; Routh, A. F. Formation of liquid core-polymer shell microcapsules. *Soft Matter* **2006**, *2* (11), 940-949.
- [155] Dinsmore, A. D.; Hsu, M. F.; Nikolaidis, M. G.; Marquez, M.; Bausch, A. R.; Weitz, D. A. Colloidosomes: selectively permeable capsules composed of colloidal particles. *Science* **2002**, *298* (5595), 1006-1009.
- [156] Su, Y.; Zhao, H.; Wu, J.; Xu, J. One-step fabrication of silica colloidosomes with in situ drug encapsulation. *RSC Adv.* **2016**, *6* (113), 112292-112299.
- [157] Keen, P. H. R.; Slater, N. K. H.; Routh, A. F. Encapsulation of amylase in colloidosomes. *Langmuir* **2014**, *30* (8), 1939-1948.
- [158] Cui, Y.; van Duijneveldt, J. S. Microcapsules Composed of Cross-Linked Organoclay. *Langmuir* **2012**, *28* (3), 1753-1757.
- [159] Williams, M.; Armes, S. P.; York, D. W. Clay-based colloidosomes. *Langmuir* **2012**, *28* (2), 1142-1148.
- [160] Mayr, L.; Amschler, S.; Edenharter, A.; Dudko, V.; Kunz, R.; Rosenfeldt, S.; Breu, J. Osmotic Swelling of Sodium Hectorite in Ternary Solvent Mixtures: Nematic Liquid Crystals in Hydrophobic Media. *Langmuir* **2020**, *36* (14), 3814-3820.
- [161] Mayr, L.; Simonyan, A.; Breu, J.; Wingert, M. J. Structural and mechanical impact of synthetic clay in composite foams made via high-internal phase emulsions. *Polym. Compos.* **2021**, *42*, 353-361.
- [162] Mayr, L.; Breu, J. Encapsulation of Fragrance in Aqueous Emulsions by Delaminated Synthetic Hectorite. *Langmuir* **2020**, *36* (37), 11061-11067.

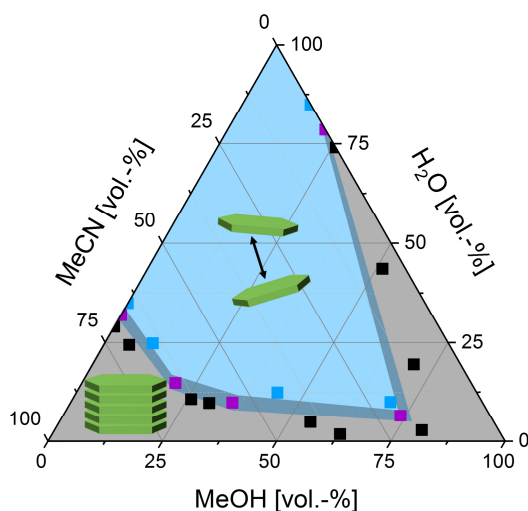
## 6 Results

### 6.1 Osmotic swelling of sodium hectorite in ternary solvent mixtures: nematic liquid crystals in hydrophobic media

Lina Mayr,<sup>1</sup> Sonja Amschler,<sup>1</sup> Andreas Edenharter,<sup>1</sup> Volodymyr Dudko,<sup>1</sup> Raphael Kunz,<sup>1</sup> Sabine Rosenfeldt<sup>1</sup> and Josef Breu<sup>1\*</sup>

Published in: *Langmuir* **2020**, 36 (14), 3814-3820

Reprinted with permission, Copyright (2020) American Chemical Society



<sup>1</sup> Department of Chemistry and Bavarian Polymer Institute, University of Bayreuth, 95447 Bayreuth, Germany

\*Corresponding author: josef.breu@uni-bayreuth.de

#### Author's individual contributions:

The concept of the publication was developed by Prof Josef Breu and me. First preliminary experiments were done by Sonja Amschler, Andreas Edenharter and Raphael Kunz. I made all the swelling experiments and measured X-ray diffraction. Sabine Rosenfeldt conducted the SAXS measurements. Volodymyr Dudko contributed with scientific discussion. The publication was written by Prof Josef Breu and me.

My contribution to this publication is 70%.

# Osmotic Swelling of Sodium Hectorite in Ternary Solvent Mixtures: Nematic Liquid Crystals in Hydrophobic Media

Lina Mayr, Sonja Amschler, Andreas Edenharter, Volodymyr Dudko, Raphael Kunz, Sabine Rosenfeldt, and Josef Breu\*



Cite This: *Langmuir* 2020, 36, 3814–3820



Read Online

ACCESS |



Metrics & More

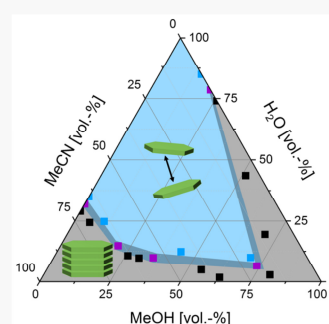


Article Recommendations



Supporting Information

**ABSTRACT:** The swelling of clay minerals in organic solvents or solvent mixtures is key for the fabrication of polymer nanocomposites with perfectly dispersed filler that contain only individual clay layers. Here, we investigated the swelling behavior of sodium hectorite in different ternary solvent mixtures containing methanol, acetonitrile, ethylene glycol, or glycerol carbonate with minimal amounts of water. We found that in these mixtures, less water is required than in the corresponding binary mixtures to allow for complete delamination by repulsive osmotic swelling. A quantitative study of osmotic swelling in a particular ternary mixture shows that organic solvents resemble swelling behavior in pure water. At hectorite contents larger than 5 vol %, the separation of individual layers scales with  $\phi^{-1}$ . At this concentration, a crossover is observed and swelling continues at a slower pace ( $\phi^{-0.5}$ ) below this value.



## INTRODUCTION

The use of clays, e.g., smectites, as fillers in polymers significantly improves gas barrier,<sup>1,2</sup> flame retardancy,<sup>3,4</sup> or mechanical properties.<sup>5–7</sup> For all these applications, the effective aspect ratio of the platy filler is the crucial parameter. The aspect ratio of layered compounds can be maximized by osmotic swelling<sup>8–10</sup> into single  $\approx 1$  nm thick 2:1 silicate layers. Being repulsive<sup>9,11</sup> in nature it allows for an utter and most gentle delamination process (a definition of delamination versus exfoliation is given elsewhere<sup>12</sup>). Contrary to liquid-phase exfoliation<sup>13</sup> that applies brute force sonication, osmotic swelling preserves the aspect ratio (diameter/thickness-ratio) inherent in the platelet diameter of the nondelaminated starting material.

A vast body of literature exists on the swelling of clays in water.<sup>14–21</sup> Comparatively, only a few, mostly older studies, focus on swelling of clay with organic media or solvent mixtures.<sup>22–24</sup>

In water, two swelling regimes exist: crystalline and osmotic swelling. Crystalline swelling is strongly dependent on water activity,<sup>19</sup> valence and hydration enthalpy of interlayer cations,<sup>25</sup> and the layer charge.<sup>11</sup> Unfortunately, natural clay minerals suffer from extensive charge heterogeneities that are reflected in a nonuniform swelling behavior of the various domains. Consequently, studying their swelling behavior is hampered by random interstratifications of different solvation levels occurring within the coherence length of the X-ray beam.<sup>16</sup> For instance, for natural montmorillonites, 0, 1, 2, and 3 water layer (WL) hydrates have been shown to coexist. In contrast, hectorite (NaHec),

$[\text{Na}_{0.5}]^{\text{inter}}[\text{Mg}_{2.5}\text{Li}_{0.5}]^{\text{oct}}[\text{Si}_4]^{\text{tet}}\text{O}_{10}\text{F}_2$ ) obtained by melt synthesis possesses a uniform charge density.<sup>26</sup> Therefore, its intercrystalline reactivity is uniform at all length scales, which facilitates characterization of swelling.

NaHec shows osmotic swelling,<sup>8</sup> having nanosheets with 1 nm thickness and a median diameter of 18  $\mu\text{m}$  which are obtained simply by immersing the as-synthesized material into deionized water.<sup>26</sup> Due to the large aspect ratio, the rotation of the nanosheets in suspension is hindered. Even very dilute suspensions of NaHec (<1 vol %) form nematic phases<sup>18</sup> as evidenced by small-angle X-ray scattering (SAXS). Negatively charged NaHec nanosheets adopt a cofacial arrangement due to strong electrostatic repulsion, and in this nematic state, adjacent clay nanosheets are not only held in a coherent cofacial geometry but are separated to long distances determined by the clay. This allows for easy diffusion of polymer chains into the galleries between adjacent nanosheets. Simply by the mixing of the aqueous nematic clay dispersions with water-soluble polymers, composite films can be cast without any restacking and all individual clay nanosheets are separated by the polymer matrix.<sup>27,28</sup>

Unfortunately, most polymers are not water-soluble. Therefore, it is highly desirable to obtain nematic phases by repulsive

Received: February 10, 2020

Revised: March 20, 2020

Published: March 20, 2020



osmotic swelling in organic solvents to facilitate the fabrication of nanocomposites. However, osmotic swelling has been shown long ago to be hampered in organic solvents.<sup>29</sup> Nevertheless, osmotic swelling of clay minerals has been observed for very few binary mixtures of organic solvents with water.<sup>30</sup> For instance, for NaHec, osmotic swelling in acetonitrile-water mixtures sets in at water contents exceeding 35 vol %.<sup>31</sup> Since it is the entropy contribution that is decisive for the repulsive nature of osmotic swelling,<sup>10</sup> it appears promising to increase the entropy of mixing contribution by applying ternary instead of binary mixtures as swelling medium. Here, the swelling of Na<sub>0.5</sub>-fluorohectorite in three different ternary solvent mixtures was investigated and osmotic swelling was indeed found to be an abundant phenomenon. Moreover, the minimum water content required to trigger osmotic swelling could be reduced significantly as compared to binary mixtures.

## EXPERIMENTAL SECTION

**Synthesis of Sodium Hectorite.** Sodium hectorite ( $[\text{Na}_{0.5}]^{\text{inter}}[\text{Mg}_{2.5}\text{Li}_{0.5}]^{\text{oct}}[\text{Si}_4]^{\text{tet}}\text{O}_{10}\text{F}_2$ , NaHec) was obtained by a melt synthesis according to a published procedure.<sup>26</sup>

**Swelling Experiments.** The hygroscopic NaHec was stored in a desiccator with a relative humidity of 43% (saturated potassium carbonate solution) to obtain the 1-WL hydrate. Clay dispersions with typically 3–4 wt % (1–2 vol %) were made by adding varying volumes of the individual solvents (Milli-Q water, acetonitrile (Merck Millipore, 99.9%), methanol (VWR, p.a.), ethylene glycol (Fluka, 99.5%), glycerol carbonate (abcr, 90%)) summing up to typically 1 mL to 30–60 mg of NaHec. Interlayer water was regarded as part of the water volume fraction.

For the quantitative evaluation of osmotic swelling in a mixture of 44 vol % methanol, 12 vol % water, and 44 vol % acetonitrile, varying amounts of NaHec (4–200 mg) corresponding to 1–11 vol % were added to 0.7 mL of the solvent mixture. All samples were equilibrated in an overhead shaker for 5 days at room temperature.

**Small Angle X-ray Scattering (SAXS).** Measurement of SAXS data was performed with a “Double Ganesha AIR” (SAXSLAB, Denmark). In this laboratory based system, X-rays are provided by a rotating copper anode (MicoMax 007HF, Rigaku Corporation, Japan) yielding to a microfocused beam. A position sensitive detector (PILATUS 300 K, Dectris) is used in different positions to cover the range of the scattering vector  $q = 0.004\text{--}0.6 \text{ \AA}^{-1}$ . Prior to the measurement, the clay suspensions were filled in 1 mm glass capillaries (Hilgenberg, code 4007610). The circularly averaged data were normalized to incident beam, sample thickness, and measurement time.

**X-ray Diffraction.** Measurement of XRD patterns were performed in transmission mode on a STOE STADI P powder diffractometer (Cu  $K_{\alpha 1}$  radiation, GE monochromator, linear position sensitive detector). Prior to the measurement, the clay suspensions were filled in 1 mm glass capillaries (Hilgenberg, code 4007610).

## RESULTS AND DISCUSSION

**Phase Diagrams.** A Gutmann donor number, which is a measure of Lewis basicity, of at least 14 was found to be prerequisite for moving  $\text{Na}^+$  from the hexagonal cavities toward the middle of the interlayer space to allow a complete solvation<sup>32</sup> while all other solvent parameters (Table 1) showed no correlation.<sup>33</sup> On the basis of this literature, acetonitrile and methanol with Gutmann donor numbers of 14.1 and 19, respectively, were used in combination with water as a first example of a ternary solvent mixture. These solvents should be able to remove  $\text{Na}^+$  from the hexagonal cavities. Obviously, an exhaustive study of all potential ternary mixtures is beyond the scope of any single paper. For the second ternary

**Table 1. Solubility Parameter, Dipole Moment, Relative Permittivity and Gutmann Donor Number of the Used Solvents**

	Hildebrand solubility parameter [MPa <sup>0.5</sup> ]	Dipole moment [D]	Relative permittivity (at 20 °C)	Gutmann Donor number [kcal mol <sup>-1</sup> ]
Water	47.9 <sup>38</sup>	1.85 <sup>39</sup>	80.1 <sup>40</sup>	18 <sup>41</sup>
Glycerol carbonate	34.1 <sup>42</sup>	5.05 <sup>42</sup>	111.5 <sup>42</sup>	nd
Acetonitrile	24.3 <sup>38</sup>	3.93 <sup>39</sup>	36.6 <sup>40</sup>	14.1 <sup>41</sup>
Ethylene glycol	29.9 <sup>38</sup>	2.36 <sup>39</sup>	41.4 <sup>40</sup>	20 <sup>41</sup>
Methanol	29.7 <sup>38</sup>	1.70 <sup>39</sup>	33.0 <sup>40</sup>	19 <sup>41</sup>

mixture, methanol was replaced by ethylene glycol. The latter is renowned for its crystalline swelling behavior, which is applied for quantitative evaluation for the montmorillonite content of bentonites.<sup>34–36</sup> As a third mixture, acetonitrile was replaced by glycerol carbonate, which may appear as a somewhat odd solvent to choose, but this rather polar monomer could be polymerized within the interlayer space into polyglycerol carbonate, a water-soluble and biodegradable polymer.<sup>37</sup>

The compositions of solvent mixtures were initially screened visually. If sediments were visible, swelling was restricted to the crystalline regime and this was subsequently verified by recording X-ray diffractograms of the sediments in suspension (Figures S1–S3, black squares in Figure 1b, Figure 2b, Figure 3b). No observable sediments and a viscosity higher than that of the pure dispersion medium were taken as a first indication for osmotic swelling. These samples were further characterized by SAXS and are displayed as blue or purple data points in the phase diagrams (Figures 1–3). At the applied clay content, nematic phases were obtained if indeed repulsive osmotic swelling had set in.<sup>18</sup> Due to the large aspect ratio of individual NaHec layers, rotation of the nanosheets in osmotically swollen suspensions is hindered and clay nanosheets are held in a coherent cofacial geometry with large separations. Consequently, SAXS is an appropriate tool to screen for osmotic swelling. SAXS curves of osmotically swollen NaHec show a  $q^{-2}$  scaling at low and intermediate  $q$  as it is typical for 2-dimensional objects scattering.<sup>18</sup> The layer separation of the nematic phases were indicated by interference peaks caused by the regular, large separation of adjacent clay nanosheets (Figure 5a). Scattering curves of samples that were not completely osmotically swollen show an additional peak at high  $q$ -values, corresponding to the basal spacing of the crystalline swollen NaHec phases (Figure 1a, purple curve).

As previously reported, in binary acetonitrile-water mixtures, osmotic swelling was observed up to a maximum acetonitrile content of 65 vol %. At 68 vol % acetonitrile, a biphasic mixture was observed with osmotically and crystalline swollen NaHec coexisting.<sup>31</sup>

Binary solvent mixtures of methanol and water required a much higher threshold of water for triggering osmotic swelling. For this binary mixture, only 15 vol % methanol was tolerated. In a mixture with 21 vol % methanol, the system is already biphasic and at 26 vol %, only crystalline swollen NaHec was observed (Figures S1 and S5).

When NaHec was swollen in ternary mixtures of methanol, water, and acetonitrile, significantly less water was found to be necessary for osmotic swelling to set in (Figure 1b). For

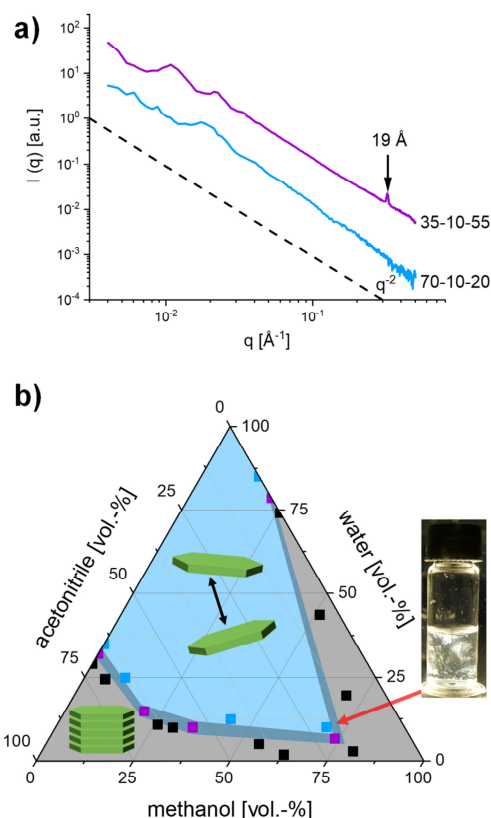


**Figure 1.** (a) SAXS curves of completely osmotically swollen (blue) and biphasic (purple) NaHec in a mixture of methanol-water-acetonitrile (numbers next to the curves are vol % of the three solvents). (b) Ternary phase diagram of NaHec swollen in methanol-water-acetonitrile mixtures (blue squares: osmotically swollen, purple squares: biphasic system, black squares: crystalline swollen, background colors are a guide for the eye to distinguish osmotic and crystalline swelling regimes; suspensions contained 1–2 vol % NaHec; insets are schematics of crystalline and osmotic swollen NaHec) along with an image of a representative nematic sample between crossed polarizers.

instance, a mixture with 35 vol % methanol and 55 vol % acetonitrile required as little as 10 vol % of water for osmotic swelling to set in (purple square in Figure 1b). This particular sample, however, still was biphasic having a small fraction of crystalline swollen phase visible in the SAXS pattern (purple curve in Figure 1a). By increasing the methanol content, complete osmotic swelling occurred at the same water content (70 vol % methanol, 20 vol % acetonitrile; see Figure 1a (blue curve) and Figure 1b (blue square)). An extension of the experiments to many more various solvent mixtures produced a ternary phase diagram (Figure 1b, Figures S4 and S5). The composition regimes for osmotic and crystalline swelling are colored in blue and black while the biphasic transition zone is marked purple. In the ternary mixtures, the threshold water content for osmotic swelling to set in was found generally to be significantly lower than in the corresponding binary mixtures. Even though for the binary water-acetonitrile and methanol-water mixtures, the latter requires a much higher water content, the ternary mixture allowing osmotic swelling with the lowest amount of water (70 vol % methanol and 20 vol %

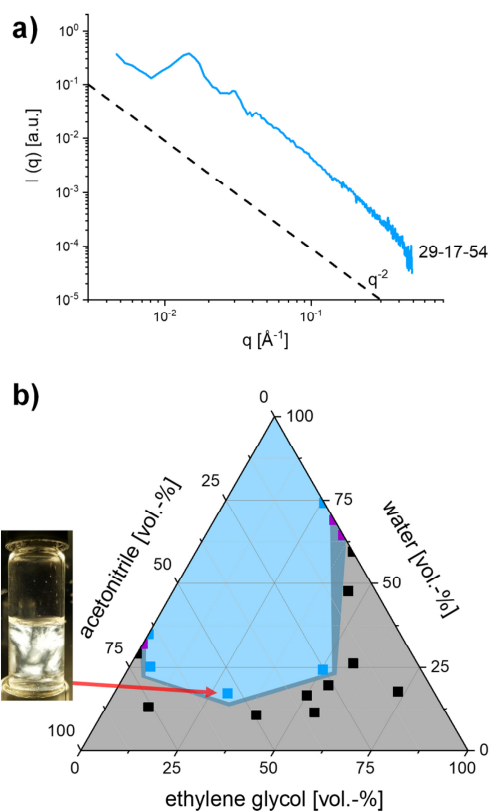


**Figure 2.** (a) SAXS curve of osmotically swollen NaHec in 29 vol % ethylene glycol, 17 vol % water, 54 vol % acetonitrile. (b) Ternary phase diagram of NaHec swollen in ethylene glycol-water-acetonitrile mixtures (blue squares: osmotically swollen, purple squares: biphasic system, black squares: crystalline swollen, background colors are a guide for the eye to distinguish osmotic and crystalline swelling regimes; suspensions contained 1–2 vol % NaHec) along with an image of a representative nematic sample between crossed polarizers.

acetonitrile) surprisingly contained more methanol than acetonitrile.

The basic features of the methanol-water-acetonitrile dispersant were resembled by a mixture of ethylene glycol, water, and acetonitrile (Figure 2b). In the binary mixture of ethylene glycol and water, osmotic swelling occurs up to 26 vol % ethylene glycol (Figures S6 and S7). This exhibited a higher tolerance of organic solvent content than that observed in binary methanol-water mixtures. Contrary to the methanol-water-acetonitrile dispersant, the lower threshold value of water to allow for osmotic swelling (17 vol %) for ethylene glycol-water-acetonitrile mixtures was on the acetonitrile-rich side of the mixture (Figure 2a, 29 vol % ethylene glycol and 54 vol % acetonitrile). Despite the rich intercalation chemistry of ethylene glycol, the absolute threshold value for the water content was actually significantly lower for methanol-water-acetonitrile (10 vol %).

The highest tolerance for organic solvent content in a binary swelling medium was observed with glycerol carbonate. In binary water-glycerol carbonate mixtures, osmotic swelling occurs at glycerol carbonate contents up to 90 vol % (Figure S8 and S9). Within a ternary mixture of methanol, water, and

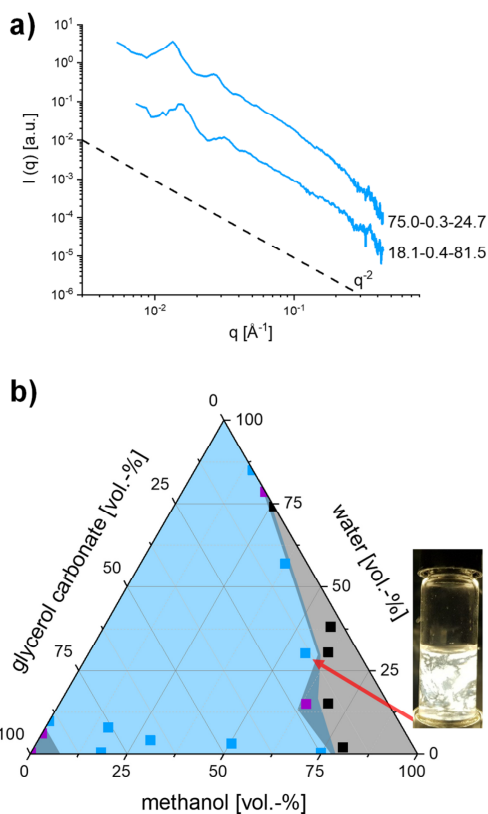


**Figure 3.** (a) SAXS curves of osmotically swollen clay in methanol-water-glycerol carbonate (numbers next to the curves are vol % of the three solvents). (b) Ternary phase diagram of NaHec swollen in methanol-water-glycerol carbonate mixtures (blue squares: osmotically swollen, purple squares: biphasic system, black squares: crystalline swollen, background colors are a guide for the eye to distinguish osmotic and crystalline swelling regimes; suspensions contained 1–2 vol % NaHec) along with an image of a representative nematic sample between crossed polarizers.

glycerol carbonate, only negligible amounts of water are necessary to allow for complete osmotic swelling (Figure 3b).

For instance, both the mixtures on the glycerol carbonate-rich side (18.1 vol % methanol, 0.4 vol % water, 81.5 vol % glycerol carbonate) and on the glycerol carbonate poor-side (75.0 vol % methanol, 0.3 vol % water, 24.7 vol % glycerol carbonate) showed complete osmotic swelling (Figure 3a). The necessary water content actually corresponds to water introduced as interlayer water in the 1-WL hydrate. No additional water was needed. The water layer is crucial for triggering osmotic swelling since completely dry NaHec did not delaminate in binary methanol-glycerol carbonate mixtures. The ternary phase diagram for NaHec swollen in methanol-water-glycerol carbonate showed the largest area representing the osmotically swollen regime (Figure 3b, blue area) of the three solvent systems tested here.

**Potential Correlation with Solvent Parameters.** Besides the postulated requirement of a Gutmann donor number of at least 14,<sup>32</sup> several other factors were discussed in literature to explain the swelling of clays with inorganic interlayer cations in organic solvents. Graber and Mingelgrin described the swelling of clays with the extended regular

solution theory normally applied for polymer solutions.<sup>43</sup> Within literature on the formation of acrylonitrile-montmorillonite complexes, Yamanaka et al. found a strong dependence on the polarizing power of the interlayer cation.<sup>44</sup> Bissada et al. worked out the influence of the cation-dipole interaction.<sup>22</sup> An evaluation of the swelling behavior of NaHec in binary solvent mixtures shows no obvious correlation between the minimal water content and Hildebrand solubility parameter, relative permittivity, or Gutmann donor number (Table 1). However, the dipole moment of the organic solvent does seem to correlate. The larger the dipole moment, the less water was necessary to set in osmotic swelling (Figure 4a). For ternary mixtures, however, the situation seems to be more complex. A correlation with the volume-weighted dipole moments of the ternary mixtures and the threshold water content needed for osmotic swelling to set in no longer exists, (Figure 4b) suggesting that other, less apparent and so far unrecognized

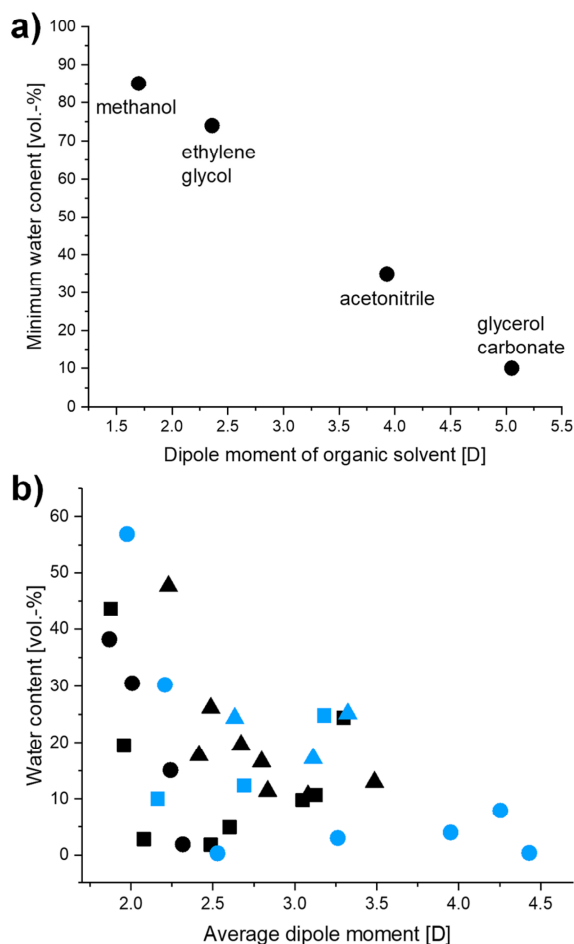


**Figure 4.** (a) Correlation between the dipole moment of organic solvents and the threshold water content needed for osmotic swelling to set in with NaHec, (b) average dipole moment (volume weighted) of ternary solvent mixtures (squares: methanol-water-acetonitrile, triangles: ethylene glycol-water-acetonitrile, circles: methanol-water-glycerol carbonate, blue: osmotically swollen NaHec, black: crystalline swollen NaHec) against the water content of the mixtures.

factors are decisive. With the available experimental data, no satisfying explanation can be given.

**Quantitative Evaluation of Osmotic Swelling.** The osmotic swelling of NaHec in one particular solvent mixture (44 vol % methanol, 12 vol % water, and 44 vol % acetonitrile) was additionally studied in a more quantitative way by following the separation of adjacent layers as a function of the volume fraction of NaHec. With decreasing NaHec content, the first peaks (001) of the scattering curves shifted toward lower  $q$ -values, which indicated an increasing layer separation (Figure 5a). Osmotic swelling of NaHec in water

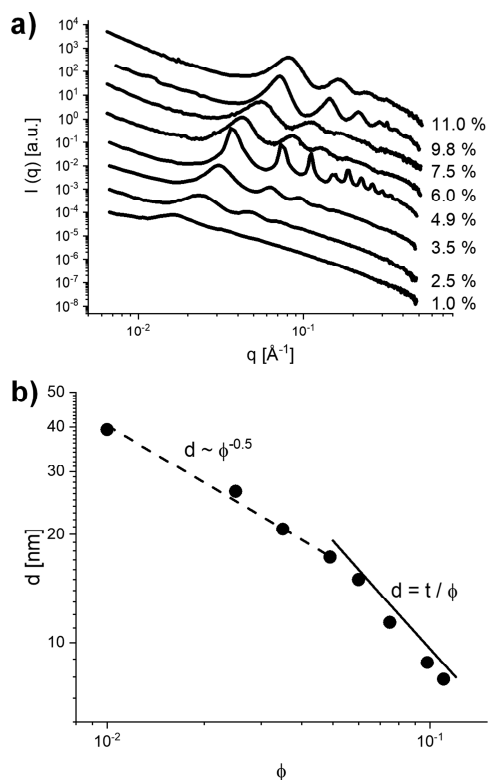


**Figure 5.** Osmotically swollen NaHec in 44 vol % methanol, 12 vol % water, and 44 vol % acetonitrile: (a) SAXS curves of different volume fractions of NaHec. (b) Observed  $d$ -spacing as a function of the volume fraction of NaHec.

comprised two subregimes depending on the volume fraction  $\phi$ . In solvent mixtures also, two subregimes were observed (Figure 5b). At high volume fractions, the separation of adjacent layers was proportional to  $t \times \phi^{-1}$ , with  $t$  being the layer thickness of the 2:1 silicate layer amounting to 9.6 Å. For NaHec contents above 5 vol %, the observed  $d$ -spacings are 15.0 nm (6.0 vol %), 11.4 nm (7.5 vol %), 8.8 nm (9.8 vol %), and 7.9 nm (11.0 vol %). This scaling indicates that all hectorite crystals have been utterly delaminated and that all silicate layers are separated to the same maximum distance utilizing the complete volume of the swelling solvent mixture available at a given solid content. This resembles the swelling behavior in pure water and indicates electrostatic repulsion. Due this repulsive nature, the modulation of the electrostatics

by the varying dielectric constant does not influence the layer separation.

At a volume fraction of NaHec of 5% ( $\phi = 0.05$ ), a crossover is observed where the slope changes to  $d \sim \phi^{-0.5}$  and swelling in this subregime continues at a slower pace. Such crossovers have also been observed for montmorillonites, nontronites,<sup>8</sup> and NaHec<sup>18</sup> during osmotic swelling in water. However, the transition between the two subregimes was observed at lower volume fractions (1.1%) for nontronite and montmorillonite and at 2.5% for synthetic NaHec. Moreover, when swelling NaHec in water, a slightly lower slope of  $\phi^{-0.66}$  was also observed in the second subregime. The reason for this crossover is not clear.

## CONCLUSION

In ternary mixtures, NaHec can be completely delaminated by repulsive osmotic swelling with less water than in corresponding binary mixtures producing nematic phases in more hydrophobic media. Although the swelling behavior lacks explanation, a synergistic effect is experimentally evidenced when swelling NaHec in a mixture of organic solvents and water. With methanol and acetonitrile, the water content could be reduced to 10 vol %. Even less water was necessary in methanol-glycerol carbonate mixtures. Here, only trace amounts of water are sufficient for complete osmotic swelling. As in water, osmotic swelling in ternary solvent mixtures comprises two subregimes with distinct dependencies on the clay content.

Osmotic swelling of NaHec with only small amounts of water may offer new, easy ways to fabricate homogeneous nanocomposites with perfectly dispersed filler nanosheets for which an organic environment is often necessary.

## ASSOCIATED CONTENT

### Supporting Information

The Supporting Information is available free of charge at <https://pubs.acs.org/doi/10.1021/acs.langmuir.0c00373>.

XRD patterns and SAXS curves that are the base of the ternary diagrams (PDF)

## AUTHOR INFORMATION

### Corresponding Author

**Josef Breu** – Department of Chemistry and Bavarian Polymer Institute, University of Bayreuth, 95447 Bayreuth, Germany; [orcid.org/0000-0002-2547-3950](https://orcid.org/0000-0002-2547-3950); Email: [josef.breu@uni-bayreuth.de](mailto:josef.breu@uni-bayreuth.de)

### Authors

**Lina Mayr** – Department of Chemistry and Bavarian Polymer Institute, University of Bayreuth, 95447 Bayreuth, Germany

**Sonja Amschler** – Department of Chemistry and Bavarian Polymer Institute, University of Bayreuth, 95447 Bayreuth, Germany

**Andreas Edenharter** – Department of Chemistry and Bavarian Polymer Institute, University of Bayreuth, 95447 Bayreuth, Germany

**Volodymyr Dudko** – Department of Chemistry and Bavarian Polymer Institute, University of Bayreuth, 95447 Bayreuth, Germany

**Raphael Kunz** – Department of Chemistry and Bavarian Polymer Institute, University of Bayreuth, 95447 Bayreuth, Germany

Sabine Rosenfeldt – Department of Chemistry and Bavarian Polymer Institute, University of Bayreuth, 95447 Bayreuth, Germany

Complete contact information is available at:  
<https://pubs.acs.org/10.1021/acs.langmuir.0c00373>

### Funding

This work was supported by the Deutsche Forschungsgemeinschaft (SFB 840 and SFB 1357).

### Notes

The authors declare no competing financial interest.

## REFERENCES

- (1) Habel, C.; Schöttle, M.; Daab, M.; Eichstaedt, N. J.; Wagner, D.; Bakhshi, H.; Agarwal, S.; Horn, M. A.; Breu, J. High-Barrier, Biodegradable Food Packaging. *Macromol. Mater. Eng.* **2018**, *303* (10), 1800333.
- (2) Grunlan, J. C.; Grigorian, A.; Hamilton, C. B.; Mehrabi, A. R. Effect of clay concentration on the oxygen permeability and optical properties of a modified poly(vinyl alcohol). *J. Appl. Polym. Sci.* **2004**, *93* (3), 1102–1109.
- (3) *Flame Retardant Polymer Nanocomposites*. John Wiley & Sons, Inc.: Hoboken, NJ, 2007.
- (4) Schütz, M. R.; Kalo, H.; Lunkenbein, T.; Breu, J.; Wilkie, C. A. Intumescent-like behavior of polystyrene synthetic clay nanocomposites. *Polymer* **2011**, *52* (15), 3288–3294.
- (5) Ziadeh, M.; Weiss, S.; Fischer, B.; Förster, S.; Altstädt, V.; Müller, A. H.; Breu, J. Towards completely miscible PMMA nanocomposites reinforced by shear-stiff, nano-mica. *J. Colloid Interface Sci.* **2014**, *425*, 143–151.
- (6) Morits, M.; Verho, T.; Sorvari, J.; Liljeström, V.; Kostianen, M. A.; Gröschel, A. H.; Ikkala, O. Toughness and Fracture Properties in Nacre-Mimetic Clay/Polymer Nanocomposites. *Adv. Funct. Mater.* **2017**, *27* (10), 1605378.
- (7) Alexandre, M.; Dubois, P. Polymer-layered silicate nanocomposites: preparation, properties and uses of a new class of materials. *Mater. Sci. Eng., R* **2000**, *28* (1–2), 1–63.
- (8) Michot, L. J.; Bihannic, I.; Maddi, S.; Funari, S. S.; Baravian, C.; Levitz, P.; Davidson, P. Liquid-crystalline aqueous clay suspensions. *Proc. Natl. Acad. Sci. U. S. A.* **2006**, *103* (44), 16101–16104.
- (9) Daab, M.; Eichstaedt, N. J.; Edenharter, A.; Rosenfeldt, S.; Breu, J. Layer charge robust delamination of organo-clays. *RSC Adv.* **2018**, *8* (50), 28797–28803.
- (10) Daab, M.; Eichstaedt, N. J.; Habel, C.; Rosenfeldt, S.; Kalo, H.; Schießling, H.; Förster, S.; Breu, J. Onset of Osmotic Swelling in Highly Charged Clay Minerals. *Langmuir* **2018**, *34* (28), 8215–8222.
- (11) Daab, M.; Rosenfeldt, S.; Kalo, H.; Stöter, M.; Bojer, B.; Siegel, R.; Förster, S.; Senker, J.; Breu, J. Two-Step Delamination of Highly Charged, Vermiculite-like Layered Silicates via Ordered Heterostructures. *Langmuir* **2017**, *33* (19), 4816–4822.
- (12) Gardolinski, J. E. F. C.; Lagaly, G. Grafted organic derivatives of kaolinite: II. Intercalation of primary n-alkylamines and delamination. *Clay Miner.* **2005**, *40* (4), 547–556.
- (13) Nicolosi, V.; Chhowalla, M.; Kanatzidis, M. G.; Strano, M. S.; Coleman, J. N. Liquid Exfoliation of Layered Materials. *Science* **2013**, *340* (6139), 1226419–1226419.
- (14) Madsen, F. T.; Müller-Vonmoos, M. The swelling behaviour of clays. *Appl. Clay Sci.* **1989**, *4* (2), 143–156.
- (15) Carrier, B.; Wang, L.; Vandamme, M.; Pellenq, R. J.; Bornert, M.; Tanguy, A.; Van Damme, H. ESEM study of the humidity-induced swelling of clay film. *Langmuir* **2013**, *29* (41), 12823–12833.
- (16) Ferrage, E.; Lanson, B.; Sakharov, B. A.; Drits, V. A. Investigation of smectite hydration properties by modeling experimental X-ray diffraction patterns: Part I. Montmorillonite hydration properties. *Am. Mineral.* **2005**, *90* (8–9), 1358–1374.
- (17) Hofmann, U.; Endell, K.; Wilm, D. Kristallstruktur und Quellung von Montmorillonit. *Z. Kristallogr. - Cryst. Mater.* **1933**, *86* (1–6), 340–348.
- (18) Rosenfeldt, S.; Stöter, M.; Schlenk, M.; Martin, T.; Albuquerque, R. Q.; Förster, S.; Breu, J. In-Depth Insights into the Key Steps of Delamination of Charged 2D Nanomaterials. *Langmuir* **2016**, *32* (41), 10582–10588.
- (19) Stöter, M.; Rosenfeldt, S.; Breu, J. Tunable Exfoliation of Synthetic Clays. *Annu. Rev. Mater. Res.* **2015**, *45* (1), 129–151.
- (20) Hansen, E. L.; Hemmen, H.; Fonseca, D. M.; Coutant, C.; Knudsen, K. D.; Plivelic, T. S.; Bonn, D.; Fossum, J. O. Swelling transition of a clay induced by heating. *Sci. Rep.* **2012**, *2*, 618.
- (21) Norrish, K. The swelling of montmorillonite. *Discuss. Faraday Soc.* **1954**, *18*, 120–134.
- (22) Bissada, K. K.; Johns, W. D.; Cheng, F. S. Cation-dipole interactions in clay organic complexes. *Clay Miner.* **1967**, *7* (2), 155–166.
- (23) Olejnik, S.; Posner, A. M.; Quirk, J. P. Swelling of Montmorillonite in Polar Organic Liquids. *Clays Clay Miner.* **1974**, *22* (4), 361–365.
- (24) Weiss, A. Organische Derivate der glimmerartigen Schichtsilicate. *Angew. Chem.* **1963**, *75* (2), 113–122.
- (25) Möller, M. W.; Handge, U. A.; Kunz, D. A.; Lunkenbein, T.; Altstädt, V.; Breu, J. Tailoring shear-stiff, mica-like nanoplatelets. *ACS Nano* **2010**, *4* (2), 717–724.
- (26) Stöter, M.; Kunz, D. A.; Schmidt, M.; Hirsemann, D.; Kalo, H.; Putz, B.; Senker, J.; Breu, J. Nanoplatelets of sodium hectorite showing aspect ratios of ~ 20 000 and superior purity. *Langmuir* **2013**, *29* (4), 1280–1285.
- (27) Tsurko, E. S.; Feicht, P.; Nehm, F.; Ament, K.; Rosenfeldt, S.; Pietsch, I.; Roschmann, K.; Kalo, H.; Breu, J. Large Scale Self-Assembly of Smectic Nanocomposite Films by Doctor Blading versus Spray Coating: Impact of Crystal Quality on Barrier Properties. *Macromolecules* **2017**, *50* (11), 4344–4350.
- (28) Wang, Z.; Rolle, K.; Schilling, T.; Hummel, P.; Philipp, A.; Kopera, B. A. F.; Lechner, A. M.; Retsch, M.; Breu, J.; Fytas, G. Tunable Thermoelastic Anisotropy in Hybrid Bragg Stacks with Extreme Polymer Confinement. *Angew. Chem., Int. Ed.* **2020**, *59* (3), 1286–1294.
- (29) Lagaly, G.; Ziesmer, S. Colloid chemistry of clay minerals: the coagulation of montmorillonite dispersions. *Adv. Colloid Interface Sci.* **2003**, *100–102*, 105–128.
- (30) Brindley, G. W. Intracrystalline Swelling of Montmorillonites in Water-Dimethylsulfoxide Systems. *Clays Clay Miner.* **1980**, *28* (5), 369–372.
- (31) Kunz, R.; Amschler, S.; Edenharter, A.; Mayr, L.; Herlitz, S.; Rosenfeldt, S.; Breu, J. Giant Multistep Crystalline Vs. Osmotic Swelling of Synthetic Hectorite in Aqueous Acetonitrile. *Clays Clay Miner.* **2020**, *469* DOI: 10.1007/s42860-019-00046-9.
- (32) Berkheiser, V.; Mortland, M. M. Variability in exchange ion position in smectite: dependence on interlayer solvent. *Clays Clay Miner.* **1975**, *23* (5), 404–410.
- (33) Onikata, M.; Kondo, M.; Yamanaka, S. Swelling of Formamide-Montmorillonite Complexes in Polar Liquids. *Clays Clay Miner.* **1999**, *47* (5), 678–681.
- (34) MacEwan, D. M. C. The identification and estimation of the montmorillonite group of minerals, with special reference to soil clays. *J. Soc. Chem. Ind., London* **1946**, *65* (10), 298–304.
- (35) Brindley, G. W. Ethylene glycol and glycerol complexes of smectites and vermiculites. *Clay Miner.* **1966**, *6* (04), 237–259.
- (36) Dowdy, R. H.; Mortland, M. M. Alcohol-Water Interactions on Montmorillonite Surfaces: II. Ethylene glycol. *Soil Sci.* **1968**, *105* (1), 36–43.
- (37) Dinh, N. T.; Mouloungui, Z.; Marechal, P. Glycerol polycarbonate, organic compositions containing same and method for obtaining said compositions. U.S. Patent 7928182 B2, April 19, 2011.
- (38) Mark, J. E. *Physical Properties of Polymers Handbook*, Second ed.; Springer: 2007.

(39) Lide, D. R. *Dipole moments* in *Handbook of Chemistry and Physics, Internet Version 2005*. CRC Press: Boca Raton, FL, 2005.

(40) Lide, D. R. *Permittivity (Dielectric Constant) of Liquids* in *Handbook of Chemistry and Physics, Internet Version 2005*. CRC Press: Boca Raton, FL, 2005.

(41) Cataldo, F. A Revision of the Gutmann Donor Numbers of a Series of Phosphoramides Including TEPA. *Eur. Chem. Bull.* **2015**, *4* (2), 92–97.

(42) Chernyak, Y. Dielectric Constant, Dipole Moment, and Solubility Parameters of Some Cyclic Acid Esters. *J. Chem. Eng. Data* **2006**, *51* (2), 416–418.

(43) Graber, E. R.; Mingelgrin, U. Clay Swelling and Regular Solution Theory. *Environ. Sci. Technol.* **1994**, *28* (13), 2360–2365.

(44) Yamanaka, S.; Kanamaru, F.; Koizumi, M. Role of interlayer cations in the formation of acrylonitrile-montmorillonite complexes. *J. Phys. Chem.* **1974**, *78* (1), 42–44.

## Supporting Information

### **Osmotic swelling of sodium hectorite in ternary solvent mixtures –**

### **Nematic liquid crystals in hydrophobic media**

*Lina Mayr<sup>1</sup>, Sonja Amschler<sup>1</sup>, Andreas Edenharter<sup>1</sup>, Volodymyr Dudko<sup>1</sup>, Raphael Kunz<sup>1</sup>,  
Sabine Rosenfeldt<sup>1</sup> and Josef Breu<sup>1\*</sup>*

<sup>1</sup>Department of Chemistry and Bavarian Polymer Institute, University of Bayreuth, 95447  
Bayreuth, Germany

\*Correspondence to J. Breu ([josef.breu@uni-bayreuth.de](mailto:josef.breu@uni-bayreuth.de))

Number of pages: 6

Number of figures: 9

Number of tables: 0

## 1. XRD patterns of suspensions in the crystalline swelling regime

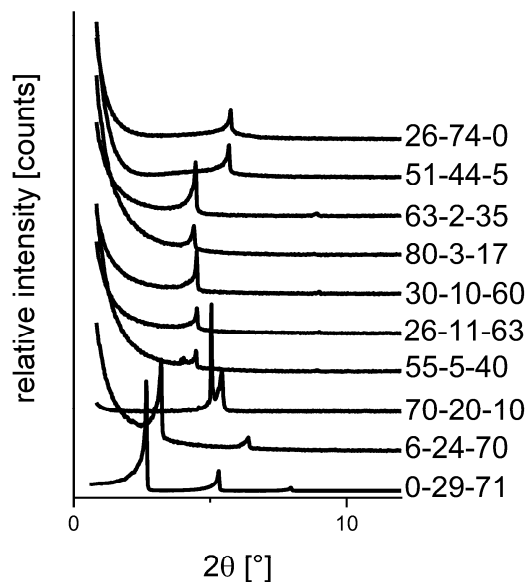
*NaHec in methanol-water-acetonitrile mixtures*

Figure S1. XRD patterns of crystalline swollen NaHec in different mixtures of methanol-water-acetonitrile (numbers next to the patterns are vol.-% of the three solvents)

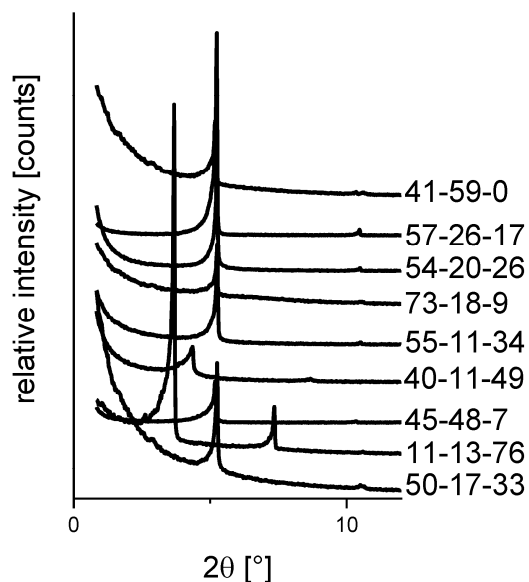
*NaHec in ethylene glycol-water-acetonitrile mixtures*

Figure S2. XRD patterns of crystalline swollen NaHec in different mixtures of ethylene glycol-water-acetonitrile (numbers next to the patterns are vol.-% of the three solvents)

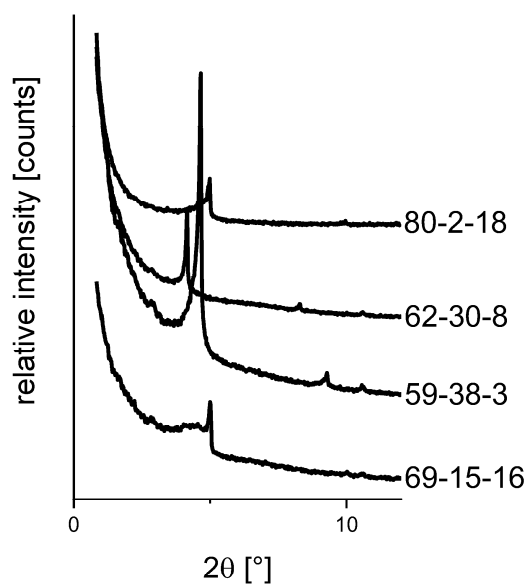
*NaHec in methanol-water-glycerol carbonate mixtures*

Figure S3. XRD patterns of crystalline swollen NaHec in different mixtures of methanol-water-glycerol carbonate (numbers next to the patterns are vol.-% of the three solvents)

## 2. SAXS curves of suspensions in the biphasic or osmotic swelling regime

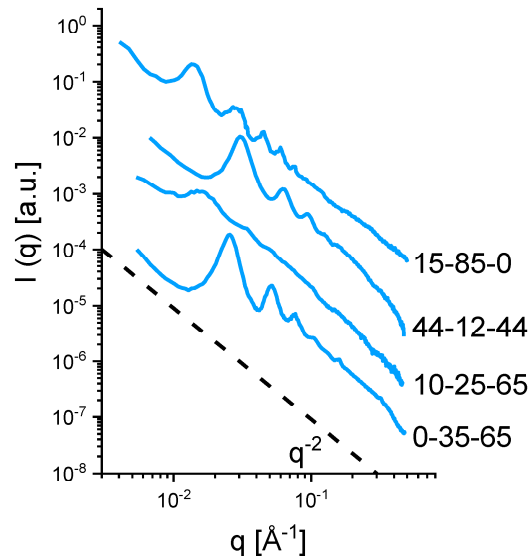
*NaHec in methanol-water-acetonitrile mixtures*

Figure S4. SAXS curves of completely osmotically swollen NaHec in different mixtures of methanol-water-acetonitrile (numbers next to the curves are vol.-% of the three solvents)

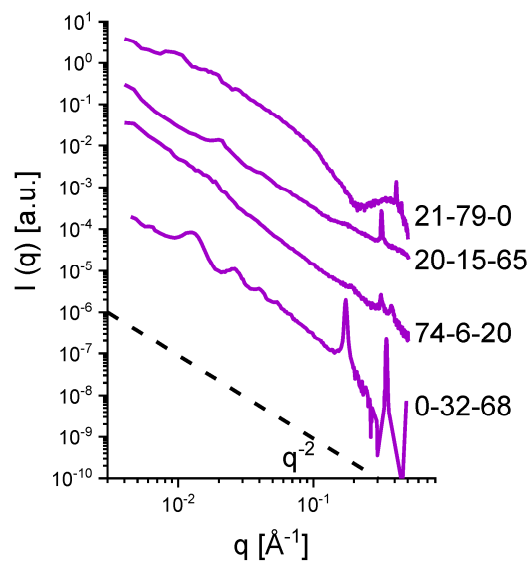


Figure S5. SAXS curves of biphasic NaHec in different mixtures of methanol-water-acetonitrile (numbers next to the curves are vol.-% of the three solvents)

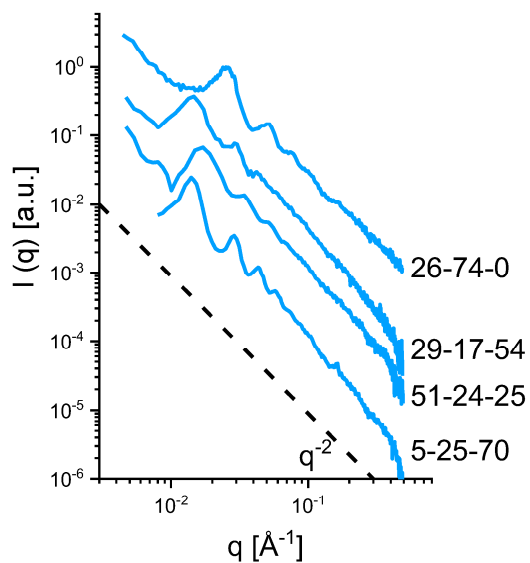
*NaHec in ethylene glycol-water-acetonitrile mixtures*

Figure S6. SAXS curves of completely osmotically swollen NaHec in different mixtures of ethylene glycol-water-acetonitrile (numbers next to the curves are vol.-% of the three solvents)

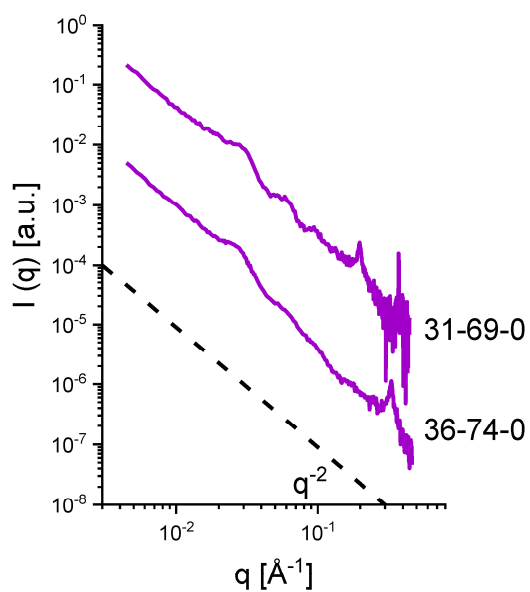


Figure S7. SAXS curves of biphasic NaHec in different mixtures of ethylene glycol-water-acetonitrile (numbers next to the curves are vol.-% of the three solvents)

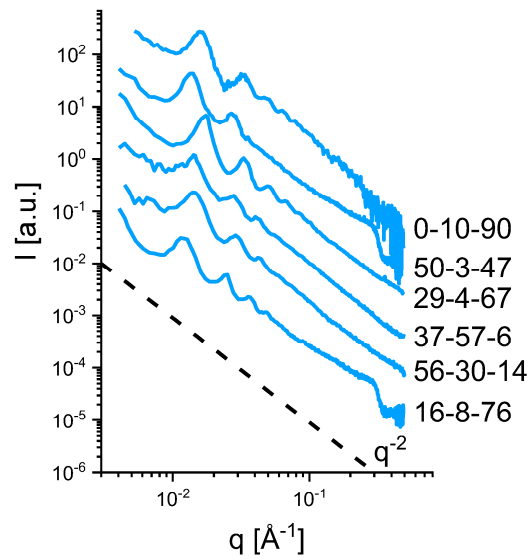
*NaHec in methanol-water-glycerol carbonate mixtures*

Figure S8. SAXS curves of completely osmotically swollen NaHec in different mixtures of methanol-water-glycerol carbonate (numbers next to the curves are vol.-% of the three solvents)

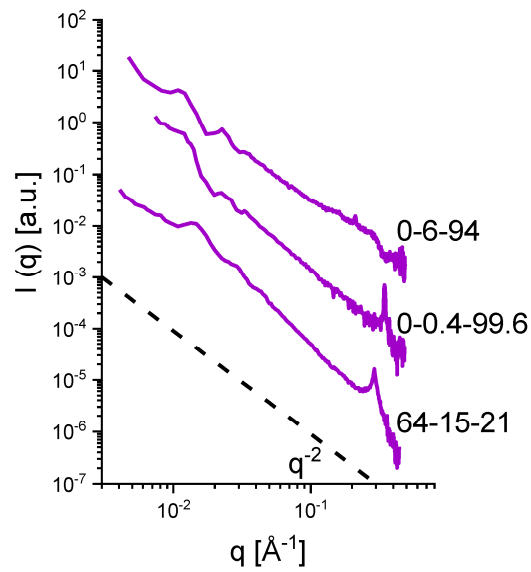


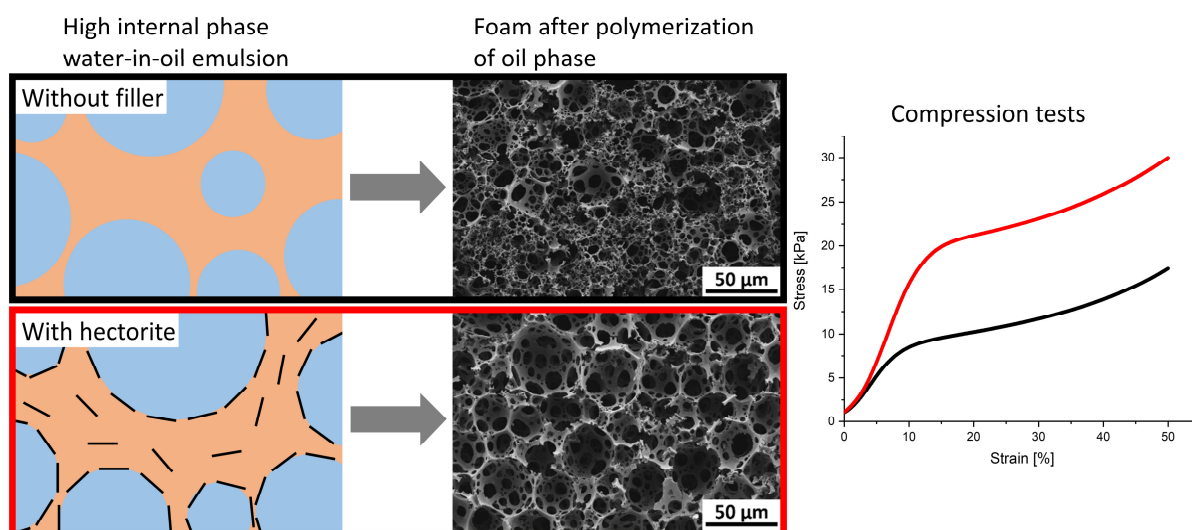
Figure S9. SAXS curves of biphasic NaHec in different mixtures of methanol-water-glycerol carbonate (numbers next to the curves are vol.-% of the three solvents)

## 6.2 Structural and mechanical impact of synthetic clay in composite foams made via high internal phase emulsions

Lina Mayr<sup>1</sup>, Arsen Simonyan<sup>2</sup>, Josef Breu<sup>1</sup> and Maxwell J. Wingert<sup>3\*</sup>

Published in: *Polymer Composites* **2021**, *42*, 353-361

Reprinted with permission, Copyright (2020) John Wiley and Sons



<sup>1</sup> Department of Chemistry and Bavarian Polymer Institute, University of Bayreuth, Universitätsstr. 30, 95440 Bayreuth, Germany

<sup>2</sup> Research & Development, Procter & Gamble, Schwalbach, Germany

<sup>3</sup> Research & Development, Procter & Gamble, Cincinnati, Ohio

\*Corresponding author: wingert.m@pg.com

### Author's individual contributions:

This publication was the result of a collaboration with Procter & Gamble. The concept was developed by all authors. I did all the syntheses and conducted all characterization methods. The publication was written by Maxwell Wingert, Prof Josef Breu and me. Arsen Simonyan contributed to scientific discussion.

My contribution to this publication is 80%.



# Structural and mechanical impact of synthetic clay in composite foams made via high-internal phase emulsions

Lina Mayr<sup>1</sup> | Arsen Simonyan<sup>2</sup> | Josef Breu<sup>1</sup> | Maxwell Joseph Wingert<sup>3</sup><sup>1</sup>Department of Chemistry and Bavarian Polymer Institute, University of Bayreuth, Bayreuth, Germany<sup>2</sup>Research & Development, Procter & Gamble, Schwalbach, Germany<sup>3</sup>Research & Development, Procter & Gamble, Cincinnati, Ohio**Correspondence**Maxwell Wingert, Research & Development, Procter & Gamble, Cincinnati, OH.  
Email: wingert.m@pg.com**Abstract**

Impacts of organophilic clay on open cell foams created from high-internal phase emulsion templating were explored. Improving mechanical properties such as compression modulus by fillers is typically most challenging to realize. We investigated the effect of two different fillers: synthetic hectorite organophilized with a custom-made organo-cation and commercial organophilic montmorillonite. Contrary to the montmorillonite, the hectorite could significantly improve the foam mechanics, up to four times for foams with a relative density of 4.1%. Investigation of bulk mechanics and the morphology of foams led to the conclusion that the foam mechanics improvement is not due to a reinforcement of the struts. Instead, the organophilic hectorite might act as a Pickering emulsifier in addition to the molecular surfactants to achieve a more consistent structure, which in particular possesses more uniform strut thickness and improved mechanical properties.

**KEYWORDS**

clay, composites, foams

## 1 | INTRODUCTION

Incorporation of layered nanomaterials like clays in polymer matrices is of great interest in research and industry since the first experiments by researchers from Toyota.<sup>[1,2]</sup> Such polymer clay nanocomposites can show improvements in gas barrier,<sup>[3,4]</sup> flame retardancy,<sup>[5]</sup> and mechanical properties.<sup>[2,6,7]</sup> Due to their large aspect ratio, they are good candidates for mechanical reinforcement. Even filler contents below 5% can significantly enhance the Young's modulus<sup>[8]</sup> and toughness.<sup>[9]</sup> As many polymers are hydrophobic and clay minerals are hydrophilic, organophilization of the filler is necessary. For this, the inorganic interlayer ions of the clay are usually exchanged against alkyl ammonium ions.<sup>[10,11]</sup> Moreover, custom-made modifiers are often used to optimize the compatibility with the polymer or to anchor polymerizable groups to the clay surface.<sup>[12–14]</sup>

Not only the incorporation of clay in polymers is of large interest, but also the formation of polymer foam

nanocomposites. One attractive way to make open cell polymer foams is the use of high-internal phase emulsions (HIPes) as templates.<sup>[15,16]</sup> In these emulsions, the dispersed phase exceeds 74% of the total volume resulting in a major phase that is present as polydisperse or polyhedral droplets in a minor continuous phase. If the continuous phase consists of monomers, the HIPE can be polymerized to form an open cell foam with highly interconnected pores and a low density.<sup>[17]</sup> In most cases, water in oil (w/o) emulsions are used to make these foams. The external phase consists of monomers, cross-linker, and molecular surfactants to stabilize the emulsion. The internal aqueous phase is mostly water. Since these foams have been made of a variety of polymers, which also can be post-modified, they have various possible applications such as catalyst supports, filtration media, absorbent materials, tissue scaffolds, smart materials, and templates for metal or inorganic open cell foams.<sup>[18,19]</sup>

Addition of fillers is one strategy to improve the utility of open cell foams, which can be fragile particularly upon tension or bending. Different fillers were incorporated in HIPE-based foams like spherical nanoparticles<sup>[20,21]</sup> or clay materials.<sup>[22–24]</sup> For example, Lépine et al synthesized foams from styrene and divinylbenzene with different montmorillonites as fillers.<sup>[25]</sup> Incorporation of montmorillonite modified with an ammonium cation with double bond increased the Young's modulus while preserving the open cell structure. At high-loading levels (>5 wt%), the mechanical behavior changed from plastic to brittle. When hydrophilic sodium montmorillonite was added through the aqueous phase, however, a bad compatibility with the monomers triggered aggregation. Consequently, no beneficial influence on the mechanical properties was observed. Thus, organophilization of clay is key for fabrication of composites based on HIPES. Berber et al found an improvement in the mechanics of foams based on polyester resin and divinylbenzene when they added alkylammonium modified montmorillonite as filler.<sup>[26]</sup> In addition, incorporating organoclay led to smaller cell sizes and a higher surface area of the foam. In general, the mechanism of mechanical reinforcement of foams is more complicated than in bulk polymers. For foams the mechanical behavior is determined not only by the mechanical properties of the polymer the struts are made from but the foam morphology is equally important. Here, we studied the influence of organophilized clay on both, the mechanics of foams and bulk polymer and on the foam morphology. For this, we used a synthetic hectorite with a narrow size distribution as filler for foams based on HIPES with low-relative densities (4%–7%). In order to minimize agglomeration of the filler, the hectorite is organophilized with a custom-made oligomeric cation.

## 2 | EXPERIMENTAL

### 2.1 | Materials

All chemicals were used as received. Cysteamine (>98%), sodium persulfate (>98%), 2,2'-azobis(2-methylpropionitrile) (AIBN, 98%), HCl in ethanol (1.25 M), lauroyl peroxide (97%), and organophilized montmorillonite ("nanoclay" containing 35–45 wt% dimethyl dialkyl [C<sub>14</sub>–C<sub>18</sub>] ammonium, organophilic montmorillonite [O-MMT]) were purchased from Sigma Aldrich. Toluene (>99.8%) and tetrahydrofuran (THF, >99.8%) were purchased from Fisher chemical. Basic aluminum oxide (Alox, Brockmann I, 50–200 μm) was purchased from Acros Organics. Magnesium sulfate (99%) was purchased from Grüssing. Sodium chloride was purchased from Bernd Kraft. 2-Ethyl hexyl acrylate was purchased from BASF. Ethylene glycol dimethacrylate was purchased from Evonik. Polyglycerol isostearate and dialkyl dimethyl

ammonium methyl sulfate (DTDMAMS) were provided by Procter & Gamble.

### 2.2 | Characterization methods

Particle size distribution was measured by static light scattering at a Retsch LA-950 (Horiba) according to ISO 13320. The hydrodynamic diameter obtained from dilute suspensions was previously shown to correlate well with the diameter of the clay platelets.<sup>[27]</sup>

<sup>1</sup>H nuclear magnetic resonance spectroscopy (NMR) was measured applying a Bruker Avance 300 (Bruker) at 300 MHz. CDCl<sub>3</sub> was used as a solvent.

Scanning electron microscopy (SEM) images were taken with a Zeiss LEO 1530 (Carl Zeiss AG) using an acceleration voltage of 3 kV. Prior to measurement, samples were cut at room temperature with a razor blade and then coated with 2 nm platinum at a Cressington Sputter Coater 208HR (Cressington Scientific Instruments). For the distributions of cell, window and strut sizes, more than 200 measurements from at least two images were done (AxioVision LE). The measured cell diameter  $D_m$  was corrected by  $D = \frac{2D_m}{\sqrt{3}}$  to take into account that the cross-sections are not at the center of the cell.<sup>[28]</sup>

Compression tests were done at a Zwick Z050 universal testing machine (Zwick Roell, testXpert II) equipped with a 0.5 kN cell load. Cylindrical samples with a diameter of 25 mm and a height of 3 mm were cut from the washed and dried foams. All measurements were done at room temperature and a compression rate of 0.3 mm/min. The samples were compressed to 50% of the original height.

Tensile tests were done at an Instron 5565 universal testing machine equipped with a 1 kN cell load. Rectangular specimens (60 x 10 mm) were cut from the polymer plates. All measurements were done at room temperature and a strain rate of 0.5 mm/min.

Krypton physisorption (Quantachrome Autosorb 1 at 77 K) was applied to calculate the surface area by BET (Brunauer-Emmett-Teller) equation.

### 2.3 | Synthesis of the oligomeric organocation (oligomeric PEHMA-NH<sub>3</sub><sup>+</sup>)

The oligomer was synthesized according to a method published by Wu et al.<sup>[29]</sup> 19.8 g of EHMA, dissolved in 150 mL of toluene, were filtrated over basic Alox to remove the inhibitor and then added together with 0.33 g AIBN to a solution of 1.5 g cysteamine in 200 mL of toluene. The mixture was purged with nitrogen for 15 minutes. Then the reaction was initiated by increasing the temperature to 85°C for 2 hours. For purification, the organic phase is

extracted three times with water and then dried over magnesium sulfate. To protonate the oligomer, HCl in ethanol was added in excess (16.2 mL, 1.25 M) before removing the solvent. The  $^1\text{H-NMR}$  spectrum of the product was recorded to determine the chain length by comparing the signals of the methylene groups neighboring to sulfur and nitrogen with the signal of the methylene groups next to the oxygen (Figure S1). An average chain length of  $n \approx 5$  resulted, which is in accordance with the applied ratio of monomer to cysteamine (5:1).

## 2.4 | Synthesis and organophilization of the layered silicate

$\text{Na}_{0.5}$ -fluorohectorite  $[\text{Na}_{0.5}][\text{Li}_{0.5}\text{Mg}_{2.5}][\text{Si}_4]\text{O}_{10}\text{F}_2$  was obtained by melt synthesis as described in literature.<sup>[30,31]</sup> To adjust the diameter to strut dimensions, an aqueous delaminated hectorite suspension (4 mg/mL) was ultrasonicated for 15 minutes applying a Hielscher UIP1000hd.

For the organophilization, a solution of the oligomeric modifier in THF (20 mL, 40 mg/mL) was added to the aqueous hectorite suspension (500 mL, 1 mg/mL) under vigorous stirring. The organophilic hectorite (HecPEHMA) was then transferred to THF by centrifugation (60 minutes, 14 000 rpm) followed by redispersion in THF.

## 2.5 | Synthesis of foams

The HIPes were synthesized using a custom-made setup. The external oil phase was filled in a PP bottle, which is placed in a heated (65°C) double jacketed beaker. The internal aqueous phase was pumped (25 mL/min) via a heating bath (70°C) into the PP bottle. The initiator solution was directly added to the PP bottle at the beginning of the addition of the aqueous phase. Emulsification was assured by an overhead stirrer at 200 rpm. After complete addition of the aqueous phase, stirring continued for another 2 minutes. Curing of the foam occurred overnight in an oven set at 80°C. Afterwards, the wet foam was cut into 3 mm thick slices with an electrical slicer. These slices were washed with water and dried afterwards.

For a typical reference emulsion, 8 g of oil phase, consisting of 65% 2-ethylhexyl acrylate, 28% ethylene glycol dimethacrylate, 6% polyglycerol isostearate, and 1% DTDMAms, was used. The aqueous phase was composed of 152 g of a 2% sodium chloride solution and 8 g of a 4 wt% solution of sodium persulfate. The water to oil ratio was systematically varied in order to get different foam densities (16:1-24:1 mass ratio).

For making composite foams with HecPEHMA, the desired amount (0.5-2 wt% referred to oil phase) of

HecPEHMA in THF was mixed with the oil phase. Prior to emulsification, THF was removed by evaporation and the suspension was ultrasonicated in an ultrasonication bath for 30 seconds to improve dispersion. O-MMT was dispersed in the oil phase in the same way.

The foam density was calculated by the mass and the dimensions of the specimens used for the compression tests. The relative density was determined by dividing the foam density by the bulk polymer density (1053 mg/cm<sup>3</sup>).

## 2.6 | Synthesis of bulk polymer plates

Lauryl peroxide (0.018 g) is dissolved in the oil phase (18 g, same composition than for the foams) as radical initiator. To produce a nanocomposite, HecPEHMA was transferred to the oil phase as described above prior to the addition of initiator. The polymerization took place between glass plates at 80°C overnight.

## 3 | RESULTS AND DISCUSSION

### 3.1 | Synthesis of HecPEHMA

Sodium fluorohectorite (NaHec) consists of parallel stacked negatively charged platelets of 1 nm thickness and 20  $\mu\text{m}$  width, separated by sodium cations.<sup>[31]</sup> Melt synthesis, moreover assures high purity and charge homogeneity. Upon immersing in water NaHec spontaneously delaminates into single 1 nm thick nanosheets preserving the original diameter yielding an average aspect ratio of 20 000.<sup>[32]</sup> To adjust the lateral platelet size to the strut size of foams, the platelets were therefore chopped down to a median diameter of 0.2  $\mu\text{m}$  (Figure S2) applying ultrasonication. For a good dispersion of NaHec in the monomer oil phase, the hydrophilic, negatively charged nanosheets were organophilized by ion-exchange with an oligomeric cation (oligomeric PEHMA-NH<sub>3</sub><sup>+</sup>), which is chemically similar to one of the monomers.

Upon addition of oligomeric PEHMA-NH<sub>3</sub><sup>+</sup> the clay instantly flocculated and the HecPEHMA could then be transferred into THF. For comparison, a commercial O-MMT was applied that had been organophilized by the supplier with dimethyl dialky (C<sub>14</sub>-C<sub>18</sub>) ammonium. Both fillers, the ultrasonicated HecPEHMA and the O-MMT, have comparable lateral sizes of typically 0.2  $\mu\text{m}$  (Figure S3).

### 3.2 | Synthesis of foams and foam properties

For comparison, foams without filler were made. The oil phase consisted of the monomer 2-ethyl hexylacrylate, the

cross-linker diethylene glycol dimethacrylate and two surfactants (polyglycerol isostearate and DTDMA). The aqueous phase contained 2% NaCl. As one of the most important properties of a foam is its density, the influence of relative density  $\rho_{rel}$  on the mechanics (compression modulus  $E$ ) was studied. For a very simplified model, Gibson and Ashby calculated a (Equation (1))

$$E = C_1 \cdot \rho_{rel}^2 \cdot E_s, \quad (1)$$

dependency (where  $E_s$  is the bulk Young's modulus and  $C_1 = 1$ ).<sup>[33]</sup> (Figure 1).

The model of Gibson and Ashby assumes that the foam mechanics are solely determined by the relative density while the foam morphology, in particular its uniformity, is consistent with varying density. In reality, however, uniformity of foams is rather inconsistent (Figure 2) and this perhaps explains the deviation from the simple model. Certainly, cell sizes and strut thicknesses vary considerably. However, improved correlations have been suggested.<sup>[34–36]</sup> Experimental data do not match the simple correlation with  $C_1 = 1$  (Figure 1) but our data rather can be best fitted with

$$E = A \cdot \rho_{rel}^B \cdot E_s, \quad (2)$$

(Equation (2), with  $A = 20.8$  and  $B = 3.2$ ).

For nanocomposites, HecPEHMA was transferred from THF to the oil phase via solvent evaporation. This has the advantage that the clay is never going through a dry state, which would inevitably trigger partial restacking of the clay platelets into band-like aggregates.

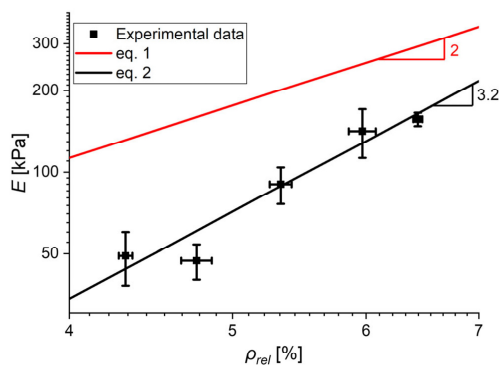


**FIGURE 1** Experimental data of compression modulus of foams without filler depending on the relative foam density compared to the model of Gibson and Ashby (red line, Equation (1)) and fitted according to Equation (2) (black line) [Color figure can be viewed at [wileyonlinelibrary.com](http://wileyonlinelibrary.com)]

This way suspensions in THF or the oil phase were obtained that were stable with no visually detectable sedimentation. With all applied HecPEHMA contents (0.5–2 wt% referred to the oil phase), the emulsions could be polymerized successfully. All foams had an open cell structure and no clay aggregates were observed in the SEM images (Figure 3, Figure S4, S5). No large voids were observed that would be associated with entrapped air.

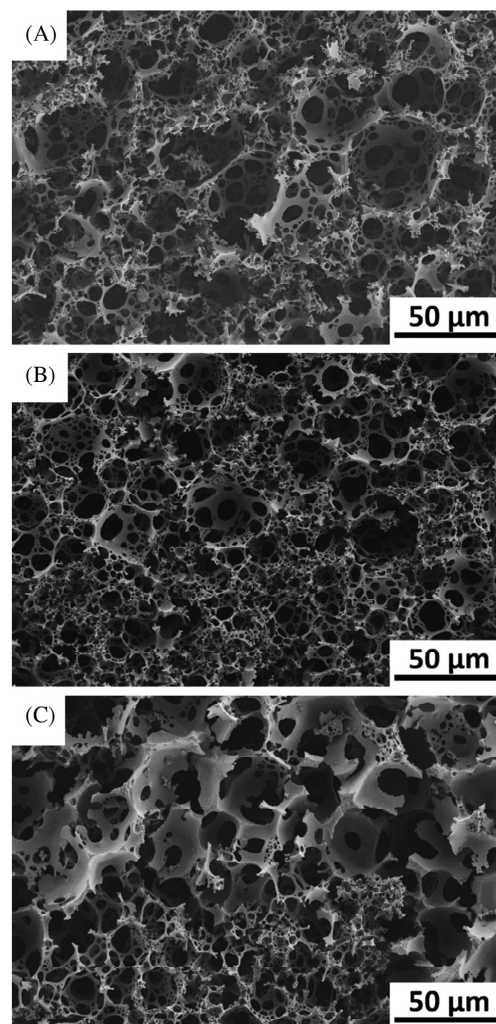
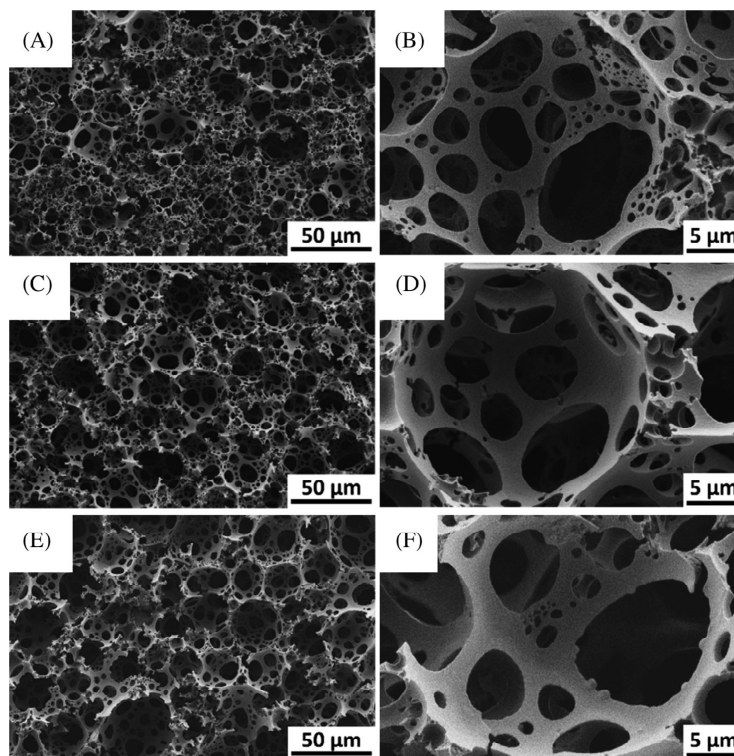


**FIGURE 2** SEM images of foams without filler and with different relative densities: A, 4.3%. B, 5.3%. C, 6.4%. SEM, scanning electron microscopy

**FIGURE 3** SEM images of foams with (A,B) no filler, (B,C) 1% HecPEHMA, and (E,F) 2% HecPEHMA. HecPEHMA, organophilic hectorite; SEM, scanning electron microscopy



The compression modulus obtained from compression tests of the composite foams was plotted vs the foam density (Figure 4B, double logarithmic scale) and all data were fitted with Equation (2). When applying 0.5% HecPEHMA as filler, the mechanical properties did not change significantly. However, increasing the filler content to 1% and 2% resulted in stronger foams as compared to reference foams with the same density (Figure 4A). Due to a nonlinear dependency of  $E$  on  $\rho_{\text{rel}}$  ( $E \propto \rho_{\text{rel}}^{1.4-1.6}$ ), the strengthening effect was more pronounced for foams with lower densities. A second important value, the yield stress  $\sigma$  showed a similar trend (Figure S6). For foams without filler a  $\sigma \propto \rho_{\text{rel}}^{3.0}$  dependency was observed whereas this changed to  $\sigma \propto \rho_{\text{rel}}^{1.3-1.7}$  for 1% to 2% HecPEHMA. This lower exponent between a linear (as measured by Jang et al.<sup>[37]</sup> and confirmed via simulation by Gaitanaros et al.<sup>[38]</sup>) and a quadratic relation may be attributed to a more regular foam morphology. For a filler content as low as 1% HecPEHMA ( $\rho_{\text{rel}}$ : 4.2%), yield stress and compression modulus could be both doubled compared to a neat foam with same density. The greatest improvement of a more than 3x increase in compression modulus and yield stress was achieved with 2%

HecPEHMA and a relative density of 4.1%. If the strengthening effect would be solely caused by reinforcement of the struts, the compression modulus of this composite can be estimated applying Halpin-Tsai theory.<sup>[39]</sup> For single 1 nm thick clay layers, this composite should then be 2.1 times stiffer than the neat foam (see Supporting information). In fact, the composite foam is four times stiffer which indicates that in addition to strut reinforcement other significant strengthening mechanisms are effective.

As a comparison to the synthetic hectorite with a custom-made organo-cation, commercial O-MMT was applied as filler (1% and 2%) as well. With a filler content of 1% O-MMT, all emulsions could be polymerized, leading to open cell foams (Figure S7). With 2% O-MMT as filler, the lowest relative density foam condition resulted in a collapsed foam structure, presumably so weak that it was unable to overcome capillary forces. It was excluded from Figure 5. All other foams possessed a generally similar morphology vs the nonfilled control (Figure S7 vs Figure 2). Contrary to the foams with 1% HecPEHMA, the foams with 1% O-MMT showed no increase in compression modulus (Figure 5) or yield stress (Figure S8) vs

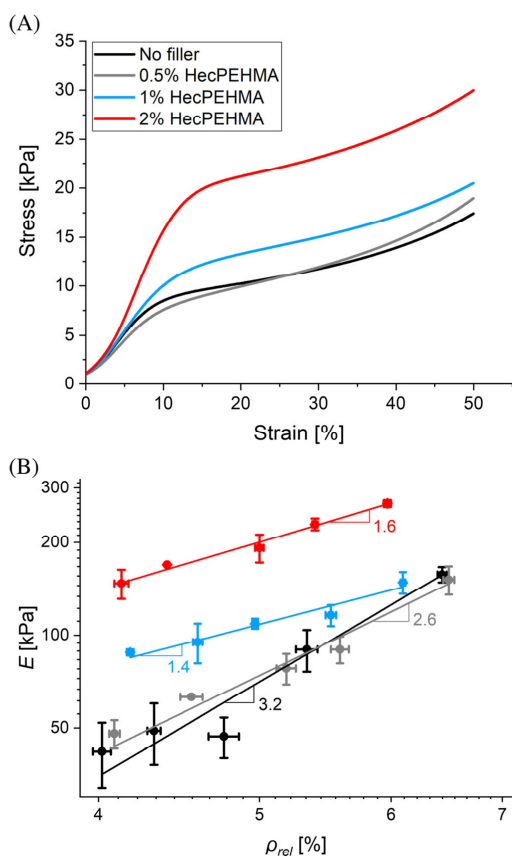


**FIGURE 4** A, Stress-strain curves of foams with and without HecPEHMA (5.0–5.3% relative density). B, Compression modulus depending on the relative foam density (black: no filler; gray: 0.5% HecPEHMA; blue: 1% HecPEHMA; red: 2% HecPEHMA; numbers next to the triangles represent values of B in Equation (2)). HecPEHMA, organophilic hectorite

neat foams. The foams with 2% O-MMT are even significantly weaker than the neat foams. The fact that more highly filled emulsions resulted in a weakening indicated that the commercial modifier is an inferior surface modifier to the custom-made oligomeric PEHMA-NH<sub>3</sub><sup>+</sup>. As will be discussed later, this is also in line with the inability of O-MMT to improve the foam structure via Pickering emulsification.

As mentioned in the introduction, two main factors affect the mechanics of foams: the mechanical properties of the struts and the foam morphology. Thus, strengthening of the foams by incorporation of HecPEHMA can have different explanations. To check whether

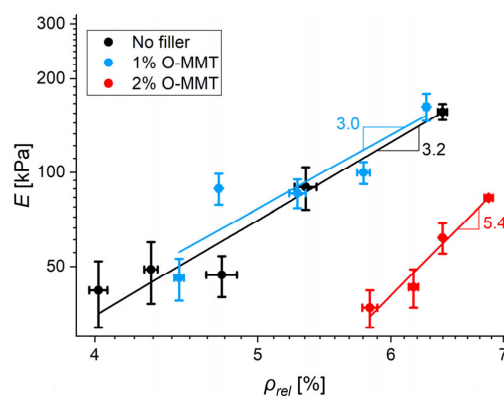


**FIGURE 5** Compression modulus depending on the foam density (black: no filler, blue: 1% O-MMT, red: 2% O-MMT; numbers next to the triangles represent values of B in Equation (2)). O-MMT, organophilic montmorillonite

HecPEHMA is able to reinforce the polymer strut itself, it was applied as filler in bulk polymer plates that were made of the same oil phase used in the emulsions. The filler content was chosen to be 2% because at this concentration, the largest reinforcement on the foam mechanics were achieved. Tensile tests of the bulk polymer plates were made to determine the effect of the filler on the mechanical properties (Table 1, Figure S9). Applying 2% HecPEHMA in polymer plates reduces tensile strength, strain at break and Young's modulus indicating the filler weakens the struts rather than reinforcing them.

The weakening of the bulk composites is in contrast to the strengthening observed for the foam composites and thus, the improvements of foam mechanics cannot be attributed to a Halpin-Tsai-type mechanism. Thus, the observed increase in compression modulus and yield stress of the foams most likely are solely related to an advantageous foam structure. Comparing the SEM images of foams with varying filler contents indeed revealed significant differences in the foam structures. In general, the foam structure is characterized by three parameters: the cell size distribution, the window size distribution and the strut thickness distribution (Figure S10). The foam structures without filler (Figure 2) and with 0.5% HecPEHMA (Figure S4) appeared very inhomogeneous. With increasing HecPEHMA content (Figure 3C–F and Figure S4), the structures became more uniform. In the unfilled foam, there are a lot of small cells (<15  $\mu\text{m}$ ) and the Sauter mean diameter ( $D_{32}$ ) was 26  $\mu\text{m}$ . With 2% HecPEHMA, the Sauter mean diameter increased to 43  $\mu\text{m}$  and the fraction of small cells became smaller (Figure 6A). But not only the cell size

**TABLE 1** Results of the tensile tests of bulk polymer plates

	No filler	2% HecPEHMA
Tensile strength	(2.3 ± 0.5) MPa	(1.3 ± 0.2) MPa
Strain at break	(4.3 ± 1.3) %	(2.8 ± 0.6) %
Young's modulus	(70.6 ± 5.3) MPa	(60.3 ± 4.1) MPa

Abbreviations: HecPEHMA, organophilic hectorite.

distributions varied, the window sizes and strut thickness showed differences as well. In the struts of the nonfilled foam many small holes (<1 μm) were visible, which resulted in a mean window diameter of 1.6 μm (Figure 6B). In addition, many struts were thinner than 0.8 μm (Figure 6C). At 2% HecPEHMA, the windows were bigger and the struts were thicker. Altogether, increasing the HecPEHMA content led to an increase in cell size, window size and strut thickness and also led to a more consistent open cell foam structure. “Consistent” does not refer to the uniformity of cell size distribution – both foams have very polydisperse cell size distributions. Instead, the unfilled foam appears to be a juxtaposition of two locally different average foam cell sizes (eg, Figure 2C). The 2% HecPEHMA foam is closer to having an ideal, random, polydisperse cell size.

In summary, observed foam structures in combination with the mechanics of the bulk plates suggest that the reinforcement of the foams is at least by large due to a more ideal open cell foam structure and not due to a strengthening of the polymer itself. This is consistent with simulation results that showed irregularities in the structure to weaken the foams.<sup>[34,40]</sup>

It is well known that increasing the average open cell foam size alone will result in larger struts but not result in a larger modulus or foam yield stress.<sup>[33]</sup> The increase in strut thickness is out of proportion with the increase in average cell size and further supports a more ideal foam structure has been created upon the introduction of sufficient Pickering-like clay particles.

Contrary to the foams with HecPEHMA, O-MMT fails to improve the foam structure but rather yield structures similar to nonfilled foams (Figure S7). Why is only HecPEHMA capable to modify the foam structure? In general, any particles as clays applied here, are surface-active materials and can stabilize droplets as Pickering emulsifiers.<sup>[41,42]</sup> If HecPEHMA dispersed in the oil phase diffuses to the interface it will stabilize the emulsion in addition to the molecular surfactants. At the higher filler contents, there is certainly more than enough clay surface available in the emulsion to cover a significant amount of the interface: The interface area in the emulsion cannot be determined reliably and

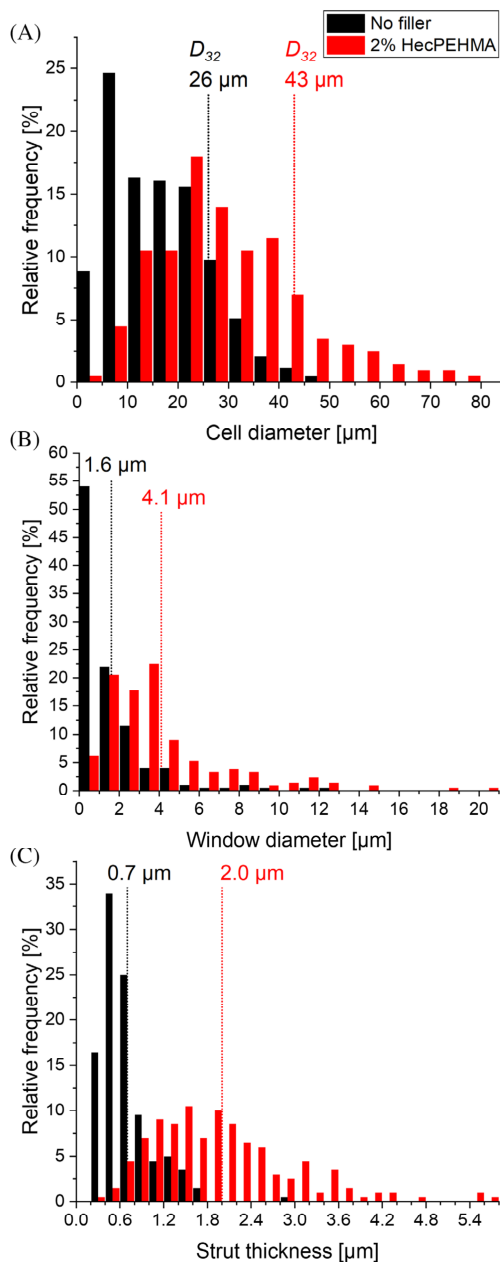


**FIGURE 6** Distribution of A, cell, B, window and C, strut sizes of a foam without filler (black) and with 2% HecPEHMA (red), numbers and dotted lines show the Sauter mean diameter ( $D_{32}$ ) or the arithmetic mean. HecPEHMA, organophilic hectorite [Color figure can be viewed at [wileyonlinelibrary.com](http://wileyonlinelibrary.com)]

moreover changes dynamically with progression of the polymerization. We therefore assume foam surface to be equivalent to the interface area as a first approximation. As determined by physisorption, the foam without filler and a relative density of 5.3% had a BET-surface area of 3.6 m<sup>2</sup>/g. If the clay platelets now are assumed to cover this surface in a monolayer, 0.5%, 1%, and 2% HecPEHMA will cover 25%, 51%, and 101%, respectively. In any case, if segregated to the interface, HecPEHMA will occupy significant amounts of the water-oil interface. Jointly with the molecular surfactants, the additional surface activity of HecPEHMA will improve emulsion stability, which might explain the more uniform structures in the polymerized foam observed.

As to the reason for the nonperformance of O-MMT we can only speculate. Pickering efficiency is related to the differences of the surface tension of the two phases and will therefore be crucially modulated by the type of modifier applied. Apparently, the similarity in chemistry provided by oligomeric PEHMA-NH<sub>3</sub><sup>+</sup> led to a better Pickering efficiency as compared to alkylammonium applied in O-MMT.

#### 4 | CONCLUSION

The mechanical behavior of foams based on HIPE is determined by two main factors: mechanical properties of the struts and the foam morphology. The latter in turn is crucially affected by the efficiency of emulsifiers applied. Any particles applied as fillers in nanocomposite foams will inevitably modify both of the above factors. In particularly anisotropic, platy fillers like clays are efficient Pickering emulsifiers. Consequently, their surface activity may have a significant if not a decisive impact on foam structure. Pickering efficiency is, however, greatly dependent on surface activity and hence on the type of modifier used to organophilize the clay filler.

Applying a synthetic clay organophilized with a custom-made modifier, which is chemically similar to the oil phase we were able to reinforce a foam based on HIPE up to 4-fold as compared to a nonfilled foam. The reinforcement was shown to be related to the improvement of the foam structure via the surface activity provided by the clay filler.

#### ACKNOWLEDGMENT

Florian Puchtler is acknowledged for the hectorite synthesis. The authors appreciate the support of the Keylab for Optical and Electron Microscopy and the Keylab for Small Scale Polymer Processing of the Bavarian Polymer Institute (BPI). Andreas Mainz is acknowledged for

helping with compression tests and Lena Geiling for conducting the BET measurement. The authors thank the North-Bavarian NMR Center for conducting the NMR measurement. Lina Mayr acknowledges the support of the Elite Network Bavaria.

#### ORCID

Josef Breu  <https://orcid.org/0000-0002-2547-3950>

#### REFERENCES

- [1] A. Okada, A. Usuki, *Macromol. Mater. Eng.* **2006**, *291*, 1449.
- [2] M. Alexandre, P. Dubois, *Mater. Sci. Eng., R* **2000**, *28*, 1.
- [3] C. Habel, M. Schöttle, M. Daab, N. J. Eichstaedt, D. Wagner, H. Bakhshi, S. Agarwal, M. A. Horn, J. Breu, *Macromol. Mater. Eng.* **2018**, *303*, 1800333.
- [4] J. C. Grunlan, A. Grigorian, C. B. Hamilton, A. R. Mehrabi, *J. Appl. Polym. Sci.* **2004**, *93*, 1102.
- [5] J. Hausner, B. Fischer, M. Stöter, A. Edenharter, J. Schmid, R. Kunz, S. Rosenfeldt, V. Altstädt, J. Breu, *Polym. Degrad. Stab.* **2016**, *128*, 141.
- [6] M. Ziadeh, S. Weiss, B. Fischer, S. Förster, V. Altstädt, A. H. E. Müller, J. Breu, *J. Colloid Interface Sci.* **2014**, *425*, 143.
- [7] M. Morits, T. Verho, J. Sorvari, V. Liljeström, M. A. Kostianinen, A. H. Gröschel, O. Ikkala, *Adv. Funct. Mater.* **2017**, *27*, 1605378.
- [8] R. R. Tiwari, U. Natarajan, *Polym. Int.* **2008**, *57*, 738.
- [9] B. Fischer, M. Ziadeh, A. Pfaff, J. Breu, V. Altstädt, *Polymer* **2012**, *53*, 3230.
- [10] M. Kotal, A. K. Bhowmick, *Prog. Polym. Sci.* **2015**, *51*, 127.
- [11] P. LeBaron, *Appl. Clay Sci.* **1999**, *15*, 11.
- [12] M. R. Schütz, H. Kalo, T. Lunkenbein, A. H. Gröschel, A. H. E. Müller, C. A. Wilkie, J. Breu, *J. Mater. Chem.* **2011**, *21*, 12110.
- [13] V. Mittal, *J. Colloid Interface Sci.* **2007**, *314*, 141.
- [14] A. Samakande, P. C. Hartmann, V. Cloete, R. D. Sanderson, *Polymer* **2007**, *48*, 1490.
- [15] N. R. Cameron, *Polymer* **2005**, *46*, 1439.
- [16] M. S. Silverstein, *Prog. Polym. Sci.* **2014**, *39*, 199.
- [17] N. Brun, S. Ungureanu, H. Deleuze, R. Backov, *Chem. Soc. Rev.* **2011**, *40*, 771.
- [18] I. Pulko, P. Krajnc, *Macromol. Rapid Commun.* **2012**, *33*, 1731.
- [19] H. Zhang, A. I. Cooper, *Soft Matter* **2005**, *1*, 107.
- [20] I. Gurevitch, M. S. Silverstein, *Macromolecules* **2011**, *44*, 3398.
- [21] K. Haibach, A. Menner, R. Powell, A. Bismarck, *Polymer* **2006**, *47*, 4513.
- [22] M. S. Ahmed, Y. H. Lee, C. B. Park, N. Atalla, *Asia-Pac. J. Chem. Eng.* **2009**, *4*, 120.
- [23] Z. Abbasian, M. R. Moghbeli, *J. Appl. Polym. Sci.* **2011**, *119*, 3728.
- [24] P. Pakeyangkoon, R. Magaraphan, P. Malakul, M. Nithitanakul, *J. Appl. Polym. Sci.* **2009**, *114*, 3041.
- [25] O. Lépine, M. Birot, H. Deleuze, *J. Polym. Sci., Part A: Polym. Chem.* **2007**, *45*, 4193.
- [26] E. Berber, F. Çıra, E. H. Mert, *Polym. Compos.* **2016**, *37*, 1531.
- [27] D. Goossens, *Sedimentology* **2007**, *55*, 65.
- [28] A. Barbetta, N. R. Cameron, *Macromolecules* **2004**, *37*, 3188.
- [29] T. Wu, A. Liu, T. Xie, G. Yang, *J. Polym. Sci., Part B: Polym.*

- Phys.* **2008**, *46*, 1802.
- [30] J. Breu, W. Seidl, A. J. Stoll, K. G. Lange, T. U. Probst, *Chem. Mater.* **2001**, *13*, 4213.
- [31] M. Stöter, D. A. Kunz, M. Schmidt, D. Hirsemann, H. Kalo, B. Putz, J. Senker, J. Breu, *Langmuir* **2013**, *29*, 1280.
- [32] S. Rosenfeldt, M. Stöter, M. Schlenk, T. Martin, R. Q. Albuquerque, S. Förster, J. Breu, *Langmuir* **2016**, *32*, 10582.
- [33] L. J. Gibson, M. F. Ashby, *Cellular Solid*, Cambridge University Press, Cambridge, **1997**.
- [34] O. E. Sotomayor, H. V. Tippur, *Acta Mater.* **2014**, *78*, 301.
- [35] H. X. Zhu, J. R. Hobdell, A. H. Windle, *Acta Mater.* **2000**, *48*, 4893.
- [36] W. E. Warren, A. M. Kraynik, *J. Appl. Mech.* **1988**, *55*, 341.
- [37] W.-Y. Jang, S. Kyriakides, *Int. J. Solids Struct.* **2009**, *46*, 617.
- [38] S. Gaitanaros, S. Kyriakides, *Int. J. Impact Eng.* **2015**, *82*, 3.
- [39] J. C. Halpin Affdl, J. L. Kardos, *Polym. Eng. Sci.* **1976**, *16*, 344.
- [40] M. H. Luxner, J. Stampfl, H. E. Pettermann, *Int. J. Solids Struct.* **2007**, *44*, 2990.
- [41] N. P. Ashby, B. P. Binks, *Phys. Chem. Chem. Phys.* **2000**, *2*, 5640.
- [42] Y. Cui, M. Threlfall, J. S. van Duijneveldt, *J. Colloid Interface Sci.* **2011**, *356*, 665.

#### SUPPORTING INFORMATION

Additional supporting information may be found online in the Supporting Information section at the end of this article.

**How to cite this article:** Mayr L, Simonyan A, Breu J, Joseph Wingert M. Structural and mechanical impact of synthetic clay in composite foams made via high-internal phase emulsions. *Polymer Composites*. 2021;42:353–361. <https://doi.org/10.1002/pc.25830>

**Supporting Info**

Structural and mechanical impact of synthetic clay in composite foams made via high internal phase emulsions

*Lina Mayr<sup>1</sup>, Arsen Simonyan<sup>2</sup>, Josef Breu<sup>1</sup> and Maxwell Wingert<sup>3\*</sup>*

*1 Department of Chemistry and Bavarian Polymer Institute, University of Bayreuth, Universitätsstr. 30, D-95440 Bayreuth, Germany*

*2 Procter & Gamble, Schwalbach, Germany*

*3 Procter & Gamble, Cincinnati, USA*

*\*Corresponding author*

## Supporting figures

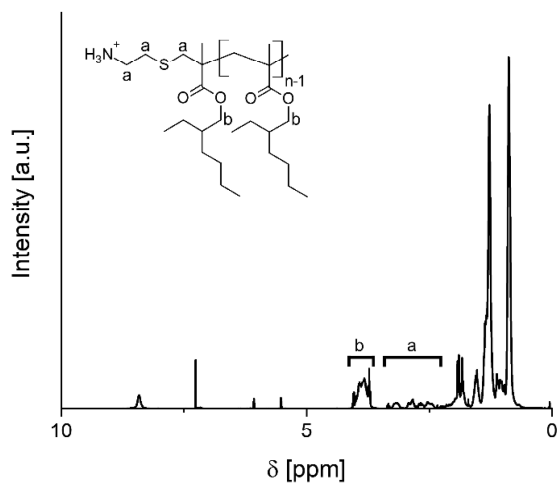
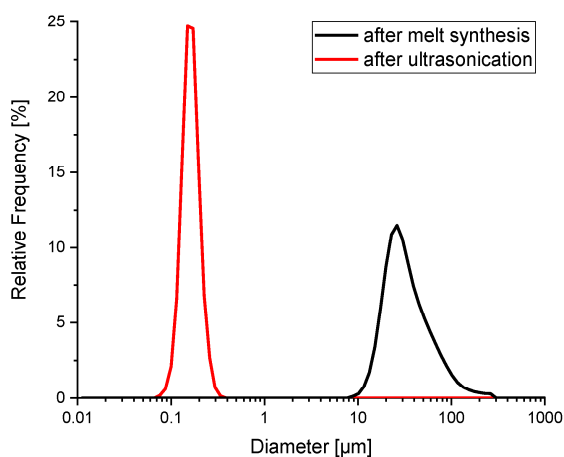
Figure S1: <sup>1</sup>H-NMR spectrum of the oligomeric cation PEHMA-NH<sub>3</sub><sup>+</sup>

Figure S2: Size distribution of NaHec in water after melt synthesis (black) and after ultrasonication (red).

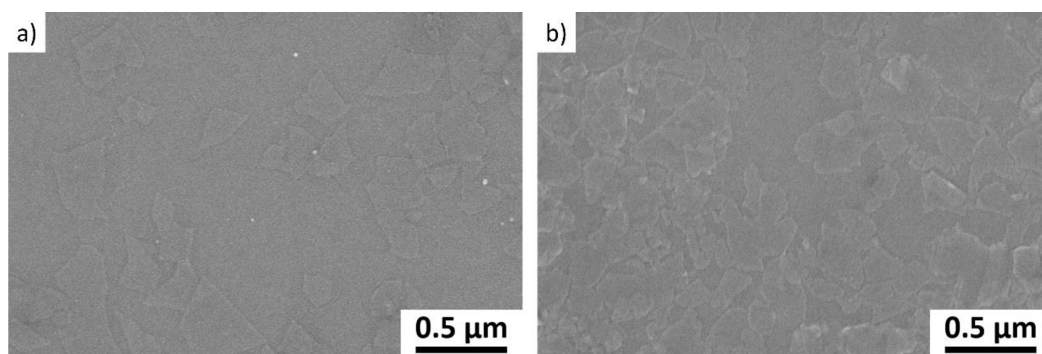


Figure S3: SEM images of HecPEHMA (a) and O-MMT (b).

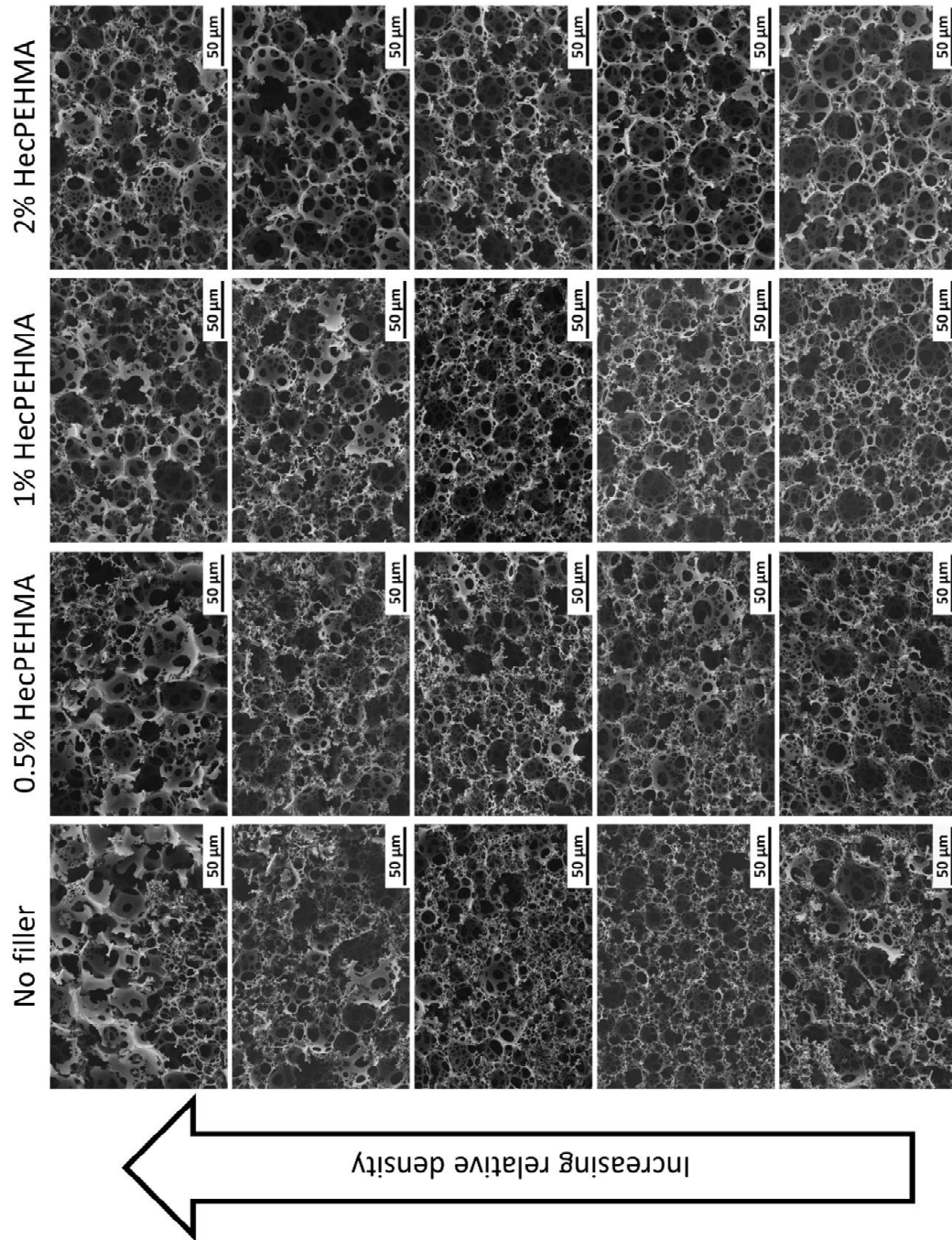


Figure S4: SEM images of foams with different HecPEHMA contents and different densities.

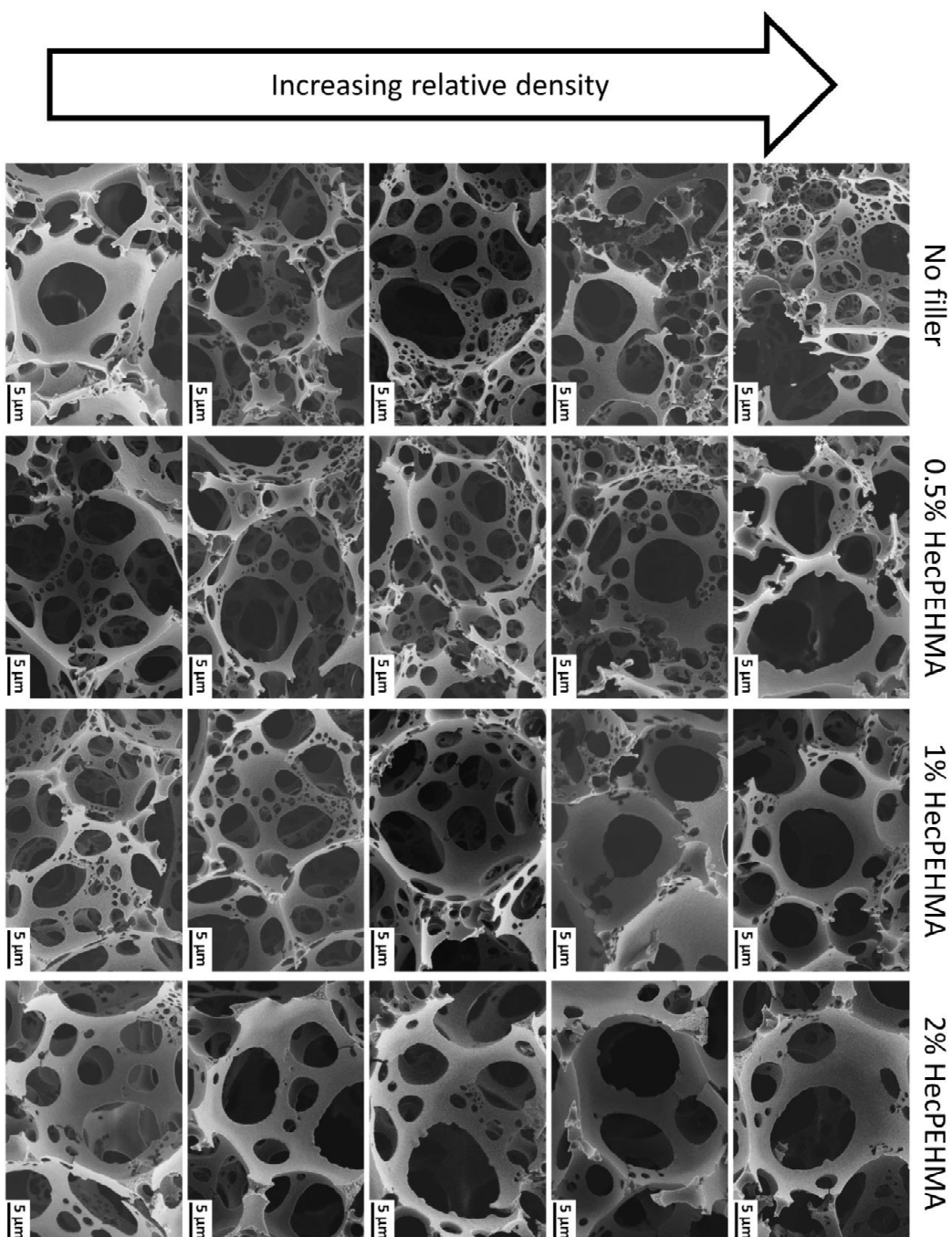


Figure S5: High magnification SEM images of foams with different HecPEHMA contents and different densities.

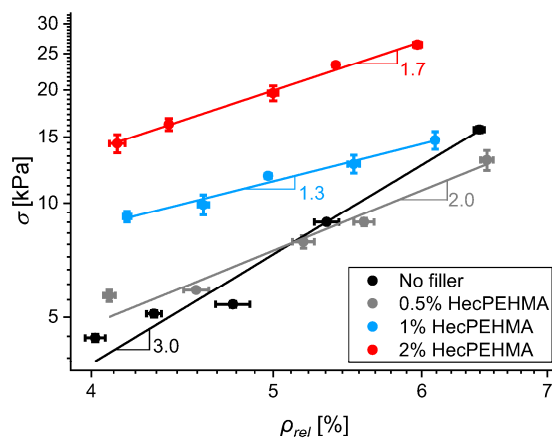


Figure S6: Yield stress depending on the foam density (black: no filler, grey: 0.5% HecPEHMA, blue: 1% HecPEHMA, red: 2% HecPEHMA, orange: 3% HecPEHMA; numbers next to the triangles represent values of  $B$  in eq.2)

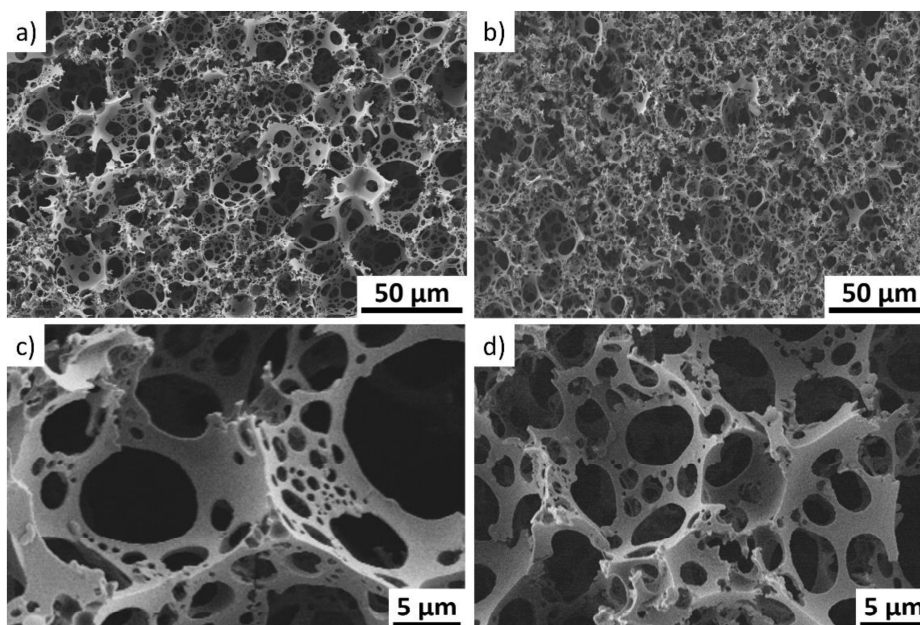


Figure S7: SEM images of foams with 1% O-MMT (a,c;  $\rho_{rel}$ : 5.3%) and 2% O-MMT (b,d;  $\rho_{rel}$ : 6.2%).

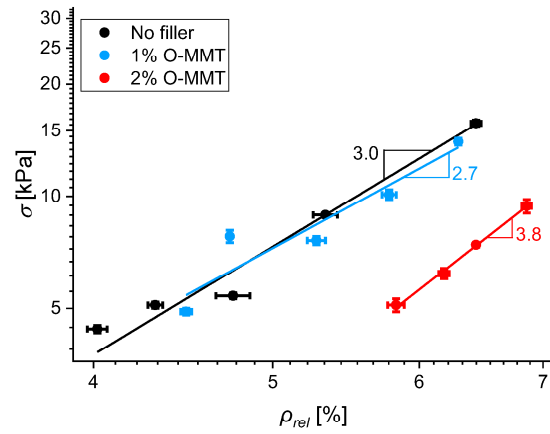


Figure S8: Yield stress depending on the foam density (black: no filler, blue: 1% O-MMT, red: 2% O-MMT; numbers next to the triangles represent values of B in eq.2)

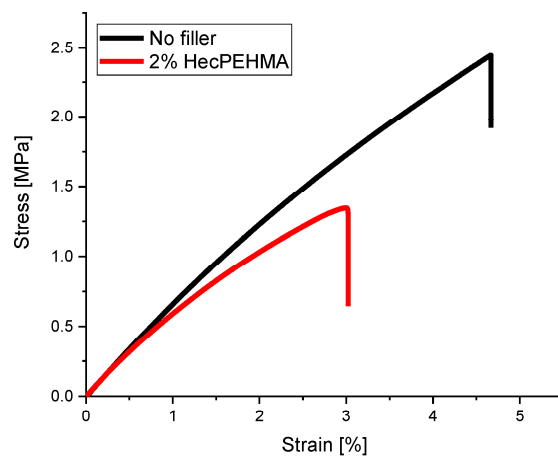


Figure S9: Stress-strain curves of tensile tests of bulk polymer plates (black: no filler, red: 2% HecPEHMA).

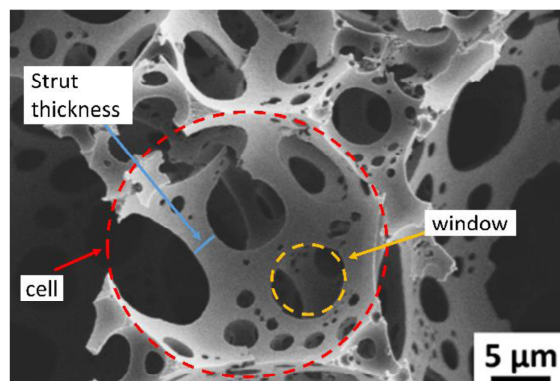


Figure S10: SEM image displaying the important parameters cell, window and strut.

### Halpin-Tsai

According to Halpin-Tsai, the Young's modulus of a composite  $E_c$  with platelets as fillers can be calculated as follows:<sup>[1-2]</sup>

$$E_c = \frac{1 + 2 \cdot 0.66 \cdot \frac{L}{h} \cdot \eta \cdot \phi}{1 - \eta \cdot \phi} \cdot E_m$$

With:  $L, h$ : length and height of the filler ( $L/h = 200$ )

$\phi$ : volume fraction of the filler

$E_m$ : Young's modulus of the matrix (42 kPa for a neat foam with 4.0% rel. density)

$E_f$ : Young's modulus of the filler (150 GPa)

$$\eta = \frac{\frac{E_f}{E_m} - 1}{\frac{E_f}{E_m} + 2 \cdot 0.66 \cdot \frac{L}{h}}$$

The volume fraction of hectorite in a foam with 2 wt.-% HecPEHMA is calculated as follows: HecPEHMA consists of 54 wt.-% hectorite and 46 wt.-% PEHMA, thus 2 wt.-% HecPEHMA means 1.1 wt.-% hectorite ( $\phi_{wt}$ ). The density of NaHec is 2.7 g/cm<sup>3</sup> and the density of PEHMA is assumed to be 1 g/cm<sup>3</sup>. Consequently, the volume fraction of hectorite is calculated as follows:

$$\phi = \frac{\phi_{wt}}{\phi_{wt} + (1 - \phi_{wt}) \cdot 2.7}$$

### Literature

<sup>[1]</sup> J. C. Halpin Affdl, J. L. Kardos, *Polym. Eng. Sci.* **1976**, 16, 344

<sup>[2]</sup> Y.-P. Wu, Q.-X. Jia, D.-S- Yu, I.-Q. Zhang, *Polym. Test*, **2004**, 23, 903

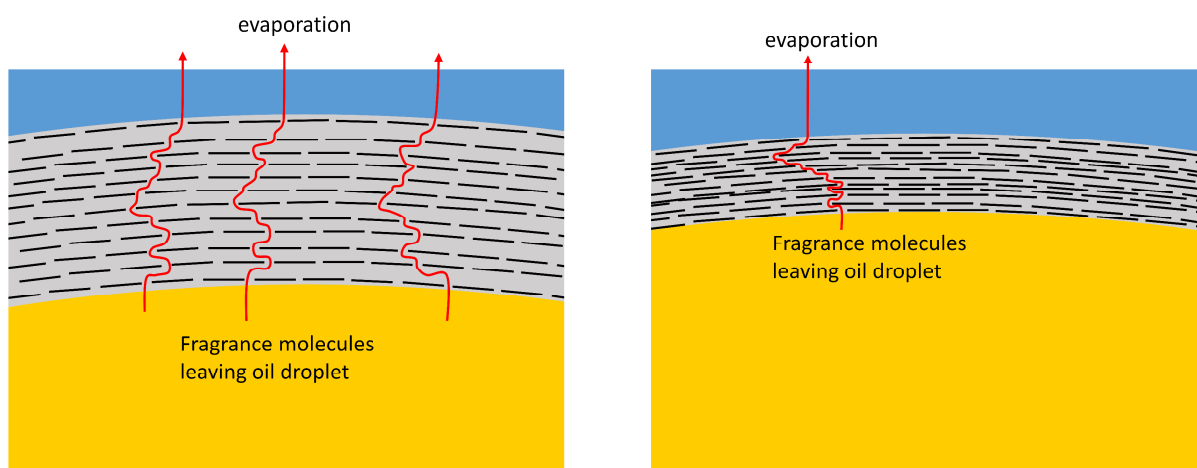


### 6.3 Encapsulation of fragrance in aqueous emulsions by delaminated synthetic hectorite

Lina Mayr and Josef Breu\*

Published in: *Langmuir* **2020**, 36 (37), 11061-11067

Reprinted with permission, Copyright (2020) American Chemical Society



Department of Chemistry and Bavarian Polymer Institute, University of Bayreuth, Universitätsstr. 30, 95440 Bayreuth, Germany

\*Corresponding author: josef.breu@uni-bayreuth.de

#### **Author's individual contributions:**

The concept of the publication was developed by Prof Josef Breu and me. I made all the experiments and analyzed the samples by laser diffraction and SEM. Furthermore, I did the interpretation of the NMR data. The publication was written by Prof Josef Breu and me.

My contribution to this publication is 90%.

# Encapsulation of Fragrance in Aqueous Emulsions by Delaminated Synthetic Hectorite

Lina Mayr and Josef Breu\*



Cite This: *Langmuir* 2020, 36, 11061–11067



Read Online

ACCESS |



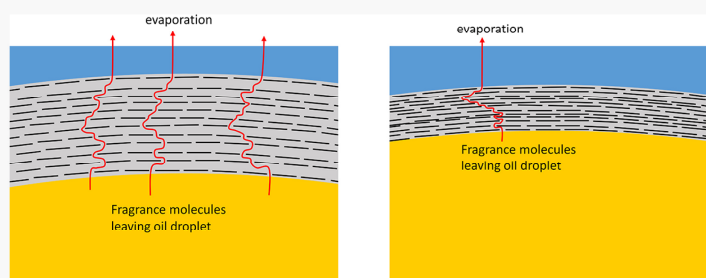
Metrics & More



Article Recommendations



Supporting Information



**ABSTRACT:** Fragrance emulsions are used in many applications in daily life. Since a lot of fragrances are quite volatile substances, their release rate from emulsions is a crucial factor. Since in most cases a mixture of fragrances is applied, the olfactory impression might change over time if the release rates of individual components differ significantly. For such applications, encapsulation with barrier materials is sought to retard release in an unselective manner. Stable fragrance-in-water emulsions were made by applying a synthetic hectorite as Pickering emulsifier which was fixed as a multilayer stack at the oil–water interface by adding poly(ethylene imine). The release of different fragrance molecules (eucalyptol, limonene,  $\alpha$ -pinene, and ethyl-2-methylbutyrate) from these emulsions was studied as the ratio between hectorite and poly(ethylene imine) was varied. While the release rates of all fragrances were retarded by the hybrid capsule acting as a nonselective barrier, the relative release was determined by the solubility of individual fragrances in the capsule material. Fragrance release could be further reduced by additional chemical cross-linking of poly(ethylene imine).

## INTRODUCTION

Emulsions find applications in various fields in daily life, like pharmaceuticals or food. Besides using molecular surfactants, emulsification can also be provided by solid particles. These so-called Pickering emulsions are of great interest as they show enhanced stability against coalescence as compared to molecular surfactants.<sup>1–3</sup> Whereas molecular surfactants in steady state equilibrium are dynamically moving between different droplets, solid particles can be assumed to be irreversibly trapped at the oil–water interface.<sup>2</sup> Two-dimensional particles (platelets), like clays, are thought to be even more stable at the interface than spherical particles as they lay flat, thus covering a large interface per particle.<sup>4</sup> In general, particles stabilizing emulsions should have a wettability intermediate between both phases. Unmodified clay minerals are very hydrophilic and thus are not able to produce stable emulsions alone. Emulsification is only assured if high salt concentrations are used.<sup>5–7</sup> This screens the repulsive forces between the platelets, lowers the zeta potential, and allows them to aggregate.<sup>8</sup> Other attempts to form stable clay Pickering emulsions include organically modified clay or adding extra surfactants.<sup>9–14</sup> For example, adsorption of

small amounts of cetyltrimethylammonium bromide (CTAB) to montmorillonite increased the stability of oil-in-water emulsions.<sup>11</sup> Increasing the amount of CTAB initially produces water-in-oil emulsions as the clay platelets become hydrophobic, while at concentrations where CTAB forms bilayers on the clay surface, oil-in-water emulsion are obtained. Cui et al. found that emulsions are more stable if the additional surfactant is more hydrophilic.<sup>9</sup> In general, a strong interaction between clay and an additional surfactant promotes their adsorption at an interface.<sup>15</sup>

As clay–polymer composite films provide superior barrier properties against gas molecules,<sup>16,17</sup> it seems promising to examine clays for the encapsulation of volatile oil droplets. In this context, the barrier properties of polyurea microcapsules for oils could indeed be improved by incorporating clays into

Received: July 9, 2020

Revised: September 2, 2020

Published: September 3, 2020



ACS Publications

© 2020 American Chemical Society

11061

<https://dx.doi.org/10.1021/acs.langmuir.0c02025>  
Langmuir 2020, 36, 11061–11067

the capsule wall.<sup>18,19</sup> Furthermore, Putlitz et al. synthesized latex particles armored with clay platelets.<sup>20</sup> This hampered solubility of the polymer, which was attributed to clay acting as a barrier on the surface of the latex particles. The cited examples apply clay solely as fillers for polymer liners at the interface rather than as Pickering emulsifier. Alternatively, montmorillonite and laponite were ion exchanged with a polycation, poly(ethylene imine) (PEI), before adding them to oil-in-water emulsions.<sup>21,22</sup> The microcapsules obtained this way were found to be highly permeable as evidenced by dye release studies indicating a disordered structure of the clay shell.<sup>21</sup>

Encapsulation of fragrance in aqueous emulsions is commercially important as such fragrance-loaded microcapsules are added to laundry detergents to keep clothing smelling fresh for longer. The release rate of oil from such microcapsules is determined by the vapor pressure and the water solubility of the oil.<sup>23</sup> Moreover, the diffusivity of the oil and its solubility in the capsule material might be rate determining if the capsule wall acts as a barrier to retard its diffusion. It was shown that spherical solid particles at the oil–water interface retard the diffusion as compared to molecular surfactants.<sup>24</sup> As compared to spherical solid particles, an enhanced retention was found for emulsions stabilized with graphene oxide layers.<sup>25</sup> In particular, multilayer stacks of two-dimensional materials can provide complete coverage of the droplet surface which cannot be realized with spherical particles.<sup>25</sup>

Here, we apply delaminated synthetic hectorite nanosheets to stabilize Pickering emulsions. The hectorite sheets restack at the interface before being fixed by irreversible PEI adsorption. The adsorbed PEI chains were subsequently cross-linked by poly(propylene glycol) diglycidylether for further stabilization of the hybrid capsule.<sup>21,22,26</sup> The release behavior of a fragrance mixture from these capsules was studied as the ratio of hectorite to PEI was varied.

## ■ EXPERIMENTAL SECTION

**Materials.** Sodium hectorite ( $[\text{Na}_{0.5}][\text{Mg}_{2.5}\text{Li}_{0.5}][\text{Si}_4]\text{O}_{10}\text{F}_2$ , Hec) was obtained by melt synthesis according to a published procedure.<sup>27</sup> Upon immersing Hec into deionized water, it spontaneously and fully delaminated into individual nanosheets of 1 nm thickness by repulsive osmotic swelling.<sup>28</sup> Since the platelet diameter of the pristine material (median 20  $\mu\text{m}$ ) was about the same as typical droplet sizes, the diameter was reduced by ultrasonication of the aqueous hectorite suspension (10 mg/mL) for 15 min using a Hielscher UIP1000hd.

Poly(ethylene imine) (PEI, average  $M_w \approx 25\,000$  by LS, average  $M_n \approx 10\,000$  by GPC, branched), poly(propylene glycol) diglycidyl ether (PPG-DGE, average  $M_n \approx 640$ ), deuterated chloroform ( $\text{CDCl}_3$ , contains 1% (v/v) TMS), and Rhodamine B isothiocyanate (mixed isomers) were purchased from Sigma-Aldrich and used as received. As model fragrances,  $\beta$ -citronellol (95%), eucalyptol (99%), (R)-(+)-limonene (97%),  $\alpha$ -pinene (98%), and ethyl-2-methylbutyrate (99%) were used as received (all from Sigma-Aldrich).

**Preparation and Characterization of the Emulsions.** The fragrance mixture applied consisted of 50 vol % citronellol, 12.5 vol % eucalyptol, 12.5 vol % limonene, 12.5 vol %  $\alpha$ -pinene, and 12.5 vol % ethyl-2-methylbutyrate. All emulsions contained 6 mL of aqueous phase and 2 mL of oil phase (fragrance mixture).

An aqueous suspension of 20 mg of ultrasonicated hectorite (3.6–4.2 mg/mL) and 2 mL of the fragrance mixture was dispersed with a Heidolph SilentCrusher M ultra turrax at 12 000 rpm. After stirring the mixture for about 20 s, an aqueous solution of PEI (10–25 mg, 20 mg/mL) was added and mixing was continued for 5 min.

For cross-linked emulsions, the fragrance mixture contained 10–30 mg of PPG-DGE. After addition of the PEI solution, mixing was continued for 2 min at room temperature followed by 3 min in a water bath (70 °C). To ensure complete reaction of the cross-linker, the emulsions were placed in an oven set at 60 °C overnight.

To label PEI with Rhodamine B, 0.53 g of PEI was dissolved in 80 mL of carbonate buffer solution (pH 10). Under stirring, 8 mg of Rhodamine B isothiocyanate in 1 mL of DMSO was added. Stirring was continued overnight. Afterward, the labeled PEI was dialyzed against water and then freeze dried.

For stability tests, the emulsions were allowed to stand for 2 weeks at room temperature.

For release studies, the emulsions were placed in an open vial and gently shaken in a fume hood for 2 weeks. To keep the volume of the emulsion constant, evaporated water was replaced. Every 2 days, an aliquot of the emulsion (~0.4 mL) was taken and the fragrance molecules were extracted to  $\text{CDCl}_3$  (0.8 mL) by vigorously shaking. The composition of the residual fragrance mixture was determined by NMR spectroscopy (Figure S1).

**Characterization Methods.** The particle size distribution of the hectorite as well as the droplet size distribution of the emulsions were measured by laser diffraction according to ISO 13320 applying a Retsch LA-950 (Horiba).

<sup>1</sup>H nuclear magnetic resonance (NMR) spectra were measured using a Bruker Avance 300 (Bruker) at 300 MHz.  $\text{CDCl}_3$  was used as a solvent.

Scanning electron microscopy (SEM) images were taken with a Zeiss LEO 1530 (Carl Zeiss AG) using an acceleration voltage of 3 kV. Prior to measurement, samples were coated with 2 nm platinum at a Cressington Sputter Coater 208HR (Cressington Scientific Instruments).

Observations of fluorescence were done with a scanning confocal PicoQuant MicroTime 200 microscope. The picosecond pulsed excitation laser (561 nm, 20 MHz repetition rate, 80 ps fwhm) was reflected by a dichroic mirror into an inverted microscope (Olympus, IX71) equipped with a water immersion objective (Olympus, UPlanSApo 60 $\times$ /1.2 W) used for focusing the laser light onto the sample and for collecting the emission from the sample. Fluorescence signal that passed through the dichroic mirror and a long-pass filter (561 nm, Semrock) was focused through a 75  $\mu\text{m}$  pinhole to a single-photon counting module (SPCM-AQRH-14-TR, Excelitas Technologies).

## ■ RESULTS AND DISCUSSION

Sodium hectorite (Hec) obtained by melt synthesis provides high purity and charge homogeneity and therefore spontaneously delaminates in single 1 nm thick platelets upon immersing in water.<sup>27,28</sup> These platelets have an average diameter of 20  $\mu\text{m}$ . To adjust the platelet size to sizes smaller than typical emulsion droplets, the platelet diameter was chopped down to ~0.2  $\mu\text{m}$  by applying ultrasonication (Figure S2). As unmodified clay platelets are too hydrophilic to stabilize emulsions, the anionic Hec was modified in situ with polycationic PEI. Addition of PEI to an aqueous Hec dispersion would instantly result in a restacking of the individual clay platelets and flocculation. Thus, we here restacked Hec at the water–oil interface. Therefore and contrary to published procedures,<sup>21,22</sup> an aqueous Hec suspension and the oil phase were first dispersed, and during this mixing process, when Hec was located at or near the interface, an aqueous PEI solution was added. This quasi in situ-fixed Hec was capable of stabilizing the emulsion. A mixture of five fragrances (citronellol, eucalyptol, limonene,  $\alpha$ -pinene, and ethyl-2-methylbutyrate) was used as oil phase in all emulsions.

The mass ratio of PEI to Hec was varied between 0.5 and 1.25, while the amount of Hec was kept constant in all

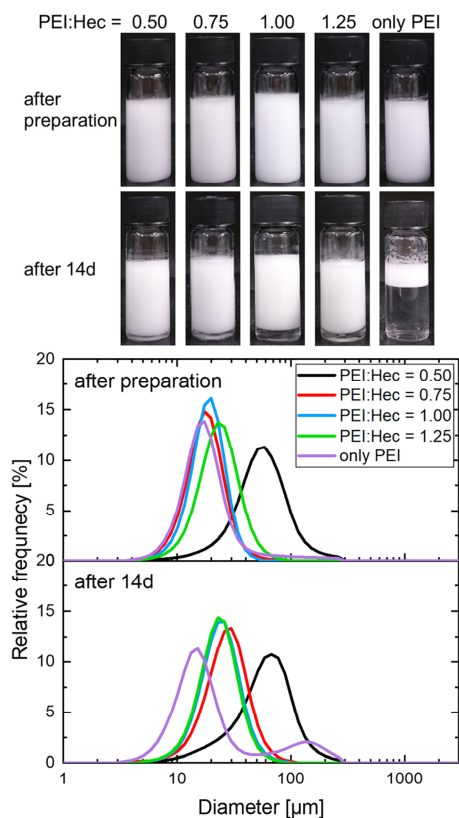


**Figure 1.** Photographs (top) and size distributions (bottom) of Hec/PEI Pickering emulsions directly after preparation and after 2 weeks in a closed vial.

emulsions. In addition, an emulsion stabilized solely with PEI (20 mg) was made for comparison. Drop tests showed that all emulsions were (o/w) type. To check the stability of the emulsions, they were stored in a closed vial for 2 weeks at

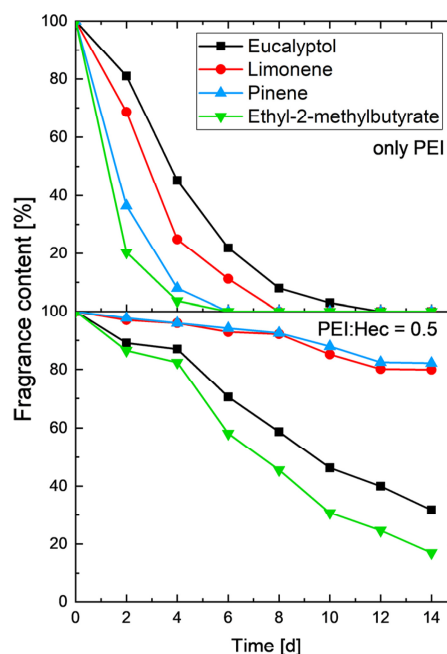


**Figure 2.** Fragrance release from an emulsion stabilized only with PEI (top) and from a Hec/PEI Pickering emulsion with PEI:Hec = 0.5 (bottom).

room temperature. After 2 weeks, the emulsion solely stabilized by PEI showed creaming resulting in a small fraction of emulsion on top of a water phase. All Hec/PEI Pickering emulsions showed only little or no creaming at all. If any, only a small fraction of water phase could be observed below the emulsion (Figure 1). Thus, Hec/PEI Pickering emulsions showed enhanced stability, most probably due to the prevention of coalescence.

The size distribution of the emulsion droplets was measured immediately after emulsification and after 2 weeks (Figure 1).

**Table 1. Physical Properties of the Hydrophobic Fragrances<sup>31–36</sup>**

	Vapor pressure at 21°C [mbar]	Water solubility at 25°C [mmol/L]	
citronellol	0.01 <sup>31</sup>	1.28 <sup>32</sup>	<chem>CC(C)C=CC(C)CO</chem>
eucalyptol	1.99 <sup>31</sup>	2.2 <sup>33</sup>	<chem>CC1(C)C2C(C1)OC2</chem>
limonene	2.12 <sup>34</sup>	0.15 <sup>35</sup>	<chem>CC1=CCC(C=C1)C</chem>
α-pinene	4.55 <sup>34</sup>	0.04 <sup>35</sup>	<chem>CC1=CC2C(C1)C=C2</chem>
ethyl-2-methylbutyrate	12.46 <sup>36</sup>	8.2 <sup>33</sup>	<chem>CC(C)C(=O)OCC</chem>

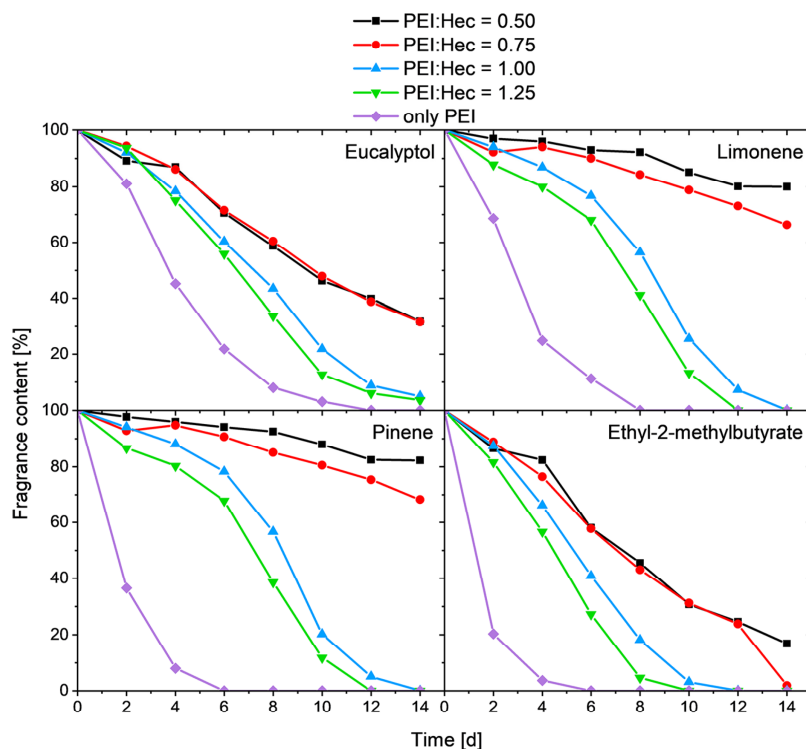


Figure 3. Fragrance release curves for Pickering emulsions with different PEI:Hec ratios.

Immediately after emulsification, the emulsion made at PEI:Hec = 0.5 had a volume-weighted mean diameter of  $58 \pm 34 \mu\text{m}$ , while all other emulsions had smaller diameters of  $18\text{--}23 \mu\text{m}$  regardless of the PEI:Hec ratio. Possibly the particles with PEI:Hec = 0.5 were not hydrophobic enough to produce smaller droplets. This ratio nevertheless ensured good stability, as the droplet size did not increase significantly after 2 weeks. All other Pickering emulsions showed also only slight increases in their mean droplet diameters. The laser diffraction results thus corroborated the visual inspection of stable emulsions. The emulsion solely stabilized by PEI had a bimodal size distribution with a fraction of larger droplets. In addition to the observed creaming, this indicates that Hec/PEI is a better emulsifier than PEI alone.

To prove the Pickering character, an emulsion with Hec/PEI was made where PEI was previously labeled with Rhodamine B to allow visualization with a fluorescence microscope (Figure S3). As PEI is a polycation, it will inevitably be adsorbed on any clay surface whether in the water phase or at the interface. We can therefore safely assume that all Hec is covered with labeled PEI. Within experimental error, all fluorescence observed in microscopy images is located at the interface. Consequently, all hectorite is located at the interface. After drying the emulsion (Figure S4), Hec/PEI could still be attributed to a shrunken capsule wall, further confirming the Pickering character.

Contrary to the literature that reports creaming of the emulsion with a comparable oil fraction and droplet size within a few hours,<sup>29,30</sup> we observed no creaming even after 2 weeks. Even after 3 months the most stable emulsion (PEI:Hec = 0.5) showed no creaming. The least stable emulsion showed little

creaming (20% aqueous phase), much less than what would be expected in equilibrium (Figure S5). As for the reason for the much retarded equilibration, we can only speculate: As compared to ordinary, surfactant-stabilized emulsions, the density of the Pickering-stabilized droplet is increased by some 10% by the much denser hectorite (2.7 g/mL) that in turn lowers the buoyancy significantly.

Moreover, as has been shown by Putlitz et al., clays at the interface mechanically enforce emulsion droplets.<sup>20</sup> These “armored” emulsion droplets will resist deformation that in turn will lead to higher effective flow resistance as compared to surfactant-stabilized emulsions and thus retard creaming kinetics.

As said before, the oil phase of all emulsions was a fragrance mixture of citronellol, eucalyptol, limonene,  $\alpha$ -pinene, and ethyl-2-methylbutyrate, allowing us to investigate the barrier properties for individual fragrances of varying vapor pressure (Table 1). Citronellol has a very low vapor pressure and exhibited negligible evaporation at room temperature. Thus, its concentration was assumed to be constant, enabling it to be used as an internal reference for the other oil components. To avoid a large decrease in the oil volume, it was used at 50 vol %. The other four fragrances were used in equal parts (by volume).

All emulsions were gently shaken in an open vial at room temperature. Periodically small aliquots of the emulsions were taken, and their fragrance composition was analyzed. Although the emulsion solely stabilized by PEI showed no phase separation when stored in a closed vial, it proved to be unstable when stored in an open vial. Within 2 days two separate phases could be observed. In this sample, ethyl-2-methylbutyrate

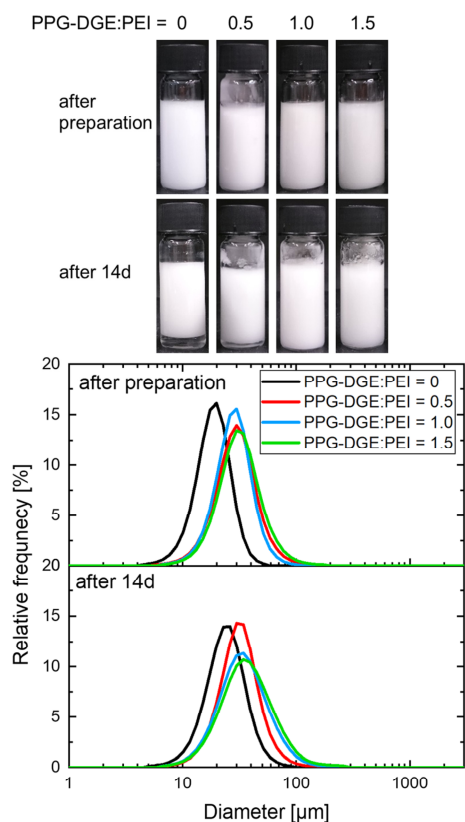


**Figure 4.** Photographs (top) and particle size distributions (bottom) of Hec/PEI Pickering emulsions directly after preparation and after 2 weeks in a closed vial (PEI:Hec = 1).

showed the fastest release followed by  $\alpha$ -pinene, limonene, and eucalyptol (Figure 2, top). As the emulsion showed phase separation, the release of the fragrance molecules was determined solely by their respective vapor pressures (Table 1). The higher the vapor pressure, the faster the rate of release. The emulsions stabilized with Hec/PEI were stable against phase separation, and the fragrance release order did not correlate with the relative vapor pressures (Figure 2, bottom). Again, ethyl-2-methylbutyrate showed the fastest release, but limonene and  $\alpha$ -pinene were retained more effectively than eucalyptol. As the emulsions were stable against phase separation, the fragrance molecules had to pass through the Hec/PEI barrier, which most likely is the rate-determining step. Permeability through the capsule will be determined by the product of solubility and diffusivity of permeates. The latter will be unselective because it is mainly based on tortuosity.<sup>37</sup> The tortuous path scales as the square of the effective aspect ratio ( $\sim 200$ ). Although PEI modification renders the hybrid capsules more hydrophobic as compared to neat Hec films, (ethoxylated) PEI nanocomposites still showed swelling with water vapor,<sup>38</sup> suggesting they are more hydrophilic than the oil. Limonene and  $\alpha$ -pinene, which showed the slowest release, both have the lowest solubility in water, indicating that limonene and  $\alpha$ -pinene are also least soluble in the hybrid capsule wall. On the other end, ethyl-2-methylbutyrate, which was released fastest, has the highest water solubility of the five fragrances. Thus, fragrance solubility within the capsule walls

actually dictates the rate of release rather than the fragrance vapor pressure. Consequently, in combination with the nonselective tortuosity, the release rates of the various fragrances became more uniform. For instance, after 4 days, ethyl-2-methylbutyrate was almost completely evaporated from PEI emulsion while 45% eucalyptol remained. With Hec/PEI (PEI:Hec = 0.5), however, 82% and 96% of ethyl-2-methylbutyrate and eucalyptol, respectively, were retained.

Besides the solubility of the fragrances in the capsule walls, fragrance adsorption on the hectorite surface or fragrance complexation with PEI might also play a role. As the polycationic PEI and the anionic Hec surface form strong ionic bonds, this appears unlikely.

All fragrances showed a retarded release in Hec/PEI Pickering emulsions than in the sample without Hec (Figure 3). Furthermore, the lower the PEI:Hec mass ratio, the slower the rate of release. For PEI:Hec = 0.5, only 20% limonene and  $\alpha$ -pinene were released after 2 weeks. Even the remaining amounts of the more water-soluble ethyl-2-methylbutyrate and eucalyptol were still 17% and 32%, respectively. In contrast, for PEI:Hec = 1.25, only very small amounts of eucalyptol could be observed after 2 weeks while all other fragrances were completely evaporated.

During the emulsification, the PEI acted like a mortar gluing multilayer stacks of anionic Hec together by an electrostatic attraction. The higher the PEI:Hec ratio, the thicker the mortar layer became between the Hec nanosheets and the distance between adjacent nanosheets will be larger. Regarding only emulsions with PEI:Hec = 0.75–1.25 (these emulsions had comparable droplet sizes), the higher the PEI:Hec ratio, the thicker the capsule around the droplet grew as the available amount of PEI was increased. However, a thicker capsule did not lead to a more effective retention of the fragrances. Hec nanosheets are impermeable toward fragrance molecules, giving rise to tortuosity. Moreover, if the gap between adjacent nanosheets becomes small, increasing tortuosity is created, resulting in nonlinear reduction of permeability as a function of increasing Hec content of the capsule.<sup>39</sup> Consequently, as the distances between the Hec nanosheets became larger with increasing PEI, the barrier was less efficient. Thus, using lower PEI:Hec mass ratios led to slower rates of fragrance release from the emulsion over time.

To enhance the stability of the PEI-Hec capsules further, PEI was additionally cross-linked by poly(propylene glycol) diglycidyl ether (PPG-DGE).<sup>21,22,26</sup> The weight ratio of PPG-DGE to PEI was varied between 0.5 and 1.5, while the ratio between PEI and Hec was kept constant (PEI:Hec = 1). All cross-linked emulsions were stable for 2 weeks, showing no creaming or phase separation. The droplet size was found to be comparable to that for the non-cross-linked emulsions and did not change significantly within 2 weeks (Figure 4). Like for the non-cross-linked emulsions, shrunken capsule walls were observed in the dried samples (Figure S4B).

Since the PEI content was kept constant in all cross-linked emulsions, tortuosity was comparable and the solubility of the fragrance molecules in the capsule determined the release rates.  $\alpha$ -Pinene and limonene were released slowest followed by eucalyptol and ethyl-2-methylbutyrate (Figure 5). As compared to the non-cross-linked emulsion, even the sample with the lowest cross-linker concentration (PPG-DGE:PEI = 0.5) already showed a significantly better retention of all fragrances. Increasing the ratio to 1.0 improved the barrier properties further, whereas an increase to 1.5 showed no additional effect.

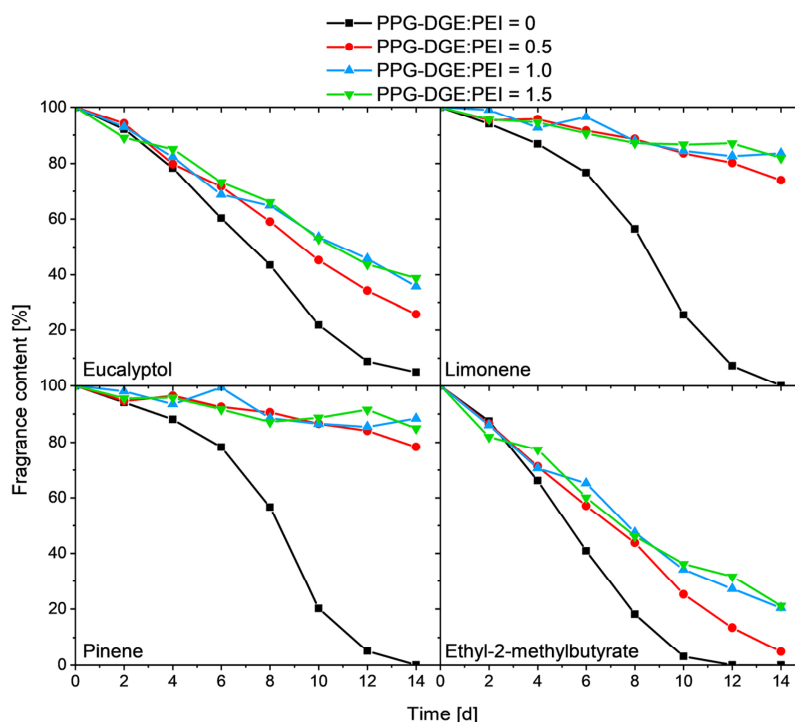


**Figure 5.** Fragrance release curves for cross-linked Pickering emulsions prepared with different PPG-DGE:PEI ratios (PEI:Hec = 1).

For PPG-DGE:PEI = 0.5, the number of amino groups (PEI) was more than 10 times higher than the number of epoxide groups (PPG-DGE). Thus, only relatively light cross-linking of the PEI chains can be achieved. However, this small amount was sufficient to hamper the diffusion of fragrance molecules through the hybrid capsule.

## CONCLUSION

Fixing delaminated hectorite nanosheets quasi in situ into multilayer stack hybrid capsules by adding polycations appears to be a general path to stable Pickering emulsions. It seems to be important to trigger the heterocoagulation of organic (PEI) and inorganic (hectorite) polyelectrolyte at the oil–water interface, since layered silicates first modified by PEI gave disordered capsules showing little to no barrier.<sup>21</sup>

In line with the tortuous path theory, increasing the polymer content in the hybrid capsule gave inferior barriers. In future work we will explore less branched polymers like poly-DADMAC (poly(diallyldimethylammonium chloride)) in order to decrease polymer content in the capsule, while more hydrophobic polymers like polyvinylpyridinium chloride will be tested in order to improve the nonselectivity of release.

## ASSOCIATED CONTENT

### Supporting Information

The Supporting Information is available free of charge at <https://pubs.acs.org/doi/10.1021/acs.langmuir.0c02025>.

NMR spectra of the fragrances and size distributions of hectorite platelets, fluorescence microscopy and scanning electron microscopy images and photographs of the emulsions after 3 months (PDF)

## AUTHOR INFORMATION

### Corresponding Author

Josef Breu – Department of Chemistry and Bavarian Polymer Institute, University of Bayreuth, 95447 Bayreuth, Germany; [orcid.org/0000-0002-2547-3950](https://orcid.org/0000-0002-2547-3950); Email: [josef.breu@uni-bayreuth.de](mailto:josef.breu@uni-bayreuth.de)

### Author

Lina Mayr – Department of Chemistry and Bavarian Polymer Institute, University of Bayreuth, 95447 Bayreuth, Germany

Complete contact information is available at: <https://pubs.acs.org/10.1021/acs.langmuir.0c02025>

### Author Contributions

The manuscript was written through contributions of all authors. All authors have given approval to the final version of the manuscript.

### Notes

The authors declare no competing financial interest.

## ACKNOWLEDGMENTS

Florian Puchtlar is acknowledged for hectorite synthesis. The authors thank the Northbavarian NMR Center for conducting the NMR measurements and appreciate the support of the KeyLab for Optical and Electron Microscopy of the Bavarian Polymer Institute (BPI). Marian Matejdes is acknowledged for conducting the fluorescence microscopy measurements. L.M. acknowledges the support of the Elite Network Bavaria. This work was supported by the Deutsche Forschungs-gemeinschaft (SFB 840, TP B3).

## REFERENCES

- (1) Pickering, S. U. Emulsions. *J. Chem. Soc., Trans.* **1907**, *91*, 2001–2021.
- (2) Binks, B. P. Particles as surfactants - similarities and differences. *Curr. Opin. Colloid Interface Sci.* **2002**, *7* (1–2), 21–41.
- (3) Chevalier, Y.; Bolzinger, M.-A. Emulsions stabilized with solid nanoparticles: Pickering emulsions. *Colloids Surf., A* **2013**, *439*, 23–34.
- (4) Wei, P.; Luo, Q.; Edgehouse, K. J.; Hemmingsen, C. M.; Rodier, B. J.; Pentzer, E. B. 2D Particles at Fluid-Fluid Interfaces: Assembly and Templating of Hybrid Structures for Advanced Applications. *ACS Appl. Mater. Interfaces* **2018**, *10* (26), 21765–21781.
- (5) Ashby, N. P.; Binks, B. P. Pickering emulsions stabilised by Laponite clay particles. *Phys. Chem. Chem. Phys.* **2000**, *2* (24), 5640–5646.
- (6) Gholamipour-Shirazi, A.; Carvalho, M. S.; Fossum, J. O. Controlled microfluidic emulsification of oil in a clay nanofluid: Role of salt for Pickering stabilization. *Eur. Phys. J.: Spec. Top.* **2016**, *225* (4), 757–765.
- (7) Bon, S. A.; Colver, P. J. Pickering miniemulsion polymerization using Laponite clay as a stabilizer. *Langmuir* **2007**, *23* (16), 8316–22.
- (8) Cauvin, S.; Colver, P. J.; Bon, S. A. F. Pickering Stabilized Miniemulsion Polymerization: Preparation of Clay Armored Latexes. *Macromolecules* **2005**, *38* (19), 7887–7889.
- (9) Cui, Y.; Threlfall, M.; van Duijneveldt, J. S. Optimizing organoclay stabilized Pickering emulsions. *J. Colloid Interface Sci.* **2011**, *356* (2), 665–71.
- (10) Lagaly, G.; Reese, M.; Abend, S. Smectites as colloidal stabilizers of emulsions I. Preparation and properties of emulsions with smectites and nonionic surfactants. *Appl. Clay Sci.* **1999**, *14* (1–3), 83–103.
- (11) Zhang, J.; Li, L.; Xu, J.; Sun, D. Effect of cetyltrimethylammonium bromide addition on the emulsions stabilized by montmorillonite. *Colloid Polym. Sci.* **2014**, *292* (2), 441–447.
- (12) Li, W.; Yu, L.; Liu, G.; Tan, J.; Liu, S.; Sun, D. Oil-in-water emulsions stabilized by Laponite particles modified with short-chain aliphatic amines. *Colloids Surf., A* **2012**, *400*, 44–51.
- (13) Whitby, C. P.; Fornasiero, D.; Ralston, J. Effect of oil soluble surfactant in emulsions stabilised by clay particles. *J. Colloid Interface Sci.* **2008**, *323* (2), 410–9.
- (14) Voorn, D. J.; Ming, W.; van Herk, A. M. Polymer-Clay Nanocomposite Latex Particles by Inverse Pickering Emulsion Polymerization Stabilized with Hydrophobic Montmorillonite Platelets. *Macromolecules* **2006**, *39* (6), 2137–2143.
- (15) Hong, J. S.; Rühls, P. A.; Fischer, P. Localization of clay particles at the oil-water interface in the presence of surfactants. *Rheol. Acta* **2015**, *54* (8), 725–734.
- (16) Habel, C.; Schöttle, M.; Daab, M.; Eichstaedt, N. J.; Wagner, D.; Bakhshi, H.; Agarwal, S.; Horn, M. A.; Breu, J. High-Barrier, Biodegradable Food Packaging. *Macromol. Mater. Eng.* **2018**, *303* (10), 1800333.
- (17) Grunlan, J. C.; Grigorian, A.; Hamilton, C. B.; Mehrabi, A. R. Effect of clay concentration on the oxygen permeability and optical properties of a modified poly(vinyl alcohol). *J. Appl. Polym. Sci.* **2004**, *93* (3), 1102–1109.
- (18) Chuanjie, F.; Xiaodong, Z. Preparation and barrier properties of the microcapsules added nanoclays in the wall. *Polym. Adv. Technol.* **2009**, *20* (12), 934–939.
- (19) Jagtap, S. B.; Mohan, M. S.; Shukla, P. G. Improved performance of microcapsules with polymer nanocomposite wall: Preparation and characterization. *Polymer* **2016**, *83*, 27–33.
- (20) Putlitz, B. z.; Landfester, K.; Fischer, H.; Antonietti, M. The Generation of “Armored Latexes” and Hollow Inorganic Shells Made of Clay Sheets by Templating Cationic Miniemulsions and Latexes. *Adv. Mater.* **2001**, *13* (7), 500–503.
- (21) Williams, M.; Armes, S. P.; York, D. W. Clay-based colloidosomes. *Langmuir* **2012**, *28* (2), 1142–8.
- (22) Cui, Y.; van Duijneveldt, J. S. Microcapsules composed of cross-linked organoclay. *Langmuir* **2012**, *28* (3), 1753–7.
- (23) Aranberri, I.; Beverley, K. J.; Binks, B. P.; Clint, J. H.; Fletcher, P. D. I. How Do Emulsions Evaporate? *Langmuir* **2002**, *18* (9), 3471–3475.
- (24) Binks, B. P.; Fletcher, P. D.; Holt, B. L.; Beausoubre, P.; Wong, K. Selective retardation of perfume oil evaporation from oil-in-water emulsions stabilized by either surfactant or nanoparticles. *Langmuir* **2010**, *26* (23), 18024–30.
- (25) Creighton, M. A.; Ohata, Y.; Miyawaki, J.; Bose, A.; Hurt, R. H. Two-dimensional materials as emulsion stabilizers: interfacial thermodynamics and molecular barrier properties. *Langmuir* **2014**, *30* (13), 3687–96.
- (26) Walsh, A.; Thompson, K. L.; Armes, S. P.; York, D. W. Polyamine-functional sterically stabilized latexes for covalently cross-linkable colloidosomes. *Langmuir* **2010**, *26* (23), 18039–48.
- (27) Stöter, M.; Kunz, D. A.; Schmidt, M.; Hirsemann, D.; Kalo, H.; Putz, B.; Senker, J.; Breu, J. Nanoplatelets of sodium hectorite showing aspect ratios of approximately 20,000 and superior purity. *Langmuir* **2013**, *29* (4), 1280–5.
- (28) Rosenfeldt, S.; Stöter, M.; Schlenk, M.; Martin, T.; Albuquerque, R. Q.; Förster, S.; Breu, J. In-Depth Insights into the Key Steps of Delamination of Charged 2D Nanomaterials. *Langmuir* **2016**, *32* (41), 10582–10588.
- (29) Dimitrova, T. D.; Gurkov, T. D.; Vassileva, N.; Campbell, B.; Borwankar, R. P. Kinetics of Cream Formation by the Mechanism of Consolidation in Flocculating Emulsions. *J. Colloid Interface Sci.* **2000**, *230* (2), 254–267.
- (30) Velez, G.; Fernandez, M. A.; Munoz, J.; Williams, P. A.; English, R. J. Role of hydrocolloids in the creaming of oil in water emulsions. *J. Agric. Food Chem.* **2003**, *51* (1), 265–9.
- (31) Hall, K. R. *Vapor Pressure and Antoine Constants for Oxygen Containing Organic Compounds*; Springer, 2000.
- (32) Yalkowsky, S. H.; He, Y. *Handbook of Aqueous Solubility Data*; CRC Press LLC, 2003.
- (33) Ferreira, V.; Pet'ka, J.; Cacho, J. Intensity and persistence profiles of flavor compounds in synthetic solutions. Simple model for explaining the intensity and persistence of their after-smell. *J. Agric. Food Chem.* **2006**, *54* (2), 489–96.
- (34) Hall, K. R. *Vapor Pressure and Antoine Constants for Hydrocarbons, and S, Se, Te, and Halogen Containing Organic Compounds*; Springer, 1999.
- (35) Fichan, I.; Larroche, C.; Gros, J. B. Water Solubility, Vapor Pressure, and Activity Coefficients of Terpenes and Terpenoids. *J. Chem. Eng. Data* **1999**, *44* (1), 56–62.
- (36) Yaws, C. L. *The Yaws Handbook of Vapor Pressure*; Gulf Professional Publishing, 2015.
- (37) Cussler, E. L.; Hughes, S. E.; Ward, W. J.; Aris, R. Barrier membranes. *J. Membr. Sci.* **1988**, *38* (2), 161–174.
- (38) Tsurko, E. S.; Feicht, P.; Nehm, F.; Ament, K.; Rosenfeldt, S.; Pietsch, I.; Roschmann, K.; Kalo, H.; Breu, J. Large Scale Self-Assembly of Smectic Nanocomposite Films by Doctor Blading Versus Spray Coating: Impact of Crystal Quality on Barrier Properties. *Macromolecules* **2017**, *50* (11), 4344–4350.
- (39) DeRocher, J.; Gettelfinger, B.; Wang, J.; Nuxoll, E.; Cussler, E. Barrier membranes with different sizes of aligned flakes. *J. Membr. Sci.* **2005**, *254* (1–2), 21–30.

**Supporting Information**

**Encapsulation of fragrance in aqueous emulsions by delaminated synthetic hectorite**

*Lina Mayr and Josef Breu\**

Department of Chemistry and Bavarian Polymer Institute, University of Bayreuth, 95447 Bayreuth, Germany

\*Correspondence to J. Breu (josef.breu@uni-bayreuth.de)

Number of pages: 4

Number of figures: 5

Number of tables: 0

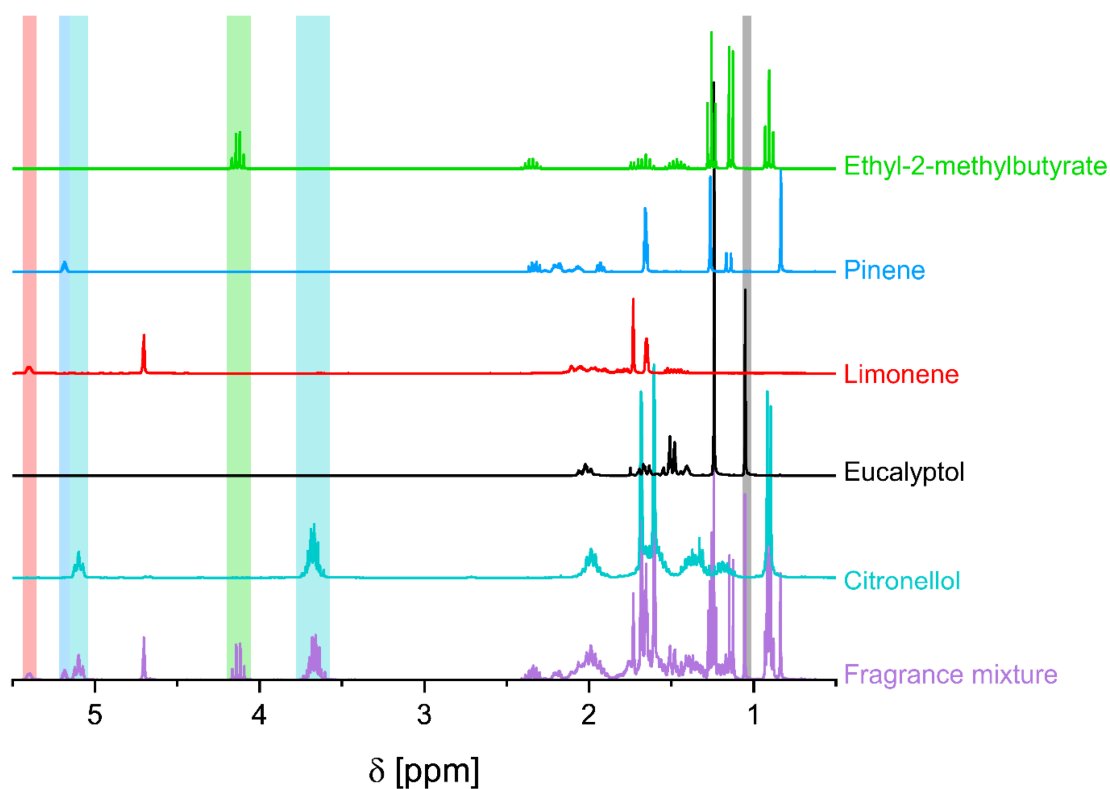


Figure S1: NMR spectra of the fragrance mixture and the individual fragrances. Colored bars show the significant peaks that were used to determine the fragrance composition (citronellol: 5.1-5.04 ppm and 3.78-3.57 ppm, eucalyptol: 1.07-1.01 ppm, limonene: 5.44-5.35 ppm, pinene: 5.22-5.15 ppm, ethyl-2-methylbutyrate: 4.20-4.05 ppm).

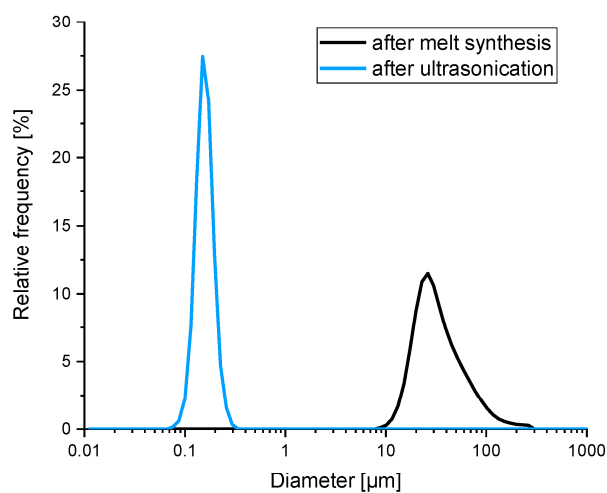


Figure S2: Platelet diameter of pristine sodium hectorite as obtained by melt synthesis (black) and after ultrasonication (blue).

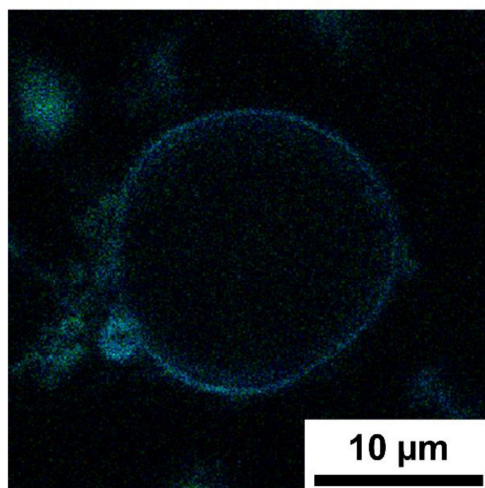


Figure S3: Fluorescence microscopy image of a Hec/PEI Pickering emulsion droplet where PEI was previously labelled with Rhodamine B (PEI:Hec = 1.0).

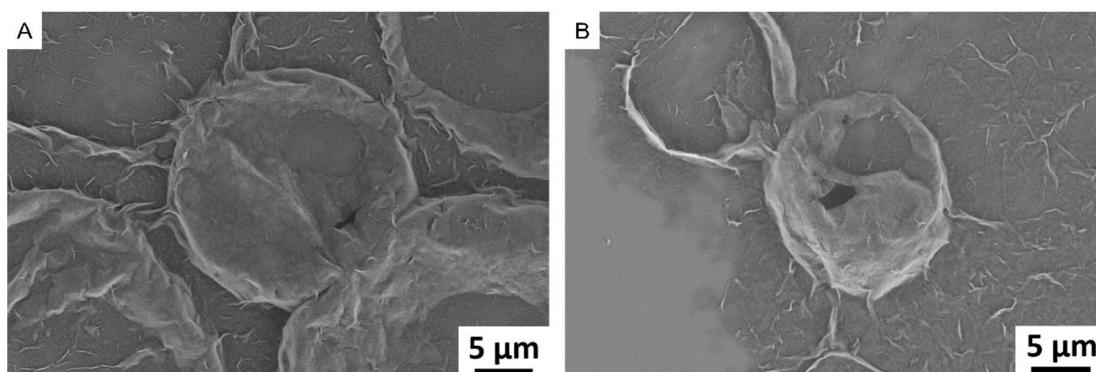


Figure S4: SEM images of dried emulsions (PEI:Hec = 1.00): A: without cross-linking, B: PPG-DGE:PEI = 1.0.

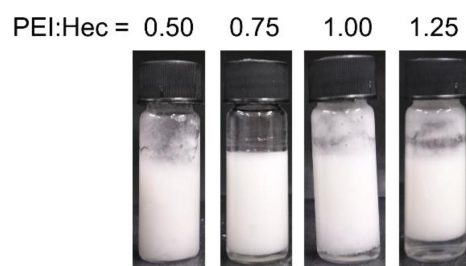


Figure S5: Photographs of Hec/PEI Pickering emulsions after three months.

---

## 7 List of Publications

Kunz, R.; Amschler, S.; Edenharter, A.; Mayr, L.; Herlitz, S.; Rosenfeldt, S.; Breu, J. Giant Multistep Crystalline Vs. Osmotic Swelling of Synthetic Hectorite in Aqueous Acetonitrile. *Clays Clay Miner.* **2020**, *67* (6), 481-487.

Mayr, L.; Amschler, S.; Edenharter, A.; Dudko, V.; Kunz, R.; Rosenfeldt, S.; Breu, J. Osmotic Swelling of Sodium Hectorite in Ternary Solvent Mixtures: Nematic Liquid Crystals in Hydrophobic Media. *Langmuir* **2020**, *36* (14), 3814-3820.

Mayr, L.; Simonyan, A.; Breu, J.; Wingert, M. J. Structural and mechanical impact of synthetic clay in composite foams made via high internal phase emulsions. *Polymer Composites* **2021**, *42*, 353-361.

Mayr, L.; Breu, J. Encapsulation of Fragrance in Aqueous Emulsions by Delaminated Synthetic Hectorite. *Langmuir* **2020**, *36* (37), 11061-11067.

Wagner, D. R.; Ament, K.; Mayr, L.; Martin, T.; Bloesser, A.; Schmalz, H.; Marschall, R.; Wagner, F. E.; Breu, J. Terrestrial solar radiation driven photodecomposition of ciprofloxacin in clinical wastewater applying mesostructured iron(III) oxide. *Environ. Sci. Pollut. Res.* **2021**, *28*, 6222-6231.

Michels-Brito, P.; Gasperini, A.; Mayr, L.; Puentes-Martinez, X.; Tenório, R.; Wagner, D. R.; Knudsen, K.; Araki, K.; Oliveira, R.; Breu, J.; Cavalcanti, L.; Fossum, J.-O. Unmodified Clay Nanosheets at the air-water interface. *Langmuir* **2021**, *37* (1), 160-170.

### Patent

US 63/044,432, Absorbent Articles Including HIPE Foam Enhanced With Clay Nanoplatelets, And Method Of Manufacture; Maxwell Wingert, Josef Breu, Lina Mayr, Steve Merrigan, Arsen Simonyan



## 8 Acknowledgement

At the end of this thesis, I would like to thank everyone who accompanied me over the last years and without whom this work would not have been possible.

First of all, I want to thank my supervisor, Prof Dr. Josef Breu, for the opportunity to join his group and to work on an exciting project with a partner from industry. Many thanks for his trust, his guidance and his support throughout the years. It was great to work in well-equipped laboratories and to do research “on a long leash”.

I would like to thank Max Wingert and Arsen Simonyan from Procter & Gamble for more than three years of fruitful collaboration, many discussions and their hospitality. Thanks to all other P&G workers in Schwalbach and Cincinnati I have met in person for their help, interesting discussions and their hospitality and thanks to them who joined our meetings and improved the project.

Thanks also to Procter & Gamble for financial support.

Furthermore, I would like to thank the whole team of AC1 and AC3. Thanks to Petra Seidler and Iris Raithel for their help in all organizational problems. Thanks to Wolfgang Milius and Thomas Martin for solving all computer problems. Wolfgang is furthermore acknowledged for his support with X-ray diffraction. Thanks to Florian Puchtler, Macro Schwarzmann and Lena Geiling for the hectorite synthesis and a great variety of measurements. Thanks to Kevin Ament, Daniel Wagner and Olena Khoruzhenko for being great lab colleagues. Thanks to Martin Rieß and Daniel for commenting on this thesis. All other colleagues from AC1 and AC3 are acknowledged for the nice atmosphere, helpfulness, relaxing coffee breaks and barbecue evenings.

I thank all my practical students and Hiwis for their help in the daily lab work.

I also would like to thank the Bavarian Polymer Institute: Martina Heider and Ulrich Mansfeld (Key Lab Electron and Optical Microscopy) for the access, introduction and help with scanning electron microscopy; Reiner Giesa (Key Lab Small Scale Polymer Processing) for the access and help with mechanical tests; Sabine Rosenfeldt (Key Lab Mesoscale Characterizations: Scattering Techniques) for conducting a lot of SAXS measurements.

I thank the North Bavarian NMR Center and Kerstin Hannemann for conducting NMR measurements.

Moreover, I would like to thank the Neue Materialien Bayreuth for the access to their Testing Center and especially Andreas Mainz for his help with compression tests.

I would like to thank Prof Dr. Jon-Otto Fossum, Paulo Brito and Leide Cavalcanti for taking me to Campinas, a great experience at the synchrotron and their help in Brazil.

I would like to thank my fellow students and friends who accompanied me during the Bachelor and Master Studies. Thanks for still meeting for Friday lunches.

Thanks to Theresa Schilling for relaxing yoga sessions and a lot of cake breaks.

A very big thank you goes to my parents and my sister who always support me – not only during this work. Thank you for everything you did for me.

Finally, I would like to thank David for proof reading, motivating, distracting and supporting me during all phases of the last years.

## 9 Erklärung des Verfassers

### **(Eidesstattliche) Versicherungen und Erklärungen**

(§ 8 Satz 2 Nr. 3 PromO Fakultät)

*Hiermit versichere ich eidesstattlich, dass ich die Arbeit selbstständig verfasst und keine anderen als die von mir angegebenen Quellen und Hilfsmittel benutzt habe (vgl. Art. 64 Abs. 1 Satz 6 BayHSchG).*

(§ 8 Satz 2 Nr. 3 PromO Fakultät)

*Hiermit erkläre ich, dass ich die Dissertation nicht bereits zur Erlangung eines akademischen Grades eingereicht habe und dass ich nicht bereits diese oder eine gleichartige Doktorprüfung endgültig nicht bestanden habe.*

(§ 8 Satz 2 Nr. 4 PromO Fakultät)

*Hiermit erkläre ich, dass ich Hilfe von gewerblichen Promotionsberatern bzw. –vermittlern oder ähnlichen Dienstleistern weder bisher in Anspruch genommen habe noch künftig in Anspruch nehmen werde.*

(§ 8 Satz 2 Nr. 7 PromO Fakultät)

*Hiermit erkläre ich mein Einverständnis, dass die elektronische Fassung der Dissertation unter Wahrung meiner Urheberrechte und des Datenschutzes einer gesonderten Überprüfung unterzogen werden kann.*

(§ 8 Satz 2 Nr. 8 PromO Fakultät)

*Hiermit erkläre ich mein Einverständnis, dass bei Verdacht wissenschaftlichen Fehlverhaltens Ermittlungen durch universitätsinterne Organe der wissenschaftlichen Selbstkontrolle stattfinden können.*

.....

Ort, Datum

.....

Lina Mayr